sanp
asnp

Schweizer Archiv für Neurologie und Psychiatrie

Archives suisses de neurologie et de psychiatrie

Swiss Archives of Neurology and Psychiatry

26.05.2010

www.sanp.ch | www.asnp.ch

Supplementum 1

Ad Swiss Archives of Neurology and Psychiatry
2010;161(4)

1st SFCNS Congress

Swiss Federation of Clinical Neuro-Societies
Swiss Neurological Society SNS
Swiss Society of Neurosurgery SSN
Swiss Society of Clinical Neurophysiology SSCN
Swiss Society of Neuropediatrics SSNP
Swiss Society of Neuroradiology SSNR
Swiss Society of Neuropathology SSNPath
and other invited societies

2.–4. June 2010, Congress Center Basel

EMH FMH Schwabe
Editores Medicorum Helveticorum

Content

Schweizer Archiv für Neurologie und Psychiatrie

Archives suisses de neurologie et de psychiatrie

Swiss Archives of Neurology and Psychiatry

Posters	Posters SSCN 1–16	3 S
	Posters SSN 17–55	8 S
	Posters SSNP 56–65	19 S
	Posters SNS 66–135	22 S
	Posters SSNR 136–161	42 S
Authors	First authors	52 S

Impressum

Offizielles Organ der Schweizerischen Neurologischen Gesellschaft und offizielles wissenschaftliches Organ der Schweizerischen Gesellschaft für Psychiatrie und Psychotherapie sowie der Schweizerischen Gesellschaft für Kinder- und Jugendpsychiatrie und -psychotherapie

Organe officiel de la Société Suisse de Neurologie et organe officiel scientifique de la Société Suisse de Psychiatrie et Psychothérapie et de la Société Suisse de Psychiatrie et Psychothérapie de l'Enfant et de l'Adolescent

Begründet im Jahre 1917 durch C. von Monakow
Fondé en 1917 par C. von Monakow

Schweizer Archiv für Neurologie und Psychiatrie

Archives suisses de neurologie et de psychiatrie

Swiss Archives of Neurology and Psychiatry

Managing Editor

Redaktion SANP
Dr. Natalie Marty
EMH Schweizerischer Ärzteverlag AG
Farnsburgerstrasse 8
4132 Muttenz
Tel. +41 (0)61 467 85 50, Fax +41 (0)61 467 85 56
e-mail: sanp@emh.ch
www.emh.ch / www.sanp.ch

Online submission

www.sanp.ch

Editors in Chief

Neurology

Prof. Dr. Andreas J. Steck
Neurologische Universitätsklinik
Universitätsspital, CH-4031 Basel

Prof. Dr. Claudio L. Bassetti
Neurocentro (EOC) della Svizzera Italiana
Ospedale Civico
Via Tesserete 46
CH-6903 Lugano
Tel. +41 (0)91 811 66 58

Psychiatry

Prof. Dr. Joachim Küchenhoff
Kantonale Psychiatrische Klinik
Bienentalstrasse 7
CH-4410 Liestal
Tel. +41 (0)61 927 71 61

Prof. Dr Jacques Besson
Service de Psychiatrie Communautaire
Rue Saint-Martin 7
CH-1003 Lausanne
Tél. +41 (0)21 316 16 01

Production

Schwabe AG
Farnsburgerstrasse 8
Postfach 832, 4132 Muttenz
Tel. +41 (0)61 467 85 85, Fax +41 (0)61 467 85 86
e-mail: druckerei@schwabe.ch

Advertising

Ariane Furrer, Assistentin Inserateregie
EMH Schweizerischer Ärzteverlag AG
Farnsburgerstrasse 8, 4132 Muttenz
Tel. +41 (0)61 467 85 88, Fax +41 (0)61 467 85 56
e-mail: afurrer@emh.ch

Subscription

For the members of the Swiss Neurological Society, the Swiss Society of Psychiatry and Psychotherapy and the Swiss Society for Child and Adolescent Psychiatry and Psychotherapy the subscription price is included in the member fee.
Subscription price for non-members: Fr. 96.–

ISSN

ISSN printedition: 0258-7661
ISSN online edition: 1661–3686

The Swiss Archives of Neurology and Psychiatry are published eight times a year.

01

Mapping bioelectric currents with high temporal resolution using magnetic resonance imaging

A.C. Nirkko[1], J. Slotboom[2], C. Kiefer[2]
[1]Neurology, University of Bern, Bern, Switzerland,
[2]Neuroradiology, University of Bern, Bern, Switzerland

Introduction: Assessment of neuronal activity with functional magnetic resonance imaging (fMRI) is indirect because it depends on the neurovascular response. Direct imaging of bioelectric currents would be preferrable, but reported attempts in vivo were not conclusive and timecourse data were not found even in vitro. To achieve this, we used a sequence with a current sensitive time window on a phantom and on human muscles, which generate up to 1000-fold larger synchronous currents upon electrical nerve stimulation.
Methods: On a clinical 3T scanner (Siemens), a gradient echo sequence (TR 25.01 ms, TE 5.00 ms) was used to image phase shift differences occurring between alternating echoes (interval 50.02 ms) in the 5 ms wide temporal window sensitive to current induced magnetic field changes. During repeated image acquisition every 4.8 sec, simultaneous electric stimulation was applied in short pulses (width 0.2 ms) at 20 Hz (interval 50.0 ms). Because the TR cycle was chosen 0.02 ms higher than the electrical stimulation interval, the electrical pulses sweeps slowly through the susceptible 5 ms window. This results in MR signal changes in the minute range which correspond to electrical currents in the msec range. The almost smooth tetanic muscle contraction prevents mechanical movement artifacts.
Results: With the phantom, the electrical currents could be depicted as planned. Using the known stimulus and the aquired data from the phantom to define the transformation from the millisecond to minutes range, the bioelectric time course from the subjects could also be recovered with the corresponding inverse transform. In addition to a sinusoidal component from residual synchronous mechanical muscle motion, a timecourse that resembled the electrophysiologic recording of the surface potential could also be found.
Conclusions: The time courses of electrical currents can be imaged with millisecond temporal resolution. This could be verified in a phantom, but is at the limits of the possible even with the comparatively large currents from human muscle. Imaging small currents from brain and nerves is therefore out of reach of the current techniques. We suggest using evoked muscle activity as a model to develop methods for direct electrical current imaging.
Supported by the Swiss National Science Foundation (SNF grant 3200B0-107499/1)

02

Applying multivariate symbolic interrelation measures to quantify peri-seizure EEG dynamics of focal onset seizures

C. Rummel, F. Amor, H. Gast, K. Schindler
qEEG group, Dept. of Neurology, Inselspital, Bern, Switzerland

Introduction: Epilepsy is the second most common neurological disorder. Only two thirds of epilepsy patients are rendered seizure-free by anticonvulsant drugs. The remaining pharmaco-resistant patients are potential candidates for epilepsy surgery. However, surgery is only possible, if the seizure onset zone may be clearly delineated and turns out to be localized in a part of the brain that may be removed without causing serious neurological deficits. Thus, to localize precisely the seizure onset zone is of paramount importance and here we will discuss how multivariate quantitative analysis of the intracranial electroencephalogram (iEEG) may support this process.
Methods: Symbolic estimates for the interrelation of two time series often yield smaller fluctuations, especially for signals dominated by low frequencies. As multivariate quantities we will study the eigenvalues and eigenvectors of matrices constructed from symmetric symbolic interrelation measures. Whereas the eigenvalues provide information about the total strength of interrelation, the eigenvectors can be exploited to identify the data channels' contribution to the interrelation patterns.
Results: The reduced fluctuation level of symbolic interrelation matrices enables more reliable interpretation of the eigenvectors, which are often highly fluctuating quantities for non-symbolic measures. In application to multi-channel iEEG we find patient specific rearrangements of the largest eigenvectors during epileptic focal onset seizures. Specifically, we find that the contributions to the largest eigenvector of the EEG channels recording from the seizure onset zone significantly drop at seizure onset. This phenomenon helps to precisely localize the seizure onset zone in space and time and may be interpreted as a "decoupling" from the ongoing large-scale collective neuronal activity.
Conclusions: Applying multivariate symbolic interrelation measures helps to precisely localize the seizure onset zone and thus provides clinically important information in the presurgical evaluation of pharmacorresistant epilepsy patients.

03

Brain LORETA functional imaging, EEG spectral power, and self-rated headache pain

P.L. Faber[1], S. Tei[2], C. Chen[3], P. Hsiao[3], D. Lehmann[1]
[1]The KEY Institute for Brain-Mind Research, University Hospital of Psychiatry, Zurich, Switzerland, [2]Department of Stress Science and Psychosomatic Medicine, Graduate School of Medicine, The University of Tokyo, Tokyo, Japan, [3]Dept. of Neurology, Taipei Veterans General Hospital, Taipei, Taiwan, Province of China

Introduction: We studied the subjective intensity of headache as reflected by EEG spectral power and by activated brain regions (functional imaging).
Methods: In 16 migraine patients without aura (6 medicated; mean age 38 ± 7.7 years; 12 women), 19-channel EEG was recorded during initial resting (4 min) on an attack-free day; 65.6 s artifact-free EEG was available on average per patient. Patients self-rated (visual-analog) headache intensity. For each of the eight independent EEG frequency bands, mean of spectral power (absolute and relative) across channels, and LORETA functional images (absolute and relative voxel strength) were computed. These values were correlated with subjective headache intensity.
Results: Correlations were negative ($p < 0.1$) with absolute power in the delta, alpha2, beta1 and 3, and gamma bands, but positive ($p < 0.1$) with relative power in delta and beta2. Absolute LORETA voxel strength (corrected for multiple testing $p < 0.1$) correlated negatively in all bands except delta; relative voxel strength correlated positively with delta through alpha1. Negative correlations with absolute LORETA voxel strength concerned only left anterior voxels in theta and alpha1, only left-hemispheric in beta1 and beta2, predominantly left in alpha1 and beta3, but more right in gamma; all positive correlations with relative strength were right anterior (delta, theta and alpha1). Medicated and unmedicated patients showed comparable tendencies.
Conclusion: With increasing headache intensity, EEG absolute power decreased, with left hemispheric localization (in some frequency bands predominantly anterior), while relative power increased exclusively right anterior. These results suggest that increasing headache intensity is associated with increasing predominant anterior left hemispheric activation (supported in part by Bial Foundation Grant #44-06).

04

Clinical Application of Simultaneous EEG/fMRI: The Bern Experience 2006–2009

R. Wiest[1], K. Jann[2], T. Koenig[2], O. Scheidegger[1], T. Dierks[2], K. Meyer[4], J. Mathis[3], K. Schindler[3], M. Hauf[1]
[1]Neuroradiology; Inselspital, Bern, Switzerland, [2]Psychiatric Neurophysiology, Bern, Switzerland, [3]Neurology, Inselspital, Bern, Switzerland, [4]Bethesda Epilepsy Clinic, Tschugg, Switzerland

Introducton: Simultaneous EEG/fMRI recordings are increasingly recognized as a method to delineate the irritative zone in patients with epilepsy. Its principal advantage is the non-invasiveness and the ability to record patients during seizure free periods. A novel technique, using Independent Component Analysis (ICA) to extract continuously fluctuating interictal epileptic activity has enhanced the detection rate of BOLD correlates that converge with electro-clinical data. Here, we present our experience with this technique in the diagnostic and presurgical workup of patients with different epilepsy syndromes.
Methods: During the evaluation period, we examined 20 patients with the ICA-based EEG /fMRI approach and with a manual spike detection technique. Subsequently, we examined 30 patients with the ICA approach. All patients received EEG (8 minutes) outside, and simultaneous EEG/fMRI (16 minutes) inside the scanner using a single-shot T2*-weighted sequence (EPI, TR/TE 4130 ms/30 ms or TR/TE 1980 ms/30 ms). ICA was applied to the EEG to extract epileptic activity as predictor for the BOLD signal in the correlation analysis.

Results: The ICA-based EEG /fMRI provided improved sensitivity in the detection of the irritative zone (16/20 pts. vs. 10/20 pts.) compared to conventional techniques [1]. Overall, in 50 patients with different epilepsy syndromes, we found 19/24 concordant BOLD correlates (compared with video-EEG) in patients with temporal lobe epilepsy, 11/11 in generalised epilepsy and 8/15 in patients with extratemporal focal epilepsy. In 7/10 patients in the presurgical workup EEG/fMRI has been integrated into the planning of the invasive EEG. In selected cases, the ICA-based predictors have been additionally used to study the temporal evolution of interictal BOLD correlates and characteristic BOLD responses in different epilepsy syndromes have been observed.
Conclusion: ICA-based simultaneous EEG /fMRI recordings provide non-invasive data about the irritative zone in patients with focal and idiopathic epilepsies. Beyond the correlation of interictal BOLD correlates with the putative seizure onset zone, they provide information about temporal evolution of the epileptic activity and brain areas involved in the interictal networks.
1 Jann K, Wiest R, Hauf, et al. Neuroimage; 2008.
This work has been granted by the SNF Grant (SPUM) 33CM30-124089 Imaging large scale networks in epilepsy.

05

Combined quantitative and neurophysiological sensory assessment reveals differences in spino-thalamic tract function within cervical and trunk dermatomes

J. Haefeli[1], J. Blum[1], A. Curt[1]
[1]Spinal Cord Injury Center, University Hospital Balgrist, Zürich, Switzerland

Introduction: Current examination of spino-thalamic tract function following spinal cord injury (SCI) is mainly limited to quantitative sensory testing. Contact heat evoked potentials (CHEPs) in combination with thermal threshold testing might be a mean to improve the assessment of segmental sensory function as related to the spino-thalamic tract. Hence, this study aimed to investigate sensory segmental characteristics of warmth and nociceptive heat perception and CHEPs within different cervical and trunk dermatomes.
Methods: In 19 healthy subjects divided into two age classes (young subjects: n = 10, mean age 28.8 ± 5.2 years; elderly subjects: n = 9, mean age 63.4 ± 3.4 years) the perception threshold, pain threshold and combined CHEPs and pain rating were examined. Five different segments (C4, C5, C6, C8 andT4) according the ASIA dermatomes were stimulated with two different temperatures (52∫C and individual pain threshold plus 3∫C).
Results: Perception thresholds of warmth showed no differences between the dermatomes while pain threshold and pain rating to heat were significantly different between dermatomes. In the cervical dermatomes C6 and C8 pain ratings were reduced and pain thresholds increased ($p < 0.05$) which related to reduced CHEPs amplitudes. CHEPs latencies were significantly ($p < 0.05$) longer for more distal segments. Regarding age class differences CHEPs amplitudes (N2, P2; N2P2) and latencies (N2, P2) demonstrated significant ($p < 0.05$) effects.
Discussion and conclusion: The combined quantitative and neurophysiological sensory assessment revealed significant differences of sensory function between cervical and trunk dermatomes. The diverse responses to heat stimulation in these dermatomes are most likely due to differences in receptor densities. These differences among segments should be concerned when investigating the sensory function of the spinothalamic tract. CHEPS as a segmental sensitive tool could complete the clinical testing of sensory thresholds to improve the assessments of the spino-thalamic tract in SCI.

06

Diffusion tensor MRI study of the spinal cord in patients with Multiple Sclerosis

J. von Meyenburg[1], B. Wilm[2], A. Weck[3], J. Petersen[4], E. Gallus[5], J. Mathys[6], E. Schätzle[7], K. von Meyenburg[8], N. Goebels[9], S. Kollias[10]
[1]Institute of Neuroradiology, University Hospital, Zürich, Switzerland, [2]Institute of Neuroradiology, University Hospital, Institute for Biomedical Engineering, University & ETH, Zürich, Switzerland, [3]Department of Neurology, University Hospital, Zürich, Switzerland, [4]Spinal Cord Injury Center, Balgrist University Hospital, Zürich, Switzerland, [5]Institute of Neuroradiology, University Hospital, Zürich, Switzerland, [6]Department of Neurology, University Hospital, Zürich, Switzerland, [7]Institute of Neuroradiology, University Hospital, Zürich, Switzerland, [8]Zürich, Switzerland, [9]Department of Neurology, University Hospital, Zürich, Switzerland, [10]Institute of Neuroradiology, University Hospital, Zürich, Switzerland

Introduction: Diffusion tensor imaging (DTI) can potentially discern axonal loss in white-matter tissue and serve as a marker for loss of tissue integrity (demyelination, axonal degeneration) [1, 2]. Limited resolution in spinal cord DWI has so far impeded focal evaluation of spinal cord tissue i.e. the differentiation between grey and white matter. Furthermore, adequate image quality was achievable only at the cervical level of the spinal cord. Recent improvements in MR pulse sequence design have overcome these problems.
Methods: Imaging was performed on a 3T Philips Achieva using a dedicated spine coil. DTI data of 28 volunteers and 41 patients with relapsing remitting MS (RRMS), secondary progressive MS (SPMS) or primary progressive MS (PPMS) (table 1) were acquired at the cervical, thoracic and lumbar levels of the spinal cord. In each region 6 transverse slices were acquired using

Table 1

Groups	Volunteers	RRMS	SPMS	PPMS	All patients
Number	28	15	14	12	41
Male/Female	14/14	5/10	9/5	8/4	22/19
Mean Age ± SD years (range)	44.8 ± 17 (21-83)	43.2 ± 8.8 (29-60)	54.4 ± 10.5 (42-74)	57 ± 14.5 (32-74)	51.1 ± 12.6 (29-74)
Mean Disease duration ± SD years (range)		8.06 ± 5.28 (2-17)	18.14 ± 11.6 (4-43)	11.1 ± 5.16 (4-18)	12.43 ± 9.34 (29-60)
Mean FA ± SD, PWM, at cervical level 5	0.71 ± 0.05	0.67 ± 0.07	0.64 ± 0.05	0.61 ± 0.07	0.64 ± 0.07
Mean FA ± SD, PWM, at thoracic level 5	0.70 ± 0.06	0.69 ± 0.07	0.69 ± 0.07	0.63 ± 0.06	0.68 ± 0.06
Mean FA ± SD, PWM, at the lumbar enlargement	0.66 ± 0.07	0.68 ± 0.11	0.68 ± 0.11	0.64 ± 0.04	0.65 ± 0.08
Mean ADC ± SD, PWM, at cervical level 5	0.88 ± 0.09	0.89 ± 0.10	0.83 ± 0.10	0.90 ± 0.09	0.90 ± 0.09
Mean ADC ± SD, PWM, at thoracic level 5	0.86 ± 0.08	0.90 ± 0.10	0.90 ± 0.11	0.87 ± 0.11	0.87 ± 0.11
Mean ADC ± SD, PWM, at the lumbar enlargement	0.89 ± 0.08	0.92 ± 0.18	0.89 ± 0.18	0.89 ± 0.79	0.89 ± 0.08

RRMS: relapsing remitting MS; SPMS: secondary progressive MS; PPMS: primary progressive MS FA: Fractional anisotropy; ADC: Apparent diffusion coefficient; PWM: Posterior white matter

References: 1] Ohgiya Y. et al, Eur Radiol. 2007;17(10):2499-504. 2] Mottershead JP, et al. J Neurol. 2003;250(11):1293-301. 3] Wilm BJ, et al. NMR Biomed. 2008 Aug 26. 4] Wilm BJ, et al. Magn Reson Med. 2007;57(3):625–30. 5] Tartaglino LM, et al. Radiology. 1995;195(3):725–32.
This study was supported by the Swiss Multiple Sclerosis Society

an outer volume suppressed reduced field of view single-shot EPI sequence [3, 4]. Fractional anisotropy (FA) and apparent diffusion coefficient (ADC) maps were calculated. Diffusivity values were evaluated in the posterior white matter (PWM) in normal appearing spinal cord tissue, i.e. spinal cord tissue without T2-hyperintense lesions.
Results: Mean fractional anisotropy in the posterior white matter (PWM) was highest in healthy subjects and lowest in the PPMS group (table 1). ADC values were lowest in volunteers and highest in the RRMS group, respectively. In the patient groups the decrease of FA was statistically significant on cervical level and showed a trend on thoracic level as compared to healthy volunteers (table 1).
Conclusions: Correlation between diffusion anisotropy and axonal density [2] in spinal MS lesions has been observed by comparing MRI images and neuropathological findings. Based on these observations our results suggest that axonal degeneration is most prominent in the PPMS group. The highest ADC values were seen in the RRMS group which might indicate that the degree of myelin loss in the RRMS patients is most prominent [2]. The fact that the PWM FA difference between patients and the control group was highest at cervical level and decreasing when moving caudally (table 1) might also reflect a decrease of inflammation in a cranio-caudal sense. This goes along with an observed decrease of T2-hyperintense lesions when moving caudally in the spinal cord [5]. Correlation between anatomical analysis with electrophysiological and clinical tests is ongoing.

07

Early muscle membrane dysfunction in porcine peritonitis

K.A. Ackermann[1], L. Brander[2], R Schröder[2], D. Tuchscherer[2], S.M. Jakob[2], J. Takala[2], W.J. Z'Graggen[3]
[1]Department of Neurology, Inselspital, Bern University Hospital and University of Bern, Bern, Switzerland, [2]Department of Intensive Care Medicine, Inselspital, Bern University Hospital and University of Bern, Bern, Switzerland, [3]Departments of Neurology and Neurosurgery, Inselspital, Bern University Hospital and University of Bern, Bern, Switzerland

Introduction: Critically ill patients often develop diffuse muscle weakness and failure to wean from mechanical ventilation. The most common cause of generalised weakness is critical illness myopathy (CIM), which has been attributed to chronic muscle membrane depolarisation. The aim of this study was to investigate muscle membrane properties by measuring velocity recovery cycles (VRCs) of muscle action potentials in the early stage of experimental sepsis. VRCs chart the changes in velocity of a muscle action potential in the wake of another, and provide an indirect indication of the afterpotentials following the muscle action potential. Hence, they are strongly dependent on membrane potential.
Methods: 25 anesthesized pigs were randomized to either fecal peritonitis (n = 11) or to non-septic controls (n = 14). Multi-fibre responses to direct muscle stimulation through needle electrodes were recorded from the front leg immediately before induction of peritonitis as well as 6, 18 and 24 hours thereafter. Latency changes were measured as conditioning stimuli were applied at inter-stimulus intervals of 2 to 1000 ms. Relative refractory period (RRP) and maximal supernormality (SN) were assessed.
Results: In septic animals, RRP was increased by 38% ($P < 0.05$) and SN was reduced by 22% ($P < 0.05$) 24 hours after induction of peritonitis compared with baseline measurements. The effect of increased RRP and reduced SN in the sepsis group was already apparent 6 hours after induction of peritonitis, whereas in the non-septic controls there were no significant differences over time. The changes in SN in the sepsis group were significantly correlated with muscle oxygenation and with serum potassium levels.
Conclusion: VRC changes in the sepsis group corresponded to muscle membrane depolarisation, which seems to be an important factor in the pathogenesis of CIM. Muscle membrane depolarisation was most likely caused by muscle hypoperfusion. VRCs provide a practicable mean for monitoring muscle membrane changes and may allow an early diagnosis of CIM.

08

High dose, fast absorbed intranasal Midazolam as a potential treatment for status epilepticus: a pharmacokinetic-pharmacodynamic study in healthy volunteers using quantitative EEG

M. Hardmeier[1], R. Zimmermann[1], M. Pflueger[2], St. Rueegg[1], S. Deuster[3], J. Drewe[4], P. Fuhr[1], M. Haschke[5]
[1]University Hospital, Clinical Neurophysiology, Basel, Switzerland, [2]University Hospital, Dept. of Psychiatry, Basel, Switzerland, [3]University Hospital, Inst. of Pharmacy, Basel, Switzerland, [4]University Hospital, Gastroenterology & Hepatology, Basel, Switzerland, [5]University Hospital, Dep. of Clinical Pharmacology, Basel, Switzerland

Introduction: Status epilepticus (SE) is a life-threatening neurologic emergency. Benzodiazepines (BZD) are the first-line treatment. Time to treatment is crucial: up to 31% of SE lasting >10 minutes are refractory to BZD. Nasal application of midazolam (MDL) has been successfully used in children; however, dosing in adults is limited by the nasal mucosal surface. Using EEG, increase in power in the beta-band after BZD-application previously correlated with antiepileptic activity. The current study evaluates the pharmacokinetic (PK) and pharmacodynamic (PD) properties of a concentrated, fast absorbed nasal formulation using quantitative EEG.
Methods: Double-blind application of MDL 5 mg i.v. (MDL5iv), and intranasal (i.n.) administration of 3 mg (MDL3in), and 6mg (MDL6in) were investigated in 12 healthy male volunteers (median age 29 y) in a cross-over design at three different days. Unit dose sprays (0.1 ml) containing 3 mg MDL with solubility/absorption enhancers (cyclodextrin/chitosan) were used. Blood was drawn at baseline and 2.5, 5, 10, 15, 20, 30, 45 and 60 min after MDL. PK analysis was performed using compartmental modelling (WinNonlin). EEG was recorded 10 min. before (baseline) until 70 min. after MDL. Artefact elimination and a fast Fourier transformation (spectral resolution: 0.5 Hz) was applied. The log transformed absolute power (Fz-Cz) in the beta1-band (14.0–17.5 Hz) was further analysed: Onset of pharmacological action was defined as the time-point, at which power rose above the mean +2x SD of its baseline for at least 60 seconds.
Results: No paradoxical or other adverse effects occurred after i.n. application. Maximum plasma concentrations (Cmax) were: 602, 110, and 63 ng/ml, for MDL5iv, MDL6in and MDL3in. Median absolute bioavailabilities of nasal administrations were 81 and 76%. The table gives the times to reach Cmax, the PD effect and clinical non-reactivity to auditory stimuli (median (range)).
Conclusions: MDL6in-absorption was faster and peak plasma concentrations higher than in previously reported nasal sprays, reaching a high bioavailability. Quantitative EEG reliably showed the fast onset of the central pharmacodynamic effect. Given the time necessary to install an i.v.-line, MDL6in provides a new and safe means for fast administration of a first dose of a highly effective antiepileptic drug in SE, even by lay people.

		MDL5iv	MDL6in	MDL3in
PK	Time to C max	n/a	425s (297–1340)	502s (297–1880)
PD	Time to PD effect	84s (68–148)	396s (238–850)	480s (288–1172)
Clinical	Time to non-reactivity	182s (162–322)	482s (282–1122)	912s (582–1342)

09

In-vivo evaluation of a combined flow restoration and mechanical thrombectomy device in a swine model of acute vessel occlusion

P. Mordasini[1], J. Gralla[1], G. Schroth[1], U. Fischer[2], M. Arnold[2], C. Brekenfeld[1]
[1]Institute of Interventional and Diagnostic Neuroradiology, Inselspital, Bern, Switzerland, [2]Department of Neurology, Inselspital, Bern, Switzerland

Background and purpose: The purpose of study was to evaluate the efficiency, thrombus-device interaction and potential complications of the stent-like Solitaire FR Revascularization Device for immediate flow restoration and mechanical thrombectomy in-vivo.
Material and methods: The device was evaluated in an established animal model in the swine. Flow restoration effect (immediately after deployment = T0, after 5 minutes = T5 and 10 minutes = T10), recanalization rate after retrieval, thromboembolic events and complications were assessed. Radio-opaque thrombi (10 mm length) were used for the visualization of thrombus-device interaction during application and retrieval of the device. The Solitaire FR (4 x 20 mm) was assessed in 15 vessel occlusions.
Results: Immediate flow restoration after deployment was achieved in 80.0% of vessel occlusions. Mean recanalization rate at T0 was 30.8%, at T5 30.7% and at T10 25.4% of initial vessel diameter. Re-occlusion occurred in 20.0% between T0 and T5 and in 13.3% between T5 and T10. Complete recanalization (TICI 3) after retrieval was achieved in 86.7%. In two cases (13.3%) partial recanalization was achieved with remaining thrombus in a side branch (TICI 2b). No thromboembolic event was observed during deployment or retrieval. Thrombus-device interaction illustrated the compression of the thrombus against the vessel wall during deployment leading to partial flow restoration. During retrieval the thrombus was retained by the stent meshes without significant thrombus compression. No vessel perforation, dissection nor fracture of the device was observed.
Conclusion: The Solitaire FR is a safe and effective combined flow restoration and thrombectomy device in-vivo. Maximal flow and thrombus compression is achieved immediately after deployment with decreasing effect with time indicating the need for retrieval to achieve recanalization.

10

Is hemifacial spasm accompanied by hemodynamic changes detectable by ultrasound? A pilot study

F. Perren[1], M.R. Magistris[1]
[1]HUG, University Hospital and Medical Faculty, Dept. Neurology, Geneva, Switzerland

Introduction: Hemifacial spasm (HFS) is a rare condition characterized by weakness, synkinesis and involuntary, intermittent, spasmodic contractions of hemifacial muscles innervated by the facial nerve. Usually, an arterial tortuosity of the posterior circulation compressing the facial nerve as it exits from brainstem induces the ephaptic axono-axonal cross-talk that sparks HFS. Magnetic resonance angiography, the actual gold standard, does not always clearly show the "vascular-nerve conflict". We sought if a noninvasive method such as color-coded duplex flow imaging (CDFI) of these arteries might be able to detect hemodynamical changes in HFS.
Methods: Nine successfully treated (botulinum toxin) consenting patients have been examined prospectively. CDFI has been performed by an experienced sonographer who was blinded to the presence of an HFS. Blood flow velocities (peak systolic, peak diastolic and mean velocities) of the vertebral (VA) (including diameter of the intraforaminal segment), posterior inferior cerebellar (PICA) and anterior inferior cerebellar (AICA) arteries were measured and side-to-side comparison was performed for all of them. Exclusion criteria included: recent stroke, vertebro-subclavian steal, stenosis, dissection, hypo- or aplasia, or occlusion.
Results: Nine patients (5 men; mean age 53.4 years) were studied. Diameters of the VAs were: 38 ± 8 mm on the right and 39.5 ± 5.5 mm on the left side. Whereas there was no significant association between mean blood flow velocities (MFV) asymmetry of the VAs and HSF (Fisher's exact p = 0.523), an elevation of MFV of the PICA and AICA was found on the side of the HFS in the 7 patients in whom these vessels could be detected by CDFI (Fisher's exact p = 0.0285; 2-tailed).
Conclusion: Despite the limited number of HFS patients studied, we found a significant association between elevation of MFV of the PICA and AICA and the side of HFS. Therefore, HFS seems to relate not only to an unfortunate malposition of an artery over the root exit zone of the facial nerve, but also to hemodynamic changes detectable by CDFI. Ultrasound techniques may become an additional tool in the detection and evaluation of the "vascular-nerve" conflict of HFS.

11

Maps of Functional Connectivity Reveal the Neural Basis of Deficits and Recovery in Patients with Ischemic Stroke

A.G. Guggisberg, J.M. Pignat, N. Gillabert, M. Di Pietro, L. Nahum, L. Allet, A.M. Lascano, I. Momjian-Mayor, M.D. Martory, C.M. Michel, K.O. Lövblad, F. Lazeyras, J.M. Annoni, R. Sztajzel, A. Schnider
Hôpitaux Universitaires de Genève, Genève, Switzerland

Introduction: Stroke is a leading cause of adult disability but techniques that help guiding and predicting the success of rehabilitation are lacking. What is needed is an imaging method that can map the functionality and the rehabilitation potential of each brain area of interest. In patients with brain tumors, the functionality of brain tissue depends on its functional connectivity with other areas. Here we assess the usefulness of non-invasive measures of functional connectivity in patients with ischemic stroke.
Methods: Twelve patients with first ever unilateral ischemic stroke in the territories of the medial and/or anterior cerebral artery were included. Spontaneous EEG activity during a no-task resting state was recorded 2 weeks and 3 months after stroke onset. In addition, standardized clinical assessments of motor and language functions were obtained. Neural activity in the brain was reconstructed using an adaptive spatial filtering technique. The imaginary component of the complex valued coherence was then calculated for pairs of brain voxels and used as an index of their functional connectivity.
Results: In the acute phase of stroke, the affected hemisphere shows relatively diffuse increases in functional connectivity in some patients. These increases are associated with better recovery after 3 months. Three months after stroke onset, the topographical distribution of functional connectivity in the alpha frequency range matches precisely the pattern of clinical deficits in each individual patient: the brain areas that are normally responsible for the affected functions show corresponding local decreases in functional connectivity. Moreover, clinical scores of force and motor capacity correlate positively with the magnitude of functional connectivity in the motor cortex, whereas scores of language skills correlate with functional connectivity in the fronto-temporal cortex.
Conclusions: The findings demonstrate that indices of functional connectivity reflect the functionality of the entire cerebral cortex without depending on patient collaboration and while requiring merely 5–10 minutes of recording time. The method has also the potential to provide important information about the mechanisms and prognostic factors of recovery after stroke.

12

Nocturnal cerebral hemodynamics in acute stroke patients during sleep disordered breathing: a near infra-red spectroscopy study

F. Pizza[2], M. Biallas[3], M. Wolf[3], U. Kallweit[1], C.L. Bassetti[4]
[1]Departmenf of Neurology, University Hospital Zürich, Zürich, Switzerland, [2]Department of Neurological Sciences, University of Bologna, Bologna, Italy, [3]Clinic of Neonatology, University Hospital Zürich, Zürich, Switzerland, [4]Department of Neurology, Neurocenter (EOC) of Southern Switzerland, Lugano, Switzerland

Introduction: Sleep disordered breathing (SDB) is a risk factor for cerebrovascular morbidity and mortality. Its impact during the acute phase of stroke is poorly known. We compared nocturnal bilateral cerebral hemodynamic changes induced by SDB in acute stroke patients, using near infra-red spectroscopy (NIRS).
Methods: Six patients (3 men and 3 women, mean age 58 ± 15 years) with acute middle cerebral artery (MCA) stroke (NIHSS score 10 ± 7, range 2–18), normal or increased daytime MCA blood flow velocity on the affected hemisphere at daytime Transcranial Doppler (TCD), and SDB (AHI 39 ± 36/h, range 5–94) were assessed by means of nocturnal polysomnography coupled with bilateral frontal NIRS recording.

Results: NIRS showed asymmetric patterns of haemoglobins' evolution on the two hemispheres induced by SDB, leading to major cerebral oxygen desaturations on the normal hemisphere (–0.80 ± 0.54% versus 0.01 ± 0.42% per second, p = 0.001). Obstructive apneas had a stronger impact than central ones on brain tissue oxygenation of the normal hemisphere (–1.17 ± 0.52% versus –0.44 ± 0.22% per second, p = 0.003).
Conclusions: During the acute phase of stroke SDB repetitively induces major cerebral oxygen desaturations on the normal hemisphere and has a more profound effect during obstructive (versus central) apneas. These new findings may reflect the asymmetry of brain metabolism and neurovascular coupling with potential clinical significance for stroke pathophysiology and recovery.

13

Primary vs secondary bilateral synchrony – insights using simultaneous EEG/fMRI

O. Scheidegger[1], K. Jann[2], T. König[2], K. Meyer[3], R. Wiest[1], M. Hauf[1]
[1]Institute for Diagnostic and Interventional Neuroradiology, Inselspital, Bern, Switzerland, [2]Department of Psychiatric Neurophysiology, University Hospital of Psychiatry, Bern, Switzerland, [3]Bethesda, Epilepsy Center, Tschugg, Switzerland

Introduction: Prevailing bilateral synchronous discharges on scalp electroencephalogram (EEG) do not allow a differentiation between primary generalized seizures and secondary bilateral synchrony in focal epilepsies. Here, we show how a comprehensive analysis of interictal simultaneous EEG/fMRI can help to differentiate primary from secondary bilateral synchrony.
Methods: Simultaneous EEG/fMRI recordings were performed in one patient suffering from idiopathic generalized epilepsy (IGE) and in one patient suffering from lesional frontal lobe epilepsy (FLE) due to a developmental venous anomaly (DVA). Both patients showed bilateral synchronous discharges on scalp EEG. An independent component analysis (ICA) factor coding for time varying interictal epileptic discharges (IED) was convolved with a hemodynamic response function to predict the blood oxygen level dependent (BOLD) signal. Voxel-wise correlations between the ICA-based predictor and the BOLD signal were computed. The temporal pattern of the BOLD correlates was analysed by shifting the convoluted predictor in intervals of 1 s from 10 s before to 10 s after the IED.
Results: Both patients showed widespread bilateral negative BOLD correlates in the association cortices of the frontal and parietal lobes beginning before and ending after the IED (duration: 12 s in IGE, 4 s in FLE). Additionally, the patient with IGE showed positive BOLD correlates 10 s prior to IED in the brainstem, evolving to a bilateral thalamic response from 8 to 0 s prior to the IED, whereas positive BOLD correlates were delineated in the cortex drained by the DVA 4 s prior to IED until 1 s after IED in the patient with FLE.
Conclusions: A pattern of brain activity that is temporally linked to brief interictal epileptic activity has been depicted in two patients with bilateral synchronous discharges. As a common pathway of propagation of epileptic activity, widespread cortical deflection resembling a default mode network evolves along physiological brain networks. Corresponding to the pathophysiologic concept of "centrocephalic crosstalk" in the patient with IGE, a thalamo-reticular network has been observed, whereas a focal onset of brain activity emerging from the delineated lesion was depicted in the patient with lesional FLE.
This study was supported in part by grant 33CM30-124089 "Imaging large scale networks in epilepsy" from the Swiss National Science Foundation.

14

Safety and efficacy of prolonged mitoxantrone therapy

C. Zecca, C. Limoni, C.L. Bassetti, C. Gobbi
Ospedale Civico Lugano, Lugano, Switzerland

Introduction: Mitoxantrone (MTX), a DNA-topoisomerase II inhibitor, is an effective first line drug for patients with malignant form of MS and a second line treatment for patients with worsening relapsing remitting MS (RRMS) or secondary progressive MS (SPMS) unresponsive to interferon beta or glatirameracetate therapy. Unfortunately, its long term employment is limited by potentially severe side effects, both dose-related and unrelated. Therefore, the vast majority of the studies supporting MTX employment in clinical practice are related to 6 months to maximal 2 year protocols of treatment. The aim of this study is to evaluate safety and efficacy of prolonged (over 2 years) MTX regimens.
Methods: Data source is the MS-registry of Ospedale Civico Lugano; all consecutive patients with worsening relapsing-remitting (RR)-MS or secondary progressive (SP)-MS treated with MTX for a minimum of 36 months since 1999 to 2009 were included. Patients were treated and followed according to the hospital internal guideline for MTX employment. Safety, tolerability and clinical/radiological measures were evaluated. Data were compared by Wilcoxon signed rank test, One sample Wilcoxon signed rank test and One sample binomial test when applicable.
Results: Twelve among 254 (4 RR, 8 SP) patients were treated with MTX for at least 36 months (median treatment duration 49.5 months) and followed for a median period of 69.5 months. Patients received a mean cumulative dose/m2 body surface of 121.8 ± 14.31. No major cardiac, oncologic nor internistic side effects were reported. After 3 years on treatment (OT) we observed no mean EDSS progression (0 ± 0.8, p = 0.861 NS). Annual relapse rate (ARR) OT was significanly lower than ARR before MTX initiation (1.41 ± 1.3 and 0.57 ± 0.57, respectively; p = 0.043). Mean number of Gd enhancing lesions was not significantly decreased after 3 years (1.56 ± 2.3 at BL and 0.1 ± 0.3 after three years OT, p = 0.13 NS); there was no significant increase in T2 lesion number after 3 years OT (mean number of new T2 lesions 1 ± 1.3, p = 0.13 NS).
Conclusion: This retrospective study suggests that MTX is effective, well tolerated and safe in MS patients also for a treatment duration over 2 years. Based on this study low/delayed MTX regimens can be considered for patients without any other therapeutic options.

15

Spike triggered reaction-time-EEG, an assessment tool for driving ability?

H.E. Krestel, C. Liechti, A. von Allmen, A. Mosbacher, J. Mathis
Inselspital, Bern, Switzerland

Introduction: Epileptic seizures at the steering wheel are a rare but critical cause of traffic accidents. Interictal epileptic activity (IEA) can cause transitory cognitive impairment, as assessed in neuropsychological tests [1]. Its impact on driving has not been extensively tested [2, 3], although guidelines often require an EEG compatible with the ability to drive. We set out to analyze the impact of IEA on reaction time in a pilot study with the perspective to establish an easy to handle tool in the routine EEG, allowing a validated judgement on the ability to drive.
Methods: So far, 9 patients in the age of 18 to 70 yrs were included. Four had absences, 3 idiopathic epilepsy with tonic clonic seizures, 2 unclassified epilepsy with generalized seizures. They all showed intermittent generalized IEA. Spike detection software (VIASYS) recognized IEA and triggered either a single light flash or an obstacle in the Java-modified Steer Clear Test (Healthdyne) ("go signals"). In the pilot experiments, he or she was instructed to press a button as rapidly as possible after the flash. In the driving simulator experiments, IEA triggered in a driving lane the appearance of an obstacle. The patient was instructed not to hit it with his virtual car by pressing a button. Reaction time (RT) was defined as the interval between the go-signal and the push of the button. RT during normal EEG served as internal control. Mean RT ± SD during IEA were compared to control by using the Wilcoxon-Mann-Whitney-Test. IEA were divided into 3 groups: classical and atypical spikes and sharp theta waves.
Results: In the flash test, RT during any type of IEA (443 ± 308 ms, n = 159) was significantly longer than RT during control (310 ± 101 ms, n = 200; p = 0.034). RT during IEA with classical spikes (674 ± 407 ms, n = 68) was significantly longer than control (332 ± 96 ms, n = 94; p <0.001), too. RT during atypical spikes (331 ± 132 ms, n = 120) was not different from control (305 ± 97 ms, n = 57; p = 0.95). During sharp theta bursts, RT (252 ± 52 ms, n = 12) did also not differ from control (228 ± 60 ms, n = 21; p = 0.21). In the driving simulator, performed in 3 patients so far, RT during any type of spikes was with 558 ± 53 ms significantly longer than during control (511 ± 62 ms, n = 52; p = 0.04). Conclusions: preliminary measurements showed that RT were prolonged during classical spikes, but not necessarily during less organized IEA. More patients are planned and RT at different time points during IEA will be assessed.
References: 1. Aarts J. Brain 1984. 2. Berkovic S. Med Law. 2000. 3. Kasteleijn D. Electroencephalogr Clin Neurophysiol 1987.

16

Validation of Copeptin as prognostic marker in ischemic stroke

G. M. De Marchis[1], M. Katan[2], A. Weck[1], H. P. Mattle[1], C. Breckenfeld[1], Ph. Schütz[2], Ch. Foerch[3], M. Seiler[4], F. Hein[4], J. Papassotiriou[4], M. Christ-Crain[2], M. Arnold[1]
[1]Inselspital, Bern, Switzerland, [2]University Hospital, Basel, Switzerland, [3]Goethe University, Frankfurt, Germany, [4]B. R. A. H. M. S., Hennigsdorf-Berlin, Germany

Objectives: The rapid and reliable estimation of prognosis in ischemic stroke is pivotal to optimize clinical care. In a recent study we demonstrated that Copeptin is a new accurate prognostic marker in ischemic stroke. This ongoing study aimed to validate Copeptin as prognostic marker in ischemic stroke.
Methods: Data of the first 198 patients with ischemic stroke who were consecutively admitted to the emergency department of the Inselspital Bern were analysed. On admission, severity of ischemic stroke was assessed by the National Institute of Health Stroke Scale (NIHSS). In all patients, Copeptin levels were measured within 24 hours of symptom onset and compared with outcome after 3 months as assessed with the modified Ranking scale (mRS).
Results: Of the 198 patients with ischemic stroke, 34% patients were female and the median age was 67 years. The median NIHSS was 5 (interquartile range [IQR] 2-14), and 61 patients (30.1%) had an unfavorable outcome (mRS >2). Copeptin levels on admission were higher in patients with an unfavorable outcome compared to those with a favorable outcome (31.9 pmol/l , IQR 15.2–76.6 versus 9.25 pmol/l, IQR 4.8–27.2, p <0.0001). After multivariate logistic regression analysis adjusted for age (OR of 1.06 [95% CI 1.03–1.10]) and NIHSS (OR of 1.19, 95% CI 1.11–1.26)), Copeptin remained an independent predictor for unfavorable outcome with an OR of 2.29 (95% CI 1.11–4.73, p = 0.02).
Conclusion: Elevated Copeptin levels measured on admission were independently associated with an unfavorable outcome three months after ischemic stroke. Our data strengthen the value of Copeptin as an independent prognostic marker in ischemic stroke.

17

5-Aminolevulic Acid Guided Partial Bone Flap Resection for Meningeomas with Cranial Invasion

S. Marbacher, D. Coluccia, O. Tomasi, H. Landolt, J. Fandino
Department of Neurosurgery, Aarau, Switzerland

Introduction: Photodynamic diagnosis (PDD) using 5-Aminolevulic Acid (5-ALA) is widely accepted for resection guidance of malignant gliomas. Recently studies demonstrated the feasibility of PDD in excising intracranial meningeomas. To date cranial involvement and the extent of bone resection is determined by preoperative imaging and intraoperative conventional white light inspection. We present our preliminary experience of PDD guided resection of meningeomas with cranial invasion.
Methods: Intra-operative PDD using 5-ALA was performed on three bone flaps in three patients affected by meningeomas with preoperative signs of cranial invasion. Intraoperative extent of resection was determined by clear fluorescence and encircled with a sterile marker. The selected area was verified under white light and excised. Additional drilling at the resection boarder was performed until residual fluorescence disappeared in the surgical field. Histopathological examination verified the extent of tumor invasion. The partial bone flap defect has been reconstructed using intraoperative template molded polymethylmethacrylate (PMMA) implants.
Results: High fluorescence was confirmed in all affected bone flaps. The extent of tumor invasion determined using 5-ALA (mean: 19.7 ± 3.1 cm^2; range: 17.2–23.5 cm^2; n = 3) exceeded that of white light examination in all cases. The consistency of tumor invasion determined by PDD using 5-ALA was confirmed by histological examination. Two tumors were diagnosed as atypical meningeoma (WHO Grade II) and one as well-differentiated meningeomas (WHO Grade I). Intraoperative partial bone flap reconstruction of excised tumor areas resulted in excellent cosmetic outcome.
Conclusion: PDD using 5-ALA is a convenient tool to determine the often difficult boundary between normal bone and tumor tissues. This small case series demonstrates that 5-5-ALA guided resection for meningeomas with cranial invasion may result in more radical tumor removal with increase of recurrence-free prognosis. Partial bone flap reconstruction of the tumor defects by intraoperative template molded PMMA is an accurate and inexpensive method that results in excellent cosmetic outcome.

18

Chronic subdural hematomas treated by burr-hole trepanation and subperiostal drainage system

W. Zumofen[1], Regli[2], Levivier[3], Krayenbühl[4]
[1]Neurochirurgie, Basel, Switzerland, [2]Neurochirurgie, Utrecht, Switzerland, [3]Neurochirurgie, Lausanne, Switzerland, [4]Neurochirurgie, Zürich, Switzerland

Objective: Most symptomatic chronic subdural hematomas are treated by subdural drainage. However, a subperiostal (i.e., extracranial) passive closed-drainage system in combination with double burr hole trepanation is used at our institution. Therefore, we wanted to analyze our results and compare them with the alternate treatment strategies reported in the current literature.
Methods: In a retrospective single-center study, we analyzed the data of all patients undergoing double burr hole trepanation with a subperiostal passive closed-drainage system. Data analysis included general patient data, complications, postoperative seizure rate, and outcome.
Results: One hundred forty-seven patients underwent surgery for 183 symptomatic chronic subdural hematomas. The perioperative mortality rate was 3.4%. Hematoma persistence or recurrence occurred in 13.1% of the cases. The postoperative seizure rate was 6.6%, and the infection rate was 1.6%, including 3 cases of superficial wound infection and 1 case with deep infection. The reintervention rate was 9.3%, including trepanation in 8.2% of the patients and craniotomy in 1.1%. The overall complication rate was 10.9%.
Conclusion: Double burr hole trepanation combined with a subperiostal passive closed-drainage system is a technically easy, highly effective, safe, and cost-efficient treatment strategy for symptomatic chronic subdural hematomas. The absence of a drain in direct contact with the hematoma capsule may moderate the risk of postoperative seizure and limit the secondary spread of infection to intracranial compartments.

19

Clinical benefit of a combined surgical and imaging suite based on flat-panel technology for neurovascular surgery

M. Kotowski, B. Schatlo, M. Jaegersberg, Ph. Bijlenga, E. Tessitore, K. Schaller, V. Pereira
Hôpitaux Universitaires de Genève, Genève, Switzerland

Objective: We report our preliminary experience of a prospective series of patients who underwent neurovascular interventions in a combined imaging, endovascular and surgical suite which allows for diagnostic as well as intraoperative imaging (CT and 3-D rotational angiography).
Methods: We combined recent Flat-Panel technology (Philips Allura Xper FD 20) with a sterile surgical and neurointerventional environment. It allows for combined neurointerventional and surgical approaches with intraoperative high-speed CT-like imaging and intraoperative 3-D rotational angiography (up to 620 projections along 240∞ in 8–10 sec, rotational speed: 30∞/55∞/s, 30 frames/sec), automated segmentation of vascular structures and intraoperative update of a frameless navigation system (Brainlab VectorVision II). The impact of intraoperative imaging on treatment strategy, workflow and feasibility of this setup was evaluated using a prospective database.

Results: Since February 2008 69 patients underwent combined neurointerventional and surgical neurovascular procedures (50 aneurysm patients, 19 arteriovenous malformations (AVMs)). In all cases intraoperative 3-D RA has been performed. 50 patients harboring 62 aneurysms underwent aneurysm clipping with an intraoperative 3-D rotational angiography for clip position control. 16% (n = 8) of patients have been reclipped due to incomplete clipping/neck remnant of the aneurysm (n = 10) or parent vessel stenosis (n = 2) leading to one intraoperative superselective thrombolysis. A 100% occlusion rate was achieved. 19 patients underwent combined neurointerventional and surgical approaches for treatment of AVMs. In 15.7% (n = 3 patients) intraoperative 3-D RA has led to additional resection of AVM remnants. We achieved complete exclusion rate of 100%.
Conclusion: A combined neurointerventional suite based on flat-panel technology is of particular value for treatment of cerebral aneurysms and AVMs. It improves the overall management of neurovascular surgery in terms of the (peri-) interventional workflow, and by preventing the necessity for extraoperatvie angiographic control with potential revision in a second operation.

20

Complex Bi-Lobular, Bi-Saccular, and Broad-Necked Microsurgical Aneurysm Formation in the Rabbit Bifurcation Model for the Study of Upcoming Endovascular Techniques

S. Marbacher[1], S Erhardt[1], D. Coluccia[1], J.A. Schläppi[3], L.K. Boxheimer[2], L. Remonda[2], J. Fandino[1]
[1]Department of Neurosurgery, Aarau, Switzerland,
[2]Deparment of Neuroradiology, Aarau, Switzerland,
[3]Department of Neursurgery, Bern, Switzerland

Introduction: Despite rapid progression of material and technique for endovascular intracranial aneurysm treatment, occlusion of large broad-necked aneurysms remains a challenge. Complex aneurysms configurations are especially at risk for incomplete occlusion, aneurysm recanalization, regrowth, and rerupture. Animal models featuring such complicate aneurysm geometries are needed to test endovascular innovations and train interventionalists.
Methods: Complex venous pouch aneurysms were surgically formed at an artificially created bifurcation of both common carotid arteries in nine adult female New Zealand rabbits. The aneurysms were evaluated using two-dimensional intra-arterial digital subtraction angiography (DSA) and contrast-enhanced three-dimensional 1.5-T magnetic resonance angiography (MRA). Operation characteristics including operation time and number of interrupted sutures were recorded.
Results: The aneurysm length, aneurysm width and neck width measured with DSA correlated with the measurements performed in 3D-1.5-T MRA. The mean aneurysm volumes measured with CE-MRA were 88.7 mm^3, 115.3 mm^3, and 95.6 mm^3 in bi-lobular, bi-saccular, and broad necked aneurysms, respectively. The mean operation time was 245 minutes (range 175 to 290 minutes). On average of 32 interrupted sutures (range 27–36) were needed to create the aneurysms.
Conclusion: This study demonstrates the feasibility of microsurgical creation of complex aneurysm in the rabbit venous pouch bifurcation model. Created aneurysm neck, dome and volume of bi-lobular, bi-saccular and broad necked aneurysms are wider than described in other studies. These new complex aneurysm formations are a promising tool for in-vivo animal testing of new endovascular devices.

21

CSF containing cystic lesion of the clivus – Case report of an exceedingly rare pathology

D. Bellut[1], D. Holzmann[2], G. de Alba Buenrostro[3], R.L. Bernays[1]
[1]Department of Neurosurgery, University Hospital Zurich, Zurich, Switzerland, [2]Department of Otorhinolaryngology, University Hospital of Zurich, Zurich, Switzerland, [3]Instituto Mexicana del Segura Social, Unidad Medica de Alta Especialidad, Guadalajara, Jalisco, Mexico

Introduction: Lesions of the clivus include meningiomas, chordomas, metastatic lesions, chondrosarkomas and pituitary adenomas. Cystic lesions of the clivus are mainly chordomas. Only some cases of meningoceles, metastases and pituitary adenomas have been described.
Case report: A 65 year old female patient for surgical treatment of an extended cystic lesion of the clivus incidentally diagnosed with MRI. MR imaging showed an extended cystic lesion of the clivus without connection to the CSF system and without contrast enhancement. The preoperative CT scan showed massive erosion of the clivus. Due to the preoperative findings it was diagnosed as a clivus chordoma. A biopsy was performed using a transnasal endoscopic approach. Opening of the clivus lead to loss of CSF. The cytological and histopathological diagnostics were in accordance with a CSF containing membranous cystic lesion of the clivus. Postoperative the patient developed CSF rhinorrhea, underwent surgery and the CSF leak could be closed. Three months after second surgery the patient was seen for follow-up and reported no signs of CSF rhinorrhea, was neurologically healthy and the CT scan showed complete removal of the lesion.
Results/Discussion: CSF containing cystic lesions of the skull are rare. They have mostly been reported after head trauma with skull fracture. To our knowledge no cases of CSF containing cysts of the clivus have been reported in the literature. A spontaneous CSF rhinorrhea could have occurred in our case. There are only five cases published in the literature with spontaneous transclival CSF rhinorrhea. None of those five previously reported cases presented with massive erosion of the clival bone as in our case. Another often discussed reason for spontaneous CSF rhinorrhea is the lateral craniopharyngeal canal. The published cases of CSF rhinorrhea due to the presence of this canal are connected with sphenoid sinus CSF leaks and not with transclival CSF leaks. There are cases of meningoceles through this canal leading to bony destruction but no involvement of the clivus as in our patient has been described.
Conclusion: Our case with an intraclival CSF containing cyst is exceedingly rare and could be misdiagnosed. Endoscopic resection and closure helped to seal the CSF fistula and establish the diagnosis. In cases of unclear cystic clival pathologies follow-ups might be a better choice of treatment as surgery has a high risk of CSF rhinorrhea.

22

Elective surgery for unruptured intracranial aneurysm in a non-university neurosurgical unit

M.A. Seule[1], M.N. Stienen[2], O.P. Gautschi[1], H. Richter[1], J.Y. Fournier[1], R. Heilbronner[1], G. Hildebrandt[1]
[1]State Hospital St. Gallen, St. Gallen, Switzerland,
[2]Ruhr-University Bochum, Bochum, Germany

Introduction: Treating patients with unruptured intracranial aneurysms (UIAs) depends on the risk of aneurysm rupture compared with the risk of treatment. The goal of this study was to delineate the operative risk from elective surgery in patients with UIAs in a non-university neurosurgical unit.
Patients and methods: Between January 1999 and November 2009 a total of 391 patients with intracranial aneurysms were treated by surgical clipping. Among them 44 patients harbouring 71 UIAs were included in this analysis. Patient data were categorized into conditions leading to the diagnosis of UIAs, aneurysm characteristics and 3-month outcome using the modified Rankin scale (mRS).
Results: The annual caseload of patients with aneurysm surgery was 36 + 8 per year. A total of 44 patients demonstrated 71 UIAs with multiple aneurysm location in 36% (n = 16). The mean age was 55 +12 years with a female/male ratio of 3:1. Conditions leading to diagnosis were history of subarachnoid hemorrhage (9%), intracranial aneurysm syndrome (9%), evaluation of headache/vertigo (36%) and others (46%). Sixty-two out of 71 UIAs were treated by clipping (n = 58) or wrapping (n = 4) procedure. Mean aneurysm size was 7.8 + 3 mm and location was exclusively in the anterior circulation. Outcome three month after elective surgery was evaluated in 39 of 44 patients up to date. Thirty-six patients (92.3%) showed no significant disability (mRS 0-1), two patients (5.1%) showed persistant focal deficits (mRS 2) and one patient (2.6%) suffered from severe surgery unrelated contralateral intracerebral hemorrhage leading to hemiparesis (mRS 4). The perioperative mortality rate was 0%.
Conclusions: Elective surgery of UIAs can be performed safely with low morbidity and no mortality rate in a non-university hospital. The effect of surgery on cognitive dysfunction has to be evaluated in further studies.

23

Fate of tumor remnants after surgery for vestibular schwannoma

A.K. Jetzer[1], L. Mariani[2]
[1]Neurochirurgische Klinik, Inselspital, Bern, Switzerland,
[2]Neurochirurgische Klinik, Universitätsspital, Basel, Switzerland

Introduction: Total resection is the gold standard of treatment for large vestibular schwannomas. The risk of postoperative neurological deficits increases with the size of the tumor and is mainly due to dissection of the last remnant of the tumor capsule from the brain stem and from the facial nerve. A strategy of subtotal tumor removal may be advantageous in selected cases, because tumor remnants may remain stable or shrink over time and because stereotactic radiosurgery may be used as an adjuvant or a salvage treatment for residual or progressive disease. We describe the fate of residual vestibular schwannoma after a less than complete resection.
Methods: We retrospectively evaluated vestibular schwannoma cases between 01/00 and 12/07 with proven residual tumor on postoperative MRI. The tumor volume of preoperative, postoperative and follow-up scans was measured. Tumor volume of the follow-up exams was compared to postoperative volume of the residual tumor and considered as progressive tumor if tumor growth was >25% and regressive if follow-up tumor volume was reduced by >25%.
Results: 40 cases were included in the study. The mean preoperative tumor volume was 8769 mm^3. The mean postoperative tumor volume was 1734 mm^3 after surgery, 1480 mm^3 at 1 year F/U and 1503 mm^3 at last follow-up (mean 36.2 months). At the 1-year F/U four patients 4(12.2%) showed tumor progression, 13(39.4%) showed stable disease and 16 (48.5%) showed tumor regression. At last follow-up (mean 36.2 months) 7 (17.5%) showed progression, 12(30%) were stable and 21(52.5%) showed regressive disease. Stable or regressive disease at last follow-up was significantly associated with larger preoperative tumor volumes. Age, gender and postoperative tumor volume were not significantly different between the different groups.
Conclusion: Most tumor remnants after resection of large vestibular schwannomas do not progress within the first years after surgery.

24

Improved microsurgical creation of venous-pouch arterial-bifurcation aneurysms in rabbits

C. Sherif[1], S. Marbacher[1], S. Erhardt[2], H. Plenk[3], J. Fandino[1]
[1]Dept. of Neurosurgery, Cantonal Hospital of Aarau, Aarau, Switzerland, [2]Dept. of Intensive Care Medicine, University of Berne, Berne, Switzerland, [3]Division of Bone and Biomaterial Research, Institute of Histology and Embryology, Medical University of Vienna, Vienna, Austria

Background and purpose: Choice of the experimental aneurysm model is essential for valid embolization device evaluations. The use of the rabbit venous-pouch arterial-bifurcation aneurysm model was so far limited by demanding microsurgery, low aneurysm patency rates and high mortality. This study aimed to facilitate microsurgery and to reduce mortality by optimized peri-/postoperative management.
Methods: Under general intravenous anesthesia aneurysms were created in 16 New Zealand White Rabbits. Using modified microsurgical techniques, a jugular vein-pouch was sutured into a bifurcation created between both common carotid arteries. Aggressive anticoagulation (intraoperatively i.v.: 1000 IU heparin, 10mg acetylsalicylic acid/kg; postoperatively s.c.: 14 days 250 IU/kg heparin/day) and prolonged postoperative analgesia (fentanyl patches: 12.5 μg/h for 72 h) were applied. Angiographic and histomorphologic characteristics of created experimental aneurysms were assessed.
Results: Reduced number of interrupted sutures and aggressive anticoagulation caused no intra-/post-operative bleeding, resulting in 0% mortality. Four weeks postoperation, angiography showed patency in 14 of 16 aneurysms (87.5%) and Oshima Type B bifurcation geometry. Mean values of parent artery diameters (2.3 mm), aneurysm-lengths (7.9 mm) and neck-widths (4.1 mm) resulted in a mean 1.9 aspect ratio. Histomorphologically, the venous pouch resembled closely human aneurysm walls. Only a benign foreign-body response to non-resorbable sutures at the vascular anastomoses was observed.
Conclusions: Venous-pouch aneurysm model creation in rabbits was substantially improved by facilitated microsurgical procedures, aggressive anticoagulation and analgesia, resulting in high aneurysm patency rates and low mortality. Favorable histological features and hemodynamics of true arterial-bifurcation aneurysms are well comparable to the majority of human aneurysms with high rupture risks.

25

Intraoperative Neurophysiological Monitoring in Neurosurgery – Motor Evoked Potentials for Brain and Spinal Cord Surgery

K.F. Kothbauer
Luzerner Kantonsspital, Luzern, Switzerland

Background: Intraoperative neurophysiological monitoring is now a requirement for a growing number of complex procedures involving the spinal cord, the brain or the brainstem. Motor Evoked Potential (MEP) monitoring is the most useful monitoring modality. MEP use in spinal cord surgery or aneurysm surgery best exemplify the benefit from these techniques to the surgeon and the patient.
Neurophysiologic methods: Motor potentials are evoked by either transcranial or direct electrical motor cortex stimulation. A “single stimulus technique” evokes D-waves recorded from the spinal cord. The “multipulse (or train) stimulation technique” evokes electromyographic responses in upper and lower extremity muscles, optimally from the thenar, hypothenar, tibialis anterior, and flexor hallucis brevis muscles. D-wave monitoring measures the peak-to-peak amplitude. For muscle MEP monitoring, the presence or absence of the response regardless of the stimulation intensity needed is measured for spinal cord surgery, and an amplitude reduction of 50% from baseline is measured for intracranial surgery.
Results: Interpretation of MEPs is reasonably fast and simple. Pre- and postoperative clinical motor findings correlate with intraoperative D-wave and MEP results. Thus correct prediction of the clinical status at any time during an operation is possible with a high accuracy. The sensitivity of muscle MEPs for postoperative motor deficits is nearly 100%, its specificity is about 90%. Thus MEP data indeed reflect the clinical “reality”. Present and stable recordings document intact motor pathways and allow the surgeon to confidently proceed with the operation. Loss of muscle MEPs and/or decrease of the D-wave amplitude together constitute a “window of warning”. It reflects a pattern of MEP change which represents a reversible injury to the motor pathways of the spinal cord. Clinically this is represented by a transient paraparesis or some other pattern of transient motor deficit of short (days) duration. Therefore the surgical strategy can be changed before an irreversible damage has occurred! Surgical actions during spinal cord operations may be waiting briefly for the recordings to recover by themselves, irrigation of the resection cavity with saline solution to wash out potassium, which blocks axonal conduction, increasing the blood pressure to improve perfusion. Even a staged resection is acceptable if intraoperative measures do not improve the recordings. Surgical interventions during brain surgery, particularly neurovascular operations usually include removal of retractor blades, elevating blood pressure and particularly correcting vascular clip placement.
Conclusion: Modern neurophysiologic techniques have become part of the tool-set used by neurosurgeons to continuously monitor the integrity of neural pathways during surgery on the brain and the spinal cord. Motor evoked potentials are particularly useful for this purpose.

26

Intrathecal Morphine analgesia after cervical and thoracic spinal cord tumor surgery – An observational pilot study

K.F. Kothbauer, B. Poblete, C. Konrad
Luzerner Kantonsspital, Luzern, Switzerland

Background: Resection of intramedullary tumors of the spinal cord frequently includes extensive incision of spinal muscles and a multilevel laminectomy. Postoperative intravenous opioid analgesia, even patient controlled analgesia may sometimes not achieve sufficient pain control. Intrathecally administered morphine provides effective pain control. it is commonly injected at lumbar levels for chronic pain treatment. To our knowledge it has not been used at thoracic or cervical levels. After intradural

surgery, morphine could easily be injected locally at the end of dural closure. Since highest morphine levels be achieved locally at the surgical site segments we postulated that this route of morphine administration would improve pain control when compared to patient controlled analgesia. Since all patients remain in the intensive care unit postoperatively this new pain treatment would be safe and it's effects could be well documented. The aim of the study was: – to improve postsurgical pain after cervical and thoracic spinal cord operations, – to demonstrate the safety of thoracic and cervical intradural application of morphine.
Materials and methods: Nine consecutive patients who underwent resection of intramedullary spinal cord tumors were studied. Informed consent was obtained. The study was approved by the institutional review board. Total intravenous anesthesia with propofol, remifentanil and ketamine was used for surgery. Before finishing the dural closure 7 mg/kg BW morphine was given via a microsurgically prepositioned intrathecal catheter which was then withdrawn with the final dural stitch. All patients were extubated in the operating room and kept in the ICU for routine postoperative monitoring. Basic analgesia with acetaminophen and metamizol was given. Intravenous morphine was added as needed. Tropisetron was given for PONV prophylaxis. Visual analog scale (VAS), blood pressure, respiratory rate(RR), oxygen saturation(SaO_2), amount of additional iv morphine given, side effects were noted at 1, 2, 4, 6, 8, 10, 12, 16, 20, 24, 48, 72 h postsurgery.
Results and discussion: (required): Six patients (7–75 years, mean 41 y) received injection at cervical (C3-C7), 3 at thoracic levels (Th2-Th12). Mean VAS was highest upon arrival at the ICU (2 of 10), mean value over the time was 1. Mean dose of additional iv morphine was 0.29 mg. Mean RR was 16. RR 8/min without changes in SaO_2 was recorded in 1 patient at 8 h. Four other patients had their RR drop below 10 at least once. After 12 h all patients had RR >10/min. Nausea and vomiting was observed in one patient, and pruritus in one patient on day 1.
Conclusion: Morphine can be given intrathecally at cervical and thoracic leveln after intramedullary surgery. It provides excellent analgesia with few side effects. Administration is save if patients are observed at an intensive care unit.

27

Invasion and migration of rat fetal and adult neural stem cells is dependent on the dorsoventral identity

M. Sailer[1], M.F. Ritz[1], A. Gerber[1], J.L. Boulay[1], G. Hutter[1], M.E. Schwab[2], R.D. McKay[3], L. Mariani[1]
[1]Neurosurgical Clinic, University Hospital of Basel, Basel, Switzerland, [2]Brain Research Institute, University of Zurich, Zurich, Switzerland, [3]National Institute of Neurological Disorders and Stroke, NIH, Bethesda, United States

Introduction: Neural stem cells (NSCs) are self-renewing cells with the capacity to differentiate into multiple cell types of the central nervous system. Much attention has been focused on the differentiation potential. It is however largely unclear which factors are involved in the induction of migration and invasion in neural stem cells. These factors are both relevant for appropriate migration of neural stem cells to injured lesions and are most probably altered in brain tumors.
Methods: E14.5 rat fetal and adult rat neural stem cells and fetal explants were exposed to a systematic series of conditions possibly relevant for migration and invasion. Migration and invasion was evaluated with in vitro observation, migration and invasion assays and RNA, protein expression.
Results: Here we find that stem cells in the proliferative zone of the cortex are mostly stationary. In contrast Fibroblast growth factor 2 (FGF2)-expanded NSCs are migratory, but show almost no potential to cross basal membranes. We were able to correlate this migratory phenotype with a ventral identity, i.e. from the medial ganglionic eminence. FGF2 and Epidermal growth factor (EGF) in combination caused NSCs to cross a 8 micrometer basal membrane assay. Further, FGF2 together with Bone Morphogenetic Protein 4 (BMP4) induced a highly invasive cell type easily crossing basal membranes. This latter phenotype could be correlated with a dorsal identity, i.e. hippocampal/choroid plexus and more dorsal with respect to the developing brain. The highly invasive phenotype (HIP) also expressed Snail1 and Snail2, two zinc finger transcription factors involved in the formation of neural crest cells and of mesoderm during embryogenesis. HIP induction by FGF2/BMP4 lead to the activation of beta-catenin, which forms part of the canonical Wnt-signaling pathway. The induction of a HIP was surprisingly also observed in adult NSCs. Our results show that the activation of FGF2/BMP4-signaling followed by Wnt-signaling forms the sequence of dorsalization with HIP induction in fetal and adult NSCs.
Conclusions: These results show that distinct factors are able to induce migration and invasion in neural stem cells. The ability of invasion is not restricted to early development but is readily available in adult neural stem cells. In our experiments the migration and/or invasion potential was not linked to the age of the cells, but to the dorsoventral position. We hypothesize that the same sequence of factors is used for brain repair and in tumor formation.

28

Long-term outcome and quality of life after cordectomy as treatment option for syringomyelia with tethered cord syndrome and myelopathy

O.P. Gautschi[1], C. Ewelt[2], M.A. Seule[1], M. Gores[1], H.J. Steiger[3], G. Hildebrandt[1], R. Heilbronner[1]
[1]State Hospital St. Gallen, Department of Neurosurgery, St. Gallen, Switzerland, [2]Westfälische Willhelms University, Department of Neurosurgery, Münster, Germany, [3]Heinrich-Heine-University, Department of Neurosurgery, Düsseldorf, Germany

Objective: Spinal cordectomy in paraplegic patient is a treatment option for the management of posttraumatic or other forms of syringomyelia, arachnopathy or tethering to manage spasticity, pain and ascending neurological dysfunction. However, there is a dearth of information concerning long-term outcome and quality of life.
Patients and methods: From February 2000 to December 2009, 18 spinal cordectomies were performed by one single surgeon (R.H.) at the Department of Neurosurgery, State Hospital St.Gallen. Indications were syringomyelia, tethered cord syndrome and arachnopathy with progressive spasticity and pain or neurological deficits of the upper limbs. Sixteen patients had a posttraumatic syringomyelia. One patient suffered from postoperative syringomyelia and one from calcifying arachnopathy after resection of a neurinoma or an ependymoma, respectively. All patients had progressive disease pattern. A follow-up with ASIA score, VAS score, Euroquol, Barthel Index, WHOQOL-BREF and quality of life (SF-36) score has been performed.
Results and conclusions: The data analysis (especially the quality of life) is at the date of the abstract submission deadline in progress and the complete set of data will be presented at the poster session of the 2010 Congress of the Swiss Federation of Clinical Neuro Societies. An interim analysis revealed that 14 patients showed stabilization or even a dramatic improvement in motor and sensory function. Four patients suffered from a persistent spasticity and 3 patients from slight deterioration in pain. There were no other surgical adverse events. Therefore, cordectomy can be considered in selected cases as a safe and useful instrument to preserve or improve functions of the upper extremities, spasticity and pain in patients with syringomyelia spinal cord tethering or arachnopathy of various aetiologies.

29

Low threshold motor mapping for complete resection of a primary motor cortex tumor without neurological deficits- a case report

K. Seidel, J. Beck, L. Stieglitz, A. Raabe
Department of Neurosurgery, Inselspital, University of Berne, Berne, Switzerland

Objective: Surgery within eloquent brain areas has always been discussed controversial because of the risk of inducing a permanent neurological deficit. We report about a case of a complete resection of a pleomorphe xanthoastrocytoma localized within the hand knob area of the primary motor cortex. The surgery was guided by low threshold motor evoked potential mapping. The patient had no postoperative neurological deficit.
Methods: Electrical stimulation for monitoring and monopolar mapping was performed with trains of five stimuli, with pulse duration of 500 μs within one pulse and an interstimulus interval of 4.0 ms. The motor threshold was defined as the stimulation intensity which elicited mMEPs from the target muscle of a minimum of 30 μV amplitude within four consecutive trails at a 0.5 Hz repetition rate.

Results: During resection the motor thresholds of the monitored muscles were stable. Monopolar motor mapping confirmed the close proximity to the primary motor area by measuring lowest motor threshold of 3 mA at the posterior part of the tumor cavity. Postoperatively the patient had no motor deficit. Early postoperative MRI showed complete resection of a histopathologically confirmed pleomorphe xanthoastrozytoma WHO grade II.
Conclusion: Surgical resection can be guided by the absolute values of motor threshold. There is probably a nonlinear relationship between stimulation intensity and distance to the critical motor structure. A threshold of 3mA in our case was not associated with a neurological deficit.

30

Meta Analysis of Patients Presenting with Acute Subdural Hematoma. Due to Ruptured Intracranial Aneurysm

S. Marbacher, O. Tomasi, J. Fandino
Department of Neurosurgery, Aarau, Switzerland

Objective: Acute subdural hematoma (aSDH) is a rare presentation of ruptured aneurysms. Fast decision-making is required to treat this life-threatening condition. The rarity of aneurysmal aSDH makes it difficult to establish reliable clinical guidelines. We performed a systematic review of clinical characteristics, diagnosis, and management of aSDH due to aneurysm rupture based on an extensive literature review. Based on this review, we propose a management flow chart.
Methods: The MEDLINE PubMed database was searched for journal articles published between 1990 and 2009 using combinations of the key words “acute subdural hematoma”, “subarachnoid hemorrhage”, and “cerebral aneurysm”. We considered all publications with two or more adult cases and detailed description of clinical characteristics and patient management. Recorded data included age, sex, initial clinical and radiological findings, diagnostic approach, intervention strategy, and outcome.
Results: Six English-language articles, with a total of 30 cases, were included in the analysis. Most of the patients were admitted with the worst SAH grade (WFNS Grade 5, n = 24) and with signs of uncal herniation. The main management strategies were urgent hematoma evacuation (n = 29), surgical aneurysm obliteration in the same procedure as urgent hematoma evacuation (n = 15), delayed coiling (n = 6), and delayed clipping (n = 5). All but two patients with fatal outcome (n = 8) were cardiopulmonary unstable during resuscitation. Favorable outcomes (GOS 5 and GOS 4, n = 18) outweighed poor outcomes (GOS 3 and GOS 2, n = 4).
Conclusions: Despite the rarity of the disease, a comprehensive management protocol can be defined by reviewing the clinical strategies used by several authors over the past 20 years. Rapid surgical decompression and aneurysm obliteration can result in favorable outcome irrespective of poor initial neurological presentation. However, patients who present in an unstable cardiopulmonary condition at the time of admission do not qualify for immediate surgery and seem to be exceptionally at risk of poor outcome.

31

Metabolic pathway of Superparamagnetic Iron Oxide Nanoparticles (SPIONs) for Sutureless Tissue Soldering and Hyperthermic Glioma Therapy – In-vivo Long Term Analysis

E. Schlachter[1], A. Bregy[1], I. Vajtai[2], A. Wirth Heller[3], T. Loennfors[6], P. Mordasini[6], G. Herrmann[4], V. Bernau[5], A. Petri Fink[5], H. Hofmann[5], A. Raabe[1], M. Reinert[1]
[1]Department of Neuosrugery, Inselspital Bern, Universitut of Bern, Bern, Switzerland, [2]Institute of Pathology, University of Bern, Switzerland, Bern, Switzerland, [3]Fachhochschule Nordwestschweiz, Muttenz, Basel-Landschaft, Muttenz, Switzerland, [4]Institute of Anatomy, University of Bern, Switzerland, Bern, Switzerland, [5]Ecole Polytechnique Fédérale de Lausanne, Lausanne, Switzerland, Lausanne, Switzerland, [6]Institute of Neuroradiology, Inselspital Bern, University of Bern, Bern, Switzerland

Introduction: The application of superparamagnetic iron oxide nanoparticles (SPION) for diagnostic procedures has gained wide acceptance in radiology practice, but therapeutic applications are still under investigation. Different uses apart from diagnosis of those SPIONs is based on two major advantages of iron oxides: their low toxicity to human beings and their high magnetization potential. If exposed to an alternating magnetic field, the harmless iron oxide particles become powerful heat sources by transforming the electromagnetic energy from the electromagnetic field into thermal energy which is heat. This heat transmission can be used either for the development of minimally invasive sutureless surgery or hyperthermia e.g. in glioma therapy. For these purposes we analyzed the pathway of SPIONs in an In-Vivo rat model using MRI, Histology and Electronmicroscopy over a period of 6 months.
Materials and methods: Different concentration of SPION were quantitatively analyzed in a 3T MR (Trio TIM, Siemens medical solutions, Erlangen, Germany) for their signal alteration (T2 relaxometry a multi-contrast spin echo (SE) sequence and R2*). A SPION-albumin complex, developed for tissue soldering, was implanted subcutaneuosly into the rat (n = 25 in three groups and followed up 6 month (1d, 3d, 15d, 4w, 3mt, 6mt) using MR-Tracking and histological analysis of local implant site, brain, liver, kidney, pancreas and spleen. Further electron microscopic analysis of the Kupffer cells of the liver and of the macrophages locally at the site of implantation was performed. Electromagnetically heated and non heated SPION-albumin complexes were studied seperately.
Results: MR-Tracking was useful for quantification and for spotting the local subcutaneous implantation. Tracking of SPIONs in the rest of the rat body gave no signal alterations and therefore showed that if particles were degraded, then below the very low and sensitive threshold of the MR apparatus. Further no pathological response was observed for all the investigated organs such as brain, liver or spleen. Liver changes in the number of Kupffer cells were found but completely identical in the SPION treated and sham-operated animals and most likely due to the trauma from surgery. Immune response initially showed more granulocytic infiltration in the non-heated and more macrophage-lymphocitic in the heated complex. Long term results showed good fibroblastic ingrowth of the implant and no foreign body reaction. The SPION-albumin complex is slowly reabsorbed over the observation period. All the rats were completely unaffected in their normal behaviour and food intake.
Conclusions: SPIONs used for tissue soldering or hyperthermic treatment can be used without any effect on the normal behaviour of rats. SPION-albumin complex is likely to be absorbed very slowly over time by the macrophage system and has no toxic effects on the brain, liver and spleen over a period of 6 month post implantation. Whole body MR Tracking of the SPION is below sensitivity and therefore unsuitable.

32

Morphological Evaluation of Bi-Lobular, Bi-Saccular, and Broad-Necked Microsurgical Aneurysms in the Rabbit Bifurcation Model

S. Erhardt[1], S. Marbacher[1], C. Sherif[1], L. Remonda[2], J. Fandino[1]
[1]Department of Neurosurgery, Aarau, Switzerland, [2]Department of Neuroradiology, Aarau, Switzerland

Introduction: Elastase induced aneurysm formation is the most frequently used experimental aneurysm model in rabbits. Limitations of this model include uncontrolled size of created aneurysms and controversial flow characteristics. The ability to vary the anatomy is a potential advantage of the microsurgical models. The aim of this work is to analyse the characteristics of three different new complex aneurysm constructions for the bifurcation model for bench testing of new endovascular devices.
Methods: Complex venous pouch aneurysms (reconstructed from lingual and facial veins) were surgically formed at an artificially created bifurcation of both common carotid arteries in New Zealand white rabbits. The aneurysm characteristics were evaluated using two-dimensional intra-arterial digital subtraction angiography (2D-DSA) and contrast-enhanced three-dimensional 1.5-T magnetic resonance angiography (3D-MRA). Measurements included aneurysm dome (length and width), aneurysm neck (neck width and neck/dome ratio) and aneurysm volume.
Results: A total of nine microsurgically created venous pouch aneurysms underwent analysis (5 bi-lobular, 2 bi-saccular, and 2 broad-necked). The overall mean neck width and aneurysm sac length of all complex aneurysms was 5.3 mm ± 1.7 mm and 8.0 mm ± 1.5 mm, respectively. The mean broad necked aneurysm width was notably broader with 7.0 mm ± 2.2 mm. The height of the saddle between the two lobes reached 5.7 mm ± 1.7 mm in bi-lobular and 6.9 mm ± 0.6 mm in bi-saccular aneurysms. There were no significant differences between 2D-DSA and 3D-MRA measurements.

Conclusions: There are only minor differences in spatial characteristics between bi-lobular and bi-saccular aneurysms. Broad-necked aneurysms do have significant different anatomical aneurysm architecture compared to bi-lobular and bi-saccular aneurysms. Our measurements confirm a good correlation between standard 2D-DSA and contrast enhanced 3D-MRA even in these complex aneurysm formations.

33

Multiple Extra- and Intradural Extra- and Intramedullary Ependymoma in the Thoracic and Lumbar Spine: Case Report

O. Tomasi, S. Marbacher, D. Coluccia, H. Landolt, J. Fandino
Department of Neurosurgery Kantonsspital Aarau, Aarau, Switzerland

Background: Spinal ependymomas, arising from ependymal cells lining the central spinal canal, are the most common glioma of lower cord, conus, and filum. Usually they are slow-growing with a natural long-history, benign, with a slight male predominance and a peak in 3rd to 6th decade. Half of spinal ependymomas are located intramedullary above the conus, and the other half occur in association with the terminal filum and the conus medullaris. Extradural and extramedullary manifestations are extremely rare. To the best of our knowledge, we present the first case of multiple intra- and extradural, intra- and extramedullary ependymoma of the thoracic and lumbar spine.
Case report: We present the case of a 35 year-old male presenting with left radicular pain and hypoesthesia L5 without motor deficits. The initial MRI and myelography demonstrated multiple intra- and extradural, intra- and extramedullar space occupying lesions at thoracic and lumbar spine at the levels Th4, Th5, L3, L4, and L5. The patient underwent a total of three surgeries for resection of the tumors at the thoracic and lumbar spine within a 1.5-year period. A total resection of the tumors could be achieved at level L1, L3, L4 and S1. The tumors in the thoracic levels were subtotally resected during a second and third surgery. The initial histological evaluation demonstrated an ependymoma WHO Grade II. Two months after the first surgery, a recurrent tumor at level L3 showed anaplastic changes and was classified as WHO III. Consequently, the patient underwent radiotherapy of the lumbar spine (LINAC; dose 4500 cGy, weekly fractioned à 300 cGy). Three years after diagnosis the patient's condition deteriorated, further therapies were refused, and the patient died.
Conclusions: We present a rare case of multiple spinal intra- and extramedular ependymoma of the thoracic and lumbar spine. Despite surgical treatment and radiotherapy in case of recurrence and anaplastic findings, the outcome is poor. This case evidenced that the outcome of spinal ependymomas might differ depending of its localization. Intradural ependymoma are usually associated with a better prognosis if totally resected. Extradural ependymoma might be associated with a higher risk of local recurrence even if total removal and radiotherapy is undertaken.

34

Multipotential pericytes in the rat spinal cord react to spinal cord compression injury

U. Graumann[1], M.-F. Ritz[2], B. Gutierrez[1], T. Janner[1], O.N. Hausmann[3]
[1]Swiss Paraplegic Research, Nottwil, Switzerland, [2]University Basel, Basel, Switzerland, [3]Hirslanden Klinik St. Anna, Lucerne, Switzerland

Introduction: Adult bone marrow (BM)-derived stem cells may contribute to vascular healing following spinal cord trauma. However, the reports from experimental transplantation studies are controversial in regard to the fate of these cells since there is indication that the stem cells give rise to pericytes but not to vascular endothelial cells. In order to elucidate the contribution of infiltrating putative endogenous BM-derived stem cells in vessel remodeling after spinal cord injury (SCI), we investigated their incidence in injured rat spinal cord tissues. In addition, the expression of angiogenic and arteriogenic factors was analyzed in a time-dependent manner.
Methods: The temporal appearance of circulating stem cells following spinal cord compression injury in rats was analyzed by immunohistology and RT-qPCR. Therefore, we investigated the expression of CD34, CD133, CXCR4, and the mobilization factor SDF-1. Blood vessel structures were visualized by stainings with Reca-1 and alpha-SMA. The expression of angiogenic and arteriogenic factors, e.g. VEGF, PDGF-BB, Ang-1, and PlGF was examined by RT-qPCR.
Results: The number of CD133 positive cells was markedly reduced 2 days post-SCI. The cells reappeared in the spinal tissues after 2 and 4 weeks of the experimental period. CD133 expressing cells colocalized with alpha-SMA and were identified as pericytes surrounding arterioles. Increasing amounts of CD34 positive cells coexpressing the macrophage/microglia marker CD11b emerged after 2 weeks post-SCI. The expression of SDF-1 was stimulated only after 3 weeks, while its receptor CXCR4 was overexpressed over a long period starting at 2 days after injury. VEGF, PDGF-BB, Ang-1, and PlGF expression was decreased with the lowest level at day 2 and 3 postinjury.
Conclusions: Our results show that resident CD133 expressing pericytes react to SCI, whereas no markers could be attributed clearly to BM-derived cells. The delayed induction of the mobilization factor SDF-1 may impede efficient neovascularization, since cavity formation has already been started 2 weeks post-SCI. The expression of factors involved in stabilization of blood vessels are negatively modulated. Disturbance of vessel integrity is a possible consequence of these modulatory effects during the phase of secondary injury after SCI.

35

Occurrence of depressive symtoms and findings of dti-imaging in patients with intracranial tumors

D. Bellut[1], A. Richter[3], Ch. Woernle[1], S. Kollias[2], H. Bertalanffy[1]
[1]Department of Neurosurgery, University Hospital Zürich, Zürich, Switzerland, [2]Department of Neuroradiology, University Hospital Zürich, Zürich, Switzerland, [3]Department of Psychiatry, University Zürich, Zürich, Switzerland

Introduction: Coping with severe illness, such as intracranial tumors, largely involves emotional factors. The epidemiology and intensity of depressive symptoms and anxiety has not been explored widely in those patients.
Methods: Patients with intracranial tumors were examined with BDI (Beck's Depression Inventory), State-Trait Anxiety Inventory (STAI) and Hamilton Depression Rating Scale (HAM-D). The results were correlated with the clinical findings (neurological examination, medical history) and the tumor characteristics (imaging, histology). In addition the patients received magnetic resonance imaging (MRI) studies with diffusion tensor imaging (DTI) and measurement of fractional anisotropy (FA) and apparent diffusion coefficient (ADC) in frontal association fibres as previous studies showed FA and ADC alterations in patients with certain types of depressions. This data was correlated with the depressive symptoms and the results of the anxiety scales.
Results: So far 60 patients have been included in the study. All patients showed different levels of anxiety. Depressive symptoms (BDI >18, HAM-D >17) were seen in 15% of the patients. Fifty-five patients underwent surgery, two received tumor embolization as treatment. There are histopathological findings for 55 patients. Most frequent diagnosis include Glioblastoma (38%), Meningioma (16%), Metastasis (12%) and Cavernoma (12%). First results from DTI imaging showed differences in patients with and without depressive symptoms regarding FA and ADC measured in certain regions of the prefrontal white matter.
Conclusions: In comparison to previous studies patients were examined with BDI, STAI, HAM-D and DTI. Depressive symptoms were found less frequently than expected and previously published in patients with intracranial tumors. Correlation of clinical findings, tumor characteristics and DTI might help to show structural changes in prefrontal white matter in patients with depressive symptoms.

36

Olfactory dysfunction in patients with Parkinson's disease is related to gray matter atrophy in regions of the olfactory cortex

B. Westermann[1], E. Wattendorf[2], P. Fuhr[3], L. Mariani[1], T. Hummel[4], A. Welge-Lüssen[5]
[1]Department of Neurosurgery, University Hospital, University of Basel, Basel, Switzerland, [2]Anatomy Unit, University of Fribourg, Fribourg, Switzerland, [3]Department of Neurology, University Hospital, University of Basel, Basel, Switzerland, [4]Smell and Taste Clinic, University of Dresden Medical School, Dresden, Germany, [5]Department of Otorhinolaryngology, University Hospital, University of Basel, Basel, Switzerland

Introduction: It is now widely accepted that early non-motor signs indicate pre-clinical stages of Parkinson's disease (PD) prior to the onset of motor symptoms. According to recent neuropathological staging concepts, impaired olfaction is assumed to indicate an early pathological process and might be associated with structural changes in primarily non-motor related brain regions.
Subjects and methods: Early PD patients (n = 15, median Hoehn and Yahr stage 1.5), moderately advanced PD (n = 12, median Hoehn and Yahr stage 2.5) and age-matched healthy controls (n = 17) participated in the study. Olfactory function was assessed in all subjects birhinally using the standardized "Sniffin' Sticks"' test battery (Burghart, Germany). According to the olfactory test, early and moderately advanced PD patients were hyposmic, whereas healthy controls were normosmic. A morphometric analysis of magnetic resonance images (voxel-based morphometry) was used to investigate gray matter atrophy related to psychophysically measured scores of olfactory function.
Results: In PD patients, but not in controls, cortical atrophy in olfactory-related brain regions correlated specifically with olfactory dysfunction. Positive correlations between olfactory performance and gray matter volume were observed in the right piriform cortex in early PD patients and in the right amygdala in moderately advanced patients.
Conclusion: The results provided first evidence that olfactory dysfunction in PD is related to atrophy in olfactory-eloquent regions of the limbic and paralimbic cortex. In addition, olfactory-correlated atrophy in these brain regions is consistent with the assumption that olfactory impairment as an early symptom of PD is likely to be associated with extranigral pathology.

37

Patency of Sacuclar, Broad-Necked, Bi-Saccular and Bi-Lobular Microsurgical Aneurysms in the Rabbit Bifurcation Model

S. Erhardt[1], S. Marbacher[1], C. Sherif[1], D. Coluccia[1], L. Remonda[2], J. Fandino[1]
[1]Deparment of Neurosurgery, Aarau, Switzerland,
[2]Department of Neuroradiology, Aarau, Switzerland

Background: The microsurgical venous-pouch arterial bifurcation model has potential advantages (ability to vary the aneurysm anatomy, favourable hemodynamic and histologic similarity to human intracranial aneurysms) compared to the rabbit elastase stump model. Long-term patency is a critical attribute of experimental models for bench testing of endovascular devices. Whereas the patency in the long-term natural course in elastase induced aneurysms is excellent, studies of patency of untreated microsurgical created aneurysms do not exist. Our purpose was to evaluate the patency of saccular, broad-necked, bi-saccular and bi-lobular microsurgical aneurysms in the rabbit bifurcation model.
Methods: Complex microsurgical aneurysms (14 saccular, 4 broad-necked, 7 bi-saccular, and 2 bi-lobular microsurgical aneurysms) were created in 27 female New Zealand white rabbits using venous pouches taken from the jugular vein and placed at the artificially constructed bifurcation. To prevent thrombosis a consequent intra- and postoperative anticoagulation (intraoperatively i.v.: 1000 IU heparin, 10 mg acetylsalicylic acid/kg; postoperatively s.c.: xx days 250 IU/kg heparin/day, xxmg, acetylsalicylic acid/kg) was performed. Patency was assessed by two dimensional intra-arterial digital subtraction angiography or three dimensional magnetic resonance angiography at xx days postsurgery.
Results: Of 27 successfully operated rabbits 21 had patent aneurysm after an average time of 37 (range 8–90) days between operation and patency control. Of the 6 animals which had thrombosed aneurysms, 2 were saccular (37 days), 2 broad-based (48 days), and 2 bi-lobular (30 days). There was only minor difference of the mean period between patent (35 days, range 8–90) and thrombosed (39 days, range 20–53) aneurysms.The complex aneurysm models showed a higher rate of occlusion, 33.3%, compared to 14.3% in the classic saccular model.
Conclusion: Compared to the rabbit elastase model and classic saccular models there is a higher rate of thrombosis. Good patency of microsurgical-created venous-pouch bifurcation aneurysm can be only achieved under strict peri- and postoperative anticoagulation regime. Despite the higher rate of spontaneous thrombosis, the complex angioarchitecture achieved with this model warrants an excellent opportunity to test new endovascular technologies.

38

Planning of cerebro-vascular surgery with a transformable Desktop-Laptop Virtual Reality Environment

R.A. Kockro[1], N. Krayenbühl[1], O. Bozinov[1], R. Bernays[1], C. Wess[1], D. Bellut[1], L. Serra[2], H. Bertalanffy[1]
[1]Department of Neurosurgery, University Hospital Zürich, Zürich, Switzerland, [2]National Neuroscience Institute, Singapore, Singapore

Introduction: Based on the technology of the Dextroscope, we have developed a stereoscopic, flat-panel neurosurgical planning station integrating a laptop which can be undocked and brought to the operating room for intra-operative viewing of the 3D planning data. We have applied this technology for the planning of 12 aneurysm-related surgical procedures.
Methods: The system includes a monitor which allows displaying polarized stereoscopic data. Wearing polarized glasses the user interacts with the 3D data by working with hand-held, tracked instruments in a virtual 3D workspace. The system enables the fusion, segmentation and simultaneous multimodal display of imaging data. A set of software tools accessible within the virtual workspace allows MRI or CT based segmentation of any structure. Surgical planning tools enable the simulation of tissue removal to define a surgical corridor. The system runs on a laptop which can be undocked to allow viewing and working with the 3D planning scenario in the operating room.
Results: Using this system for the planning and discussion of aneurysm surgery resulted in an efficient way to understand the complexity of anatomical and pathological spatial relationships. The anatomy of the aneurysm itself, the parent vessel, the aneurysm neck, neighboring vessel branches, adjacent cranial nerves and the skull base could be studied. During surgery the system's viewpoint could be adjusted to the surgical viewpoint and hence the interactive visualization of the anatomy of the aneurysm helped to anticipate the clip's position. To improve the mode of interaction with detached laptop we are currently working on an intra-operative 3D user interface.
Conclusion: The stereoscopic display of complimentary 3D imaging information embedded in a virtual work space provided an effective platform for preoperative planning. The interactive display of the surgical plan on a laptop in the operating room allowed seeking additional orientation during critical parts of surgery. The system may help to diminish the learning curve of vascular neurosurgery by providing an artificial patient-specific simulation environment.

39

Primer extension based quantitative polymerase chain reaction reveals consistent differences in the methylation status of the MGMT promoter in diffusely infiltrating gliomas (WHO grade II–IV) of adults

E. Vassella[1], I. Vajtai[1], N. Bandi[1], M. Arnold[1], V. Kocher[1], L. Mariani[1]
[1]Institut für Pathologie, Universität Bern, Bern, Switzerland, [2]Universitätsspital Basel, Basel, Switzerland

Diffusely infiltrating gliomas (WHO grade II–IV) are the most common primary brain tumours in adults. These tumours are not amenable to cure by surgery alone, so that biomarkers of eligibility for adjuvant modalities are being called for to guide therapeutic decision making. Epigenetic silencing of the O6-methylguanine-DNA methyltransferase (MGMT) gene by promoter methylation has been associated with longer survival in patients with high grade gliomas who receive alkylating chemotherapy; and molecular testing for the methylation status of the MGMT promoter sequence is considered among the most relevant of such markers. We developed a primer extension based assay adapted to formalin-fixed paraffin-embedded tissues that allows the quantitative assessment of the methylation status of the MGMT promoter. This assay is very sensitive, highly reproducible, and provides valid test results in nearly 100% of cases. Our results indicate that oligodendrogliomas, empirically known to entail a relatively favourable prognosis, also represent the most homogeneous entity in terms of MGMT promoter methylation. Conversely, astrocytomas, which are more prone to spontaneous progression to higher grade malignancy, are significantly more heterogeneous. In addition, we show that the degree of promoter methylation correlates with the prevalence of loss of heterozygosity on chromosome arm 1p in the oligodendroglioma group, but not the astrocytoma group. Our results may potentially have important implications for clinical molecular diagnosis.

40

Prognostic Value of Growth Hormone in patient with Intracerebral Hemorrhage

W. Zumofen[1], Zweifel[1], Katan[2], Mariani[1], Müller[4], Christ-Crain[3]
[1]Department of Neurosurgery, Basel, Switzerland, [2]Department of Neurology, Basel, Switzerland, [3]Department of Endocrinology and Clinical Nutrition, Basel, Switzerland, [4]Department of Internal Medicine, Aarau, Switzerland

Background and purpose: Early prognosis of outcome is important for optimized care and treatment decision in patient with spontaneous intracerebral haemorrhage (ICH). Endocrine alterations of the hypothalamic-pituitary-axis (HPA) are one of the first measurable alterations after cerebral ischemia Human growth hormone (GH) has shown to have a prognostic value in various diseases and has been implicated in the development of atherosclerosis. We evaluated the prognostic accuracy of GH in patients with an acute ICH.
Methods: In a prospective observational study in 40 consecutive patients with ICH, GH was measured on admission by an immunoradiometric assay. The prognostic value of GH to predict 30 day mortality and 90 day functional outcome was assessed. Favorable functional outcome was defined as Barthel score >85 points and Modified Rankin Scale <3 points.
Results: GH levels were increased in patients who died within 30 days as compared to survivors (0.45 (IQR 0.20-1.51) vs 1.51 (IQR0.91–4.08), p = 0.032) and in patients with an unfavorable functional outcome as compared to patients with a favorable functional outcome after 90 days (0.26 (IQR 0.16–0.62) vs 0.67 (IQR 3.1–1.76), p = 0.043). For the prediction of death, receiver-operating-characteristics revealed an area under the curve (AUC) for GH of 0.78 (95%CI 0.60–0.96) which was in the range of the Glasgow Coma Scale (AUC 0.82 (95%CI 0.59–1.00)).
Conclusions: If confirmed in a large trial, GH is a prognostic marker in patients with an ICH might be an additional valuable tool for risk stratification and decision making in the acute phase of ICH patients.

41

Quality of life and outcome after treatment of ruptured cerebral aneurysms: results of a single center in Switzerland

L.S. Lucia Schwyzer, J.F. Javier Fandino, E.S. Evelin Szyjkowski, S.M. Serge Marbacher, R.E. Rolf Ensner, A.M. Angel Mironov, H.L. Hans Landolt
Kantonsspital Aarau, Aarau, Switzerland

Object: To evaluate the subjective outcome and quality of life of patients who suffered from aneurysmal subarachnoid hemorrhage who underwent endovascular coiling or microsurgical clipping in a single center.
Methods: For this retrospective single-center study we included patients who underwent aneurysm occlusion at the Kantonsspital Aarau between January 2000 and December 2006. The quality of life (QoL), the functional status and the level of independence were assessed by means of the SF-12 Health Survey, the modified Rankin Scale (mRS) and the Barthel Index. The questionnaires were sent to the patients and completed by themselves. A total of 104 patients with a mean age of 53.14 years (range 18-80 yrs) were included in the study. In 63 (60.6%) of the cases the aneurysm was clipped and in 41 (39.4%) of the cases endovascular coiling was performed.
Results: The SF-12 scores for the PCS (Physical Component Summary) and MCS (Mental Component Summary) were similar for both clipped (PCS 45.35; MCS 46.55) and coiled (PCS 46.31; MCS 47.87) patients. The mean values for the PCS were in average 4.17 points and for MCS 2.79 points lower when compared to the mean of the US population with a mean of 50 (SD 10). The mean Barthel-Index for the whole group was 92.26 (SD 16.8) and was almost identical for both the clipped (mean 92.54; SD 16.21) and coiled (mean 91.83; 17.9) patients (p = 0.56). The modified Rankin scores did not differ between the coiled and clipped patients (mean coiled 1.63; mean clipped 1.56; p = 0.97)
Conclusions: The functional as well as the mental health scores between the two groups of clipped and coiled patients which were treated at our center did not demonstrate a significant difference but were for both groups lower when compared with the population-based scores. Although the neurologic condition as well as the imaging result on admission was worse in the coiled group, the long-term results do not differ significantly.

42

Quantitative analysis of 06-Methylguanine DNA Methyltransferase (MGMT) promoter methylation in patients with low-grade gliomas

A. Ochsenbein[1], A.D. Schubert[1], E Vassella[3], L. Mariani[2]
[1]Inselspital, Bern, Switzerland, [2]Universitätsspital Basel, Basel, Switzerland, [3]Universität Bern, Bern, Switzerland

Background: Loss of heterozygosity (LOH) on the chromosomes 1p and 19q is associated with sensitivity to alkylating agents like temozolomide (TMZ) in patients with low-grade gliomas; whether methylation of the MGMT-promoter, a predictive factor in glioblastoma patients, also correlates with tumor response to temozolomide in low-grade gliomas is unclear.
Methods: We performed a retrospective analysis of patients with histologically verified low-grade gliomas (WHO Grade II) who were treated with TMZ for tumor progression at our hospital between November 1999 and November 2007. Objective tumor response was assessed by MRI at 6-month intervals. LOH of microsatellite markers on chromosomes 1p and 19q was determined by polymerase chain reaction (PCR) amplification of the matched pairs of blood and tumor DNA. A methylation-specific, primer extension based PCR method was developed to quantitatively assess the MGMT methylation status in the tumour tissue.
Results: Twenty-two patients with a median age of 53 y (range 27–72) were included in the study; 59% were male. Seven patients had prior surgical resection of the tumor. Histological classification revealed 10 oligodendrogliomas, 7 oligoastrocytomas and 5 astrocytomas. All patients were treated with TMZ 200 mg/m^2 day 1–5 in a 4 wk cycle. Grade 3–4 hematological toxicity occurred in 32% of the patients (9% leucopenia, 23% thrombocytopenia). The progression free survival was 32 months. Combined LOH 1p and 19q was found in 14 pts; 1 patient had LOH 1p alone and 1 patient LOH 19q alone. The LOH status could not be determined in two patients and was normal in the remaining four. MGMT promoter methylation was detectable in 20 pts by conventional PCR and quantitative analysis revealed a methylation status between 12–100%. The volumetric response to chemotherapy analyzed after 6 months by MRI correlated with the level of MGMT promoter methylation (p = 0.012).
Conclusion: Quantitative methylation-specific PCR of the MGMT promoter correlates with radiological response to chemotherapy with temozolomide in WHO grade II gliomas.

43

Role of the perfluorocarbon oxycyte upon tissue preservation after transient focal ischemia in a rat model

A. Bregy[3], M. Zambrana[1], J. Diaz[1], H. Bramlett[1], R. Bullock[2], A. Raabe[3], M. Reinert[3]
[1]The Miami Project to Cure Paralysis, Miller School of Medicine, Miami, FL, United States, [2]Neurological Surgery, Miller School of Medicine, Miami, FL, United States, [3]Department of Neurosurgery, University of Bern, Bern, Switzerland

Introduction: Stroke is the leading cause of disability in adults and is the second most common cause of death but will probably soon become number one since the incidence of acute cerebrovascular events (stroke and transient ischaemic attack combined) currently exceeds the incidence of acute coronary heart disease. Stroke can be classified into two different groups, infarcts which are due to local vascular obstruction and hemorrhages in brain parenchyma or subarachnoid space. Stroke is a reduction in blood supply to the brain due to vessel occlusion and not only a decrease in oxygen availability to the tissue as in hypoxia. Infarcts are responsible for around 80% of all the strokes. When oxygen and glucose are low, aerob adenosine triphosphate (ATP) production is impaired and e.g. ion pumps, necessary for cell survival, affected in their function. This leads to a release of glutamate, an excitatory neurotransmitter which is considered as a major cause of neuronal injury. Glutamate in the extracellular space leads to calcium influx into the cells and activation of digesting enzymes and failure of mitochondria. Ischemia itself leads to oxygen free radicals and other reactive oxygen species which initiate elements of apoptosis. It is thus possible to prevent ischemic cell death by an increase in the oxygen supply to the tissue by using the perfluorocarbon Oxycyte consisting of very small particles, about 0.2 microns in diameter, which facilitates their passage through capillaries and partially blocked vessels where red blood cells cannot pass.

Methods: In our study we determined if increasing the delivery of oxygen as soon as possible after onset of ischemia, by administration of Oxycyte (9 mL/kg, i.v.) will be neuroprotective and reduce infarct size in a rat model of temporary middle cerebral artery occlusion (tMCAO).
Results: Although there was no statistical significant difference in brain volume, volume of infracted hemisphere and volume of stroke (analyzed microscopically) in Oxycyte vs control group ($p = 0.4558$, $p = 0.6251$ and $p = 0.8938$ respectively) a clear difference in survival of the animals was found. 2 animals in the Oxycyte group died because of a subarachnoid hemorrhage which could be found by post mortem investigation whereas in the control group 5 animals were found with lethal bleeding. 1 animal in the Oxycyte group died because of the size of the infarct, possibly due to size of edema with consecutive herniation, and 2 animals were found in the control group.
Conclusion: The results of our study indicates the benefit of the use of the perfluorocarbon Oxycyte in a condition like stroke. Further animal studies are considered.

44

Sonication of catheter tips for improved detection of microorganisms on external ventricular drainages and ventriculo-peritoneal shunts

G.F. Jost[1], M. Wasner[1], E. Taub[1], L. Mariani[1], A. Trampuz[2]
[1]Universitätsspital Basel, Basel, Switzerland, [2]Centre Hospitalier Universitaire Vaudois, Lausanne, Switzerland

Introduction: Diagnosis of infections involving internal or external neurosurgical drainage devices is challenging and no single reliable microbiological tests exists. In a pilot study we have used sonication to study the colonization in 18 explanted external ventricular drainages (EVD) or ventriculo-peritoneal shunt devices (VPS). This technique dislodges biofilm bacteria prior to culture from the surface of implanted materials.
Methods: Removed devices were sonicated in saline (40 kHz, 1 min, 0.25 W/cm^2), the resulting fluid was cultured aerobically and anaerobically at 37 °C and bacterial counts were enumerated. Ventricular cerebrospinal fluid was cultured separately.
Results: Sonication cultures grew significantly more bacteria (13/18, 72%) than cultures of aspirated ventricular cerebrospinal fluid (CSF) (7/18, 39%) ($p < 0.001$, 95% confidence interval 26% to 40%). Positive sonication cultures of EVD catheters yielded a median of >100 colony forming units (CFU) (min. 60, max. >100). For positive sonication cultures of VPS the median was 100 CFU (min. 20, max. >1000). All patients with bacteria in CSF had also positive sonication cultures from the removed ventricular drainage/shunt. Interestingly, two patients with positive sonication findings, but sterile CSF cultures, became afebrile immediately after the ventricular catheter had been removed. As there was no alternative infectious focus, these two patients probably presented a subclinical meningitis caused by the colonized ventricular catheters.
Conclusion: Sonication culture of ventricular drainages and ventriculo-peritoneal shunts improves the microbiological assessment and may reveal a higher incidence of colonized catheters than formerly reported.

45

Subdural drainage system vs. subperiostal drainage system in the treatment of chronic subdural hematoma with burr hole trepanation – a single center experience of 113 cases

D. Bellut, Ch. Woernle, J.K. Burkhardt, N. Krayenbuehl, H. Bertalanffy
Department of Neurosurgery, University Hospital Zurich, Zurich, Switzerland

Introduction: Chronic subdural hematomas are mainly found in elderly patients. Surgery is the recommended treatment of choice in patients with symptomatic hematomas. In literature burr hole trepanation with intraoperative irrigation and subdural draining is favored, but recently a technique with a subperiostal drainage system showed equal to superior results. Here we present for the first time a comparison of those two techniques performed by the same surgeons of a single center.
Methods: In a retrospective study 113 cases of patients receiving surgery for 143 symptomatic chronic subdural hematomas were analyzed. Only those patients were included who received double burr hole trepanation and subdural or subperiostal closed drainage system as first surgical treatment. The decision whether to place subdural or subperiostal drainage system were made by the operating surgeon. Patient characteristics, clinical data, surgery characteristics, follow-up examinations, pre-, postoperative and follow-up imaging studies as well as outcome and complications were analyzed.
Results: Patient characteristics and hematoma size were comparable in the two groups of our study. The overall outcome showed no differences between the two groups. There was a higher rate of subdural fluid collection at follow up and a higher rate of reoperations in the group receiving subperiostal drainage system but a lower rate of mortality and severe complications.
Conclusion: In our experience there is a higher rate of hematoma rest and a higher rate of reoperations in patients receiving burr hole trepanation and subperiostal drainage system. But as severe complications are seen less frequent and mortality is less frequent as well in those patients this could be the treatment of choice in patients with predictable high risk for surgery- and non-surgery related complications.

46

Terson hemorrhage in aneurysmal subarachnoid hemorrhage

M.N. Stienen[2], A. Harders[1], S. Lücke[1]
[1]Dept. of Neurosurgery, University Hospital Bochum Langendreer, Bochum, Germany, [2]Dept. of Neuroanatomy and Molecular Brain Research, Ruhr-University Bochum, Bochum, Germany

Introduction: The concomitance of vitreous and/or subhyaloid hemorrhage (Terson syndrome; TS) and aneurysmal subarachnoid hemorrhage (SAH) has frequently been shown. However, there is a broad variation of reported prevalence of TS and only few cases are diagnosed in the neurosurgical unit. In this prospective study the authors determined the incidence of Terson syndrome (TS) in patients suffering from SAH and attempted to identify the prognostic relevance in terms of patient outcome.
Methods: Over a period of 12 months a total of 69 patients suffering from SAH were included in this analysis. The admitting Glasgow Coma Scale scores (GCS), Hunt&Hess grades, and Fisher grades were documented. All participants were ophthalmologically examined. The exact anatomical localisation of the aneurysm was recorded. Surgical clipping and endovascular coiling was performed in 48 patients. At discharge from the hospital the outcome was assessed using the Glasgow Outcome Scale (GOS).
Results: In a 1-year period, a total of 69 SAH patients (17 men and 52 women) with a mean age of 54.2 years (range 27–86 years) were admitted to our clinic. 11 patients (15.9%) revealed a TS within 24 hours after the aneurysm rupture (3 men and 11 women). In 6 patients the TS occurred bilaterally, in the remaining 5 patients only the right eye was affected. The hemorrhage was in a statistically significant correlation with either high Fisher- (3.0 vs. 2.36) or Hunt & Hess (4.0 vs. 2.82) scores or low GCS (5.0 vs. 11.96) scores. Especially aneurysms of the internal carotid artery (ICA; 4 patients) predisposed in a significant way for the development of TS in our cohort. Compared with the non-TS group, patients with TS displayed significantly higher mortality (36.4% vs. 11.6%) and worse functional outcome as being reflected by GOS 2 (27.3% vs. 5.8%), even though this observation was not significant.
Conclusion: Terson hemorrhage is a frequent clinical finding in SAH patients. It is likely to occur in severe SAH with high Hunt & Hess- and Fisher- scores and low GCS scores. Presence of TS may indicate a severe hospital course and a worse functional outcome of the patient. Especially in SAH patients bearing ruptured ICA aneurysms, an ophthalmological examination should be performed. Early recognition of TS is important since diminution of visual acuity even to functional blindness in the bilateral cases may be highly hindering to the patient and hamper the rehabilitation process considerably.

47

The role of oxycyte, a perfluorocarbon given after thoracic spinal cord injury in a rat model

A. Bregy[1], A. Singh[1], A. Marcillo[1], M. Zambrana[1], J. Diaz[1], R. Bullock[2], D. Dietrich[1], A. Raabe[3], M. Reinert[3]
[1]The Miami Project to Cure Paralysis, Miller School of Medicine, Miami, FL, United States, [2]Neurological Surgery, Miller School of Medicine, Miami, FL, United States, [3]Department of Neurosurgery, University of Bern, Bern, Switzerland

Introduction: Spinal cord injury (SCI) is a two-phase process, consisting of primary and secondary injuries. The term "secondary injury" describes the complex interaction of pathophysiological and biochemical mechanisms initiated by the primary injury. Anatomical, biochemical and physiological studies have demonstrated that ischemia develops just after severe contusion or compression injury of the cord. Focal cord ischemia may lead to critical tissue hypoxia within and adjacent to the injured cord segments. This Hypoxia leads to a shift away from aerobic metabolism and limits ATP production. An imbalance between energy demand and availability results in consequent mitochondrial damage in neurons and glia and may lead to neuronal death, and axonal interruption as well as demyelination. Improving oxygen availability in the first few hours after SCI may thus re-activate neurons and axons, hence allowing restoration of ion pumping, resting membrane potential, and electrical activity. One of several ways to enhance oxygen delivery to the injured cord includes enhancing oxygen transport by using a perflurocarbon (PFC). PFC particles are very small, about 0.2 microns in diameter, which facilitates their passage through capillaries and partially blocked vessels where red blood cells cannot pass. We determined if increasing the delivery of oxygen as soon as possible after injury, by administration of a perfluorocarbon oxygen carrier; Oxycyte will be neuroprotective following contusive spinal cord injury (SCI), and whether it can contribute to functional recovery.
Methods: Therefore we administered Oxycyte (9 ml/kg i.v.) a 60% w/v solution and compared this to vehicle controls. Female Sprague Dawley rats were injured and then subjected to behavioral testing (BBB) foot print analysis and histological evaluation of healthy white and gray matter tissue volumes.
Results: Behaviorally, Oxycyte administered rats displayed a significantly faster recovery of function compared to vehicle controls in open-field locomotion during the first 6 weeks (Vehicle 10.8 ± 0.8, Oxycyte 12.4 ± 0.3) and the functional recovery persisted for 7 weeks though the effect was not significant. At the endpoint of the experiment (8 weeks), foot print analysis revealed a significantly improved stride length ($p < 0.05$) and foot placement ($p < 0.001$) compared to vehicle. There was a decrease in the foot fall errors with the administration of Oxycyte ($p = 0.08$). Stereological quantification of the preserved tissue volumes after 8 wk of injury revealed that Oxycyte treated rats had significantly more preservation of white (7.72 ± 0.85 mm^3 vs 5.64 ± 0.85 mm^3; ($p < 0.05$) 37% increase) accompanied by an increase in grey (2.4 ± 0.65 mm^3 vs 1.67 ± 0.32 mm^3; 31% increase) as compared to the intralipid controls.
Conclusion: Results of our studies clearly indicate a neuroprotective effect of Oxycyte after SCI in rats and clinical trials, and studies in larger animals, will be considered.

48

The spinal dural arteriovenous fistulae and their surgical treatment

M.F. Oertel[1], V. Rohde[2], M. Mull[3], T. Krings[4], J.M. Gilsbach[1], A.K. Thron[3], F.J. Hans[1]
[1]Department of Neurosurgery, RWTH Aachen University, Aachen, Germany, [2]Department of Neurosurgery, Georg-August-University, Goettingen, Germany, [3]Department of Neuroradiology, RWTH Aachen University, Aachen, Germany, [4]Department of Medical Imaging, University of Toronto, Toronto, Canada

Introduction: Spinal dural arteriovenous fistulae (SDAVF) are exceedingly rare but remain the most common type of vascular malformations affecting the spinal cord. Based on our experience with the largest series of surgically treated SDAVF and the analysis of the longest postoperative follow-up interval of patients with SDAVF reported so far the aim of the present study was to characterize the clinical, diagnostical, therapeutical and outcome data associated with patients suffering from SDAVF and to predict prognosis from surgical therapy.
Methods: Between 1990 and 2005, 110 SDAVF in 107 patients (23 females, 84 males) were angiographically confirmed and microsurgically treated at the University Hospital Aachen. The mean patient age was 60 years (range, 23 to 86 years). The presenting symptoms were consistent with progressive myelopathy (106/107) or included isolated pain syndrome (1/107). Thoracic location (69/110) was predominant followed by the lumbar (31/110), sacral (6/110) and cervical (4/110) site. During surgery, 1/110 concurrent intradural perimedullary fistula was identified and obliterated. All patients were available for short-term examination (≤3months) and 62/107 patients for hitherto long-term follow-up evaluation (≥4 years, range 4 to 15 years) postoperatively. The clinical outcome was assessed using the Aminoff and Logue scale.
Results: Early postoperatively, 79/107 patients improved neurologically, no clinical change was seen in 26/107 patients and 2/107 patients deteriorated after surgery. 51/62 of the patients available for long-term evaluation remained improved (46/62) or stabilized (5/62), 11/62 patients subsequently deteriorated postoperatively. Surgery-related complications included 3/107 wound healing disturbances, 2/107 subcutaneous accumulations of CSF and 1/107 spinal epidural haematoma, requiring reoperation in 2/107 cases. A second operation because of a residual and recanalized (5/107) or dual SDAVF (3/107) was indicated in 8/107 cases.
Conclusions: Patients with SDAVF are perfect candidates for surgical management whereas microsurgical obliteration of SDAVF represents an effective, secure and curative approach for the treatment of SDAVF resulting in persistent clinical improvement and preventing progressive neurological deterioration in the majority of patients. Surgical-associated complications, reoperations, recurrences and secondary deterioration are rarely encountered and good long-term clinical outcome could be expected.

49

The use of a web-based audiovisual patient information system in preoperative patient education

O.P. Gautschi[1], M.N. Stienen[2], C. Hermann[1], D. Cadosch[3], M.A. Seule[1], J.Y. Fournier[1], G. Hildebrandt[1]
[1]State Hospital St. Gallen, St. Gallen, Switzerland, [2]Ruhr-University Bochum, Bochum, Germany, [3]University of Western Australia, Crawley, Australia

Introduction: In the current climate of increasing awareness, patients are demanding more knowledge about forthcoming operations. The patient information accounts for a considerable part of the physician's daily clinical routine. Unfortunately, only a small percentage of the information is understood by the patient after solely verbal elucidation, and even in the use of auxiliary materials, there is still room for improvement. New ways in patient information have to be found to satisfy patient's rising expectations. It is consistent with the spirit of the time to use modern media for broad and demonstrative patient information.
Methods: In a prospective study, 84 consecutive stationary patients, scheduled for a specific neurosurgical procedure were asked to use a web-based audiovisual patient information system. A combination of pictures, text, tone and video about the planned surgical intervention could be recalled on the internet before an elective surgical intervention. For patients not familiar with the internet, the clearly designed program was presented on a tablet personal computer the day before surgery. All patients and their treating surgeons were then asked to complete a questionnaire.
Results: Eighty-two percent of all participants found that the audiovisual patient information system lead to a better understanding of the forthcoming operation. 82% found that the information system was a very helpful preparation before the pre-surgical interview with the surgeon. 91% of all participants considered it meaningful to provide this kind of preoperative education also to patients planned to undergo other surgical interventions. 83% were altogether "very content" with audiovisual patient information system and 85% would recommend the system to others. In the majority of cases (61%) the corresponding surgeon assessed the patient information system as substantial benefit to the preoperative dialogue.
Conclusions: This new approach of patient information had a positive impact on patient education as is evident from high satisfaction scores. By using this information system, the patient can take an active part in the preoperative dialogue with the physician starting from a better level of information. Thus, time can be saved and used more efficiently to answer important questions. Because patient satisfaction with the informed consent process and understanding of the presented information improved substantially, the audiovisual patient information system clearly benefits both surgeons and patients.

50

The value of intraoperative MRI to predict improvement of visual fields defects after transphenoidal resection for pituitary tumors

S.Z. Zosso[1], S.B. Berkmann[1], H.P.K. Killer[1], J.F. Fandino[1], H.L. Landolt[1]
[1]Neurosurgery, Aarau, Switzerland, [2]Ophthalmology, Aarau, Switzerland

Introduction: Pituitary macroadenomas with suprasellar expansion may cause ophthalmologic deficits due to compression of the optic chiasm. Therefore, the advantage of intraoperative MRI (iMRI) by showing residual tumor adjacent to the optic chiasm, which can be immediately resected, might improve functional outcome of these patients. The aim of this study was to evaluate the correlation between visual improvement and intraoperative optic decompression evaluated with iMRI in patients undergoing transphenoidal resection of pituitary adenomas.
Methods: A total of 31 patients (23 male, 8 female) who underwent transphenoidal resection of pituitary macroadenoma from March 2007 to September 2009, were included in this study. iMRI (PoleStar, Medtronic) was performed prior and after resection. Tumor volume ranged between 0,94 and 55,73 cc (mean 9,89 cc). Preoperative visual field defects included hemianopsia (n = 15, 48%), quadrant anopsia (n = 15, 48%). One patient had no visual deficit prior to surgery. Preoperative vision deficit was documented in 25 (81%) patients. Intraoperative resection was classified as R0: no remnant tumor, R1: partial resection, R2: tumor debulking/biopsy.
Results: The iMRI performed after first resection attempt showed in 17 (55%) patients a no remnant tumor (R0). In 8 (26%) and 6 (19%) patients a resection grade R1 and R2 was documented, respectively. Additional resection of residual tumor after a second iMRI was performed in 8 cases (4 suprasellar, 2 parasellar, 2 intrasellar). The final iMRI showed no residual tumor in two patients. A resection grade R1 could be achieved in three cases with resection grade R2. In 6 cases (4 suprasellar, 2 intrasellar) no additional resection was performed. Postoperatively, normal visual field could be documented in 24 (77%) patients. In 2 patients an improvement was documented. Five patients did not showed improvement of the visual fields defects. Normal vision after surgery was documented in 22 (71%) patients, an improvement in 5 patients, no changes in 4 patients. Compression of the chiasm on the final iMRI correlated with persistence of visual field defects and visual deficits in 80% and 100% of the cases, respectively.
Conclusion: Intraoperative MRI findings correlate with improvement of visual fields defects and vision deficits after transphenoidal resection of pituitary tumors with compression of optic structures.

51

Thermal Model for Optimisation of Vascular Laser Tissue Soldering

S. Bogni[1], O. Stumpp[1], A. Bregy[2], M. Reinert[2], M. Frenz[1]
[1]Institute of Applied Physics, Department of Biomedical Photonics, University of Bern, Bern, Switzerland, [2]Department of Neurosurgery, Inselspital Bern, University of Bern, Bern, Switzerland

Laser tissue soldering (LTS) is a promising technique for tissue fusion. However, thermal damage of the tissue during laser procedure has always been an important and challenging problem. As in LTS of arterial blood vessels the vessel wall, especially the endothelium must not be damaged, a precise knowledge of the temperature distribution within the vessel is therefore very important. We developed a finite element model (FEM) to simulate the temperature distribution within blood vessels during LTS. Temperature measurements were used to control and calibrate the model. With the model we tested different parameters such as irradiation length, laser power, absorption coefficient, thickness of the solder-layer and pulsed energy deposition on their impact to the temperature distribution within the soldering joint in order to find optimal settings for LTS of blood vessels. A mathematical model has been developed to describe our endovascular soldering technique. The model was able to reproduce temperatures of the solder surface we measured during in-vitro experiments. With the model the impact of different soldering parameters on the temperature distribution was calculated. The model suggests a pulsed energy deposition as the most convincing way of denaturaiting the solder by lowering the intima temparture exposition.

52

Two-dose evaluation of efficacy and safety of perfluorocarbon Oxycyte™ in diffuse traumatic brain injury in the rat

A. Bregy[3], M. Zambrana[1], J. Cesar Diaz[1], A. Singh[1], W.D. Dietrich[2], R. Bullock[1], A. Raabe[3], M. Reinert[3]
[1]The Miami Project to Cure Paralysis, Miller School of Medicine, Miami, FL, United States, [2]University of Miami, Miller School of Medicine, Department of Neurosurgery, Miami, FL, United States, [3]Inselspital Bern, Department of Neurosurgery, Bern, Switzerland

Approximately 1/3 of severe CNS injury patients show reduced oxygen tension (< 25 mm Hg $ptiO_2$), often due to reduced cerebral blood flow (CBF), e.g. caused by narrowed vessels, during the first 6 to 24 hours following injury, which can lead to post-traumatic brain damage and a significantly worse the outcome These secondary insults include hypoxia, ischemia, excitotoxicity, apoptosis, and metabolic failure (Mackintosh et al., 1996). It is well known that neuronal tissue especially hippocampal areas of CA1/CA3 and dentate gyrus are extremely vulnerable to several types of secondary insults, such as hypoxia, ischemia and hypoglycemia, which are considered the major pathophysiological mechanisms leading to neuronal death hours or days after injury. Reperfusion after ischemia may be associated with inflammation and oxidative stress leading to the so called reperfusion injury. During hypoxia/ischemia, improvement of oxygen delivery may be of therapeutic benefit to ameliorate the damage associated with reperfusion. One way to increase oxygen delivery is by augmentation of dissolved oxygen in the blood by using perfluorocarbons (PFC). Perfluorocarbon emulsions have improved outcomes in stroke models. In our study we examined the effect of administration of Oxycyte™ a third-generation perfluorocarbon on brain tissue oxygenation and histological damage after a moderate lateral fluid percussion injury (LFPI) followed by a delayed hypoxic insult. In our studies adult male Sprague-Dawley rats were allocated to 2 different groups: Group-1: LFPI treated with 9mL/kg i.v. Oxycyte™ versus Intralipid control, 10 min post-injury. The following day a second administration of the Oxycyte™ versus Intralipid (9 mL/kg i.v.) was combined with a 30 minute hypoxic phase. Brain tissue oxygenation was measured by a LicoxÆ probe placed in the damaged area during hypoxia and reperfusion. In a second group of animals the histological damage in hippocampal neuronal cell count was assessed. Results of our acute experiments indicated higher oxygenation levels in the brain tissue of Oxycyte™ treated rats within the hypoxic period as compared to controls. In the reperfusion phase of the experiment, control animals showed higher oxygen levels during reperfusion, whereas Oxycyte™ treated animals achieved pre-hypoxic oxygen levels. Hippocampal neuronal cell count showed higher amount of survived cells in the Oxycyte™ group compared to the control group. Taken together, these data show that Oxycyte™ improves oxygen delivery to brain tissue in hypoxic conditions after traumatic brain injury in rats and seems to protect damaged neuronal cells within the hippocampus. Administration of 2 doses of Oxycyte™ appear safe, and therefore might reduce secondary hypoxic / ischemic damage, after TBI.

53

Recurrent intracranial aneurysms after successful neck clipping

M.E. Beltagy[1], C. Muroi[2,3], H.G. Imhof[4], J. Fandino[3], Y. Yonekawa[4]
[1]Department of Neurosurgery, University of Cairo, Egypt, [2]University Hospital Zurich, Zurich, [3]Department of Neurosurgery, Kantonsspital Aarau, Aarau, [4]University of Zurich, Zurich

Background: We report our experience on recurrent aneurysms after primarily completely clipped cerebral aneurysms. Mechanism of recurrence and its recommendable management are discussed.
Methods: The database consisted of 1016 consecutive patients who underwent clipping of ruptured and unruptured aneurysms in an 15 years period from 1993 through 2007.
Results: Out of these patients, 9 patients were found to be treated for recurrent aneurysms after successful complete clippings of initial aneurysms: 6 patients initial surgery before 1992, while 3 patients during the period. Mean elapsed time between their first clipping and the recurrence of aneurysm was 13.3 ± 7.8 years. Recraniotomy was performed in 7 patients, in which 6 patients underwent reclipping of the aneurysms with

or without removal of the old clips. One patient was treated by construction of extracranial-intracranial EC-IC bypass plus coating of the aneurysm. Endovascular occlusion of the parent artery was performed in one patient and the rest one patient expired without any. Recurrent aneurysms could be classified into 3 types according to the relation of their new aneurysm neck to the old clip.
Conclusion: Recurrent aneurysms after complete clipping occurred around 0.02%/year and took place after a period of 25 years at longest and 13.3 years on the average. Classification of recurrent aneurysms into three types might serve to select their appropriate surgical management.

54

Upright, multiposition MRI of the Spine – Highlights after 4 years of experience with "fmri" (functional MRI of the Spine)

D.L. Kaech[1], J.P. Elsig JP[2]
[1]Neurosurgery, Kantonsspital Graubünden, CH-7000 Chur, [2]Upright MRI Zentrum Zürich, Baslerstrasse 30, CH-8048 Zürich

Introduction: Imaging of the spine during axial loading and in various positions is now possible with the top-front open, upright, weight-bearing, dynamic-kinetic 0.6 Tesla MRI, which is also called "stand-up™ or upright™, multi-position™, true MRI™ and finally fmri®", i.e., functional MRI of the spine.
Material and Methods: Patients with recurrent positional or motion dependent spinal and/or radicular pain, including neurogenic claudication, were inverstigated in upright seated or standing position, including flexion-extension, and sometimes rotation imaging.
Results: Illustrative cases include cervical and lumbar spinal instability, lateral rotational instability, dynamic spinal cervical and lumbar stenosis and position-dependent disc herniations. This is particularly valuable in patients with a previous unremarkable or only mildly abnormal recumbent MRI. Other examples of the advantages of this method are protruding synovial cysts causing a significant stenosis during retroflexion, while the canal looked only slightly narrow during anteflexion, with some fluid in the distended intervertebral joints. In an ice hockey player, who previously experienced an episode of transient traumatic quadriplegia, fmri revealed a C3-C4 disc herniation and a buckling of the ligamentum flavum increasing during retroflexion with unilateral retrolisthesis resulting in a dynamic segmental stenosis with compression of the cord. In patients with increasing neck pain years after a car accident a missed odontoid fracture with associated instability was disclosed. In patients with prior spinal fusion procedures, motion and axial loading-dependent mobile stenosis/instability at an adjacent segment were detected.
Conclusion: This open MRI imaging modality enables a better correlation between patient complaints, clinical and imaging findings, and in the near future could become the imaging modality required before performing complex surgical spinal procedures. It gives us the possibility to assess load and motion dependent physiological and pathological changes within the intervertebral foramina and the spinal canal. Our experience shows that fmri technology is able to clarify whether there is a latent, possibly 3-D instability, i.e., a mechanical cause of neural compression. It has the potential to replace myelography – exception made for patients with ferromagnetic implants and major tremor – for evaluating operated patients with recurrent problems. The quality control, i.e. the assessment of position and function of spinal implants is a central concern of the surgeon, because it can determine the future of a technology but above all the future of patients. The MRI compatible "Discocerv®" cervical disc prostheses, but also other implants as Dynesys® and X-Stop® have been studied with upright, positional and kinetic, i.e. functional MRI. The present experience confirms the positive statements made by the pioneers, as published by Jinkins et al. Finally this open, upright, multi-position MRI is a new diagnostic option for obese and claustrophobic patients.

55

Can we extrapolate ISUIA results to the population?

P. Bijlenga, M. Jägersberg, V. Mendes-Perreira, M.C.J.M. Sturkenboom, R. Risselada, P. Singh, P. Lawford, G. Zilani, J. Byrne, T. Doczi, J. Macho, J. Blasco, E. Vivas, T. Sola, C. Friedrich, K.O. Lovblad, D. Rüfenacht, C. Schaller, A. Frangi

Objective: According to the International Study of Unruptured Intracranial Aneurysms (ISUIA), anterior circulation (definded as anterior communicating artery (Acom), anterior cerebral artery (ACA), middle cerebral artery (MCA) and internal carotid artery (ICA)) aneurysms less than 7 mm of diameter are of minimal rupture risk. However, it is general neurosurgical experience that Acom aneurysms are frequent and often rupture below 7 mm of size. Do Acom aneurysms behave differently from other anterior circulation aneurysms?
Methods: We studied the prospectively recruited patients of the multicenter @neurIST project. The prevalence of unruptured aneurysms by location was compared between ISUIA reported figures and @neurIST data. The Odd ratio (including confidence interval and p-value) of aneurysm rupture was compared between Acom and the other anterior and posterior circulation locations. Average sizes (mean, SD) of unruptured and ruptured aneurysms were calculated.
Results: Of 263 unruptured aneurysms in the @neurIST study, 207 (78%) were found in the anterior circulation (ISUIA 61%) and among these 48 (23%) were aneurysms of the Acom (ISUIA 10% for both ACA and Acom). The higher prevalence of these aneurysms in the @neurIST collective was significant ($p < 0.001$). The Odd ratios for aneurysm rupture between the Acom and anterior circulation, Acom and MCA, Acom and ICA and Acom and posterior circulation locations were 2.7 (1.8–4.1, $p < 10^{-6}$), 4.0 (2.4–6.4, $p < 10^{-7}$), 6.4 (3.7–11.1, $p < 10^{-11}$) and 1.4 (0.9–2.3, not significant), respectively. Unruptured and ruptured aneurysm sizes were 6.3 ± 4.4 mm and 6.8 ± 7.2 mm for the Acom, 5.3 ± 3.7 mm and 7.1 ± 5.7 mm for the MCA, 6.0 ± 4.6 mm and 6.8 ± 8.4 mm for the ICA and 6.0 ± 3.5 mm and 7.3 ± 4.5 mm for the posterior circulation, respectively.
Conclusion: The prevalence of unruptured aneurysms of the anterior circulation is significantly higher in the @neurIST study than reported in ISUIA. Acom is the most frequent location of aneurysms observed in @neurIST. Acom aneuryms are mostly discovered ruptured and express similar behavior to posterior circulation aneurysms in contrast to MCA and ICA aneurysms. Anterior circulation rupture risk proposed by ISUIA does, in our opinion, not apply to Acom aneurysms.

56

Canavan Disease a clinical course in a non-Jewish child with a novel mutation

H. Schober[1], J. Luetschg[1], I. Hoeliner[1], A. Fussenegger[1], M. Witsch-Baumgartner[2], S. Kalb[2], B. Simma[1]
[1]Landeskrankenhaus, Feldkirch, Austria, [2]Division of clinical genetics, Medical university, Innsbruck, Austria

Introduction: Canavan disease is a severe autosomal rezessive inherited progressive leucodystrophy caused by Aspartoacylase (ASPA) deficiency, which results in increased brain N-acetyl-L-aspartic acid (NAA) concentrations and reduced myelin lipid synthesis. Genetically two mutations comprise the majoritiy of mutant alleles in Jewish patients, mutations in the ASPA gene among non Jewish patients seem to be different and more diverse. The purpose of this case report is to present a female with the infantile form of Canavan's disease and a new mutation of the ASPA gene.
Method: The clinical, MRI, biochemical and molecular genetic data of a non Jewish female infant will be presented.
Case report and results: The female infant is the first child of an unrelated, healthy non jewish couple. At the age of 6 months she showed a macrocephaly, sparse social interaction, hypotonia with poor head control, intermittend spasticity and feeding problems. The MRI showed a leucodystrophy and in the MR spectroscopy a typical NAA peak in the white matter. In the molecular analysis of the ASPA gene (NM_000049.2) a compound heterocygosity for p.P 181T (c.541C>A in exon 4), and c.432G>A in exon 2 was found The mother is heterocygote for p.P181T and the father is heterocygous for c.432G>A. During the follow up examinations an intermittend increasing spasticity, a poor social contact and almost no psychomotor development were observed. Since

there is no causal therapy only symptomatic interventions (physiotherapy, baclofen and tizanidine) were possible.
Conclusion: Canavan's disease is very rare in non-Jewish caucasion popupulation. In children with macrocephaly, severe developmental delay and increasing spasticity the diagnosis is made by MRI and metabolic investigations (NAA peak in the white matter). Mutation analysis can show novel mutations of the ASPA gene particularly in patients with non-Jewish ancestry.

57

Cerebellar clefts: confirmation of the neuroimaging pattern

A. Poretti[1], TAGM Huisman[2], F.M. Cowan[3], E. Del Giudice[4], P.Y. Jeannet[5], D. Prayer[1], M.A. Rutherford[3], A.J. du Plessis[7], C. Limperopoulos[8], E. Boltshauser[1]
[1]Department of Pediatric Neurology, University Children's Hospital, Zürich, Switzerland, [2]Division of Pediatric Radiology, Russell H. Morgan Department of Radiology and Radiological Science, The Johns Hopkins University School of Medicine, Baltimore, United States, [3]Department of Paediatrics and Imaging Sciences Department, MRC Clinical Sciences Centre, Hammersmith Campus, Imperial College, London, United Kingdom, [4]Section of Child Neuropsychiatry, Department of Pediatrics, University "Federico II", Naples, Italy, [5]Pediatric Neurology and Neurorehabilitation Unit, Centre Hospitalier Universitaire Vaudois, Lausanne, Switzerland, [6]Department of Neuroradiology, Medical University, Vienna, Austria, [7]Fetal-Neonatal Neurology Research Program, Department of Neurology, Children's Hospital Boston and Harvard Medical School, Boston, United States, [8]Department of Neurology and Neurosurgery, School of Physical and Occupational Therapy, and Pediatrics, McGill University, Montreal, Canada

Introduction: In 2008 we described neuroimaging and clinical findings in children with cerebellar clefts (Poretti A et al., Neuropediatrics, 2008) and proposed that these clefts represent disruptive changes following prenatal cerebellar hemorrhage. We now report an additional series expanding on our experience.
Methods: Analysis of clinical and neuroimaging findings of 9 patients with cerebellar cleft collected from multiple institutions.
Results: The clefts were located in the left cerebellar hemisphere in 5 cases, in the right in 3, and bilaterally in one child who had bilateral cerebellar hemorrhages as a preterm at 30 weeks gestation. In one patient born at 24 weeks of gestation a unilateral cerebellar hemorrhage has been found at the age of 4 months. Other typical cerebellar findings included disorderly alignment of the folia and fissures, irregular grey/white matter junction, and abnormal arborisation of the white matter in all cases. The cerebellar cleft extended into the fourth ventricle in 3 cases. Supratentorial abnormalities (periventricular nodular heterotopias, atretic occipital encephalocele, and ventriculomegaly) were found in 4 cases. The 9 patients were 3 months to 12.4 years (mean: 4 years) old at the latest follow-up. All but 2 patients were born at term. The early postnatal course was unremarkable in all but 3 cases. Truncal ataxia or expressive language delay were present in 4 patients, oculomotor apraxia, muscular hypotonia, mild cognitive impairment, or attention deficit hyperactivity disorder in 2, and dysarthria in 1.
Conclusions: We confirm the neuroimaging pattern of cerebellar clefts. The documented fetal cerebellar hemorrhage in our first series, the uneventful perinatal history, and the neuroimaging similarities with the previous reported cases argue for residual disruptive changes after a prenatal cerebellar hemorrhage. Exceptionally, as now documented in 2 patients, cerebellar clefts can be found also after neonatal cerebellar hemorrhages in preterm infants. The outcome in these children was variable ranging from almost normal development to mild developmental impairment and language and speech disorders.

58

Cerebral Sinus Venous Thrombosis in Swiss Children

S. Grunt[1], K. Wingeier[1], E. Wehrli[1], E. Boltshauser[2], A. Capone[3], J. Fluss[4], D. Gubser-Mercati[5], P.Y. Jeannet[6], E. Keller[7], J.P. Marcoz[8], T. Schmitt-Mechelke[9], P. Weber[10], M. Weissert[11], M. Steinlin[1]
[1]Department of Neuropaediatrics, University Children's Hospital, Berne, Switzerland, [2]Department of Neuropaediatrics, University Children's Hospital, Zürich, Switzerland, [3]Department of Neuropaediatrics, Children's Hospital, Aarau, Switzerland, [4]Neuropaediatrics, Paediatric Subspecialties Service, University Children's Hospital, Genève, Switzerland, [5]Champreveyres 4, Neuchâtel, Switzerland, [6]Department of Neuropaediatrics, University Children's Hospital, Lausanne, Switzerland, [7]Department of Neuropaediatrics, Children's Hospital, Chur, Switzerland, [8]Rue de Lausanne 20, Sion, Switzerland, [9]Department of Neuropaediatrics, Children's Hospital, Luzern, Switzerland, [10]Department of Neuropaediatrics, University Children's Hospital, Basel, Switzerland, [11]Department of Neuropaediatrics, Children's Hospital, St. Gallen, Switzerland

Aim: Describe the characteristics of paediatric cerebral sinus venous thrombosis (CSVT) in Switzerland.
Methods: Data on clinical features, neuroimaging, risk factors and treatment were collected for all children younger than 16 years old suffering from CSVT in Switzerland between January 2000 and December 2008. A follow-up examination and a cognitive assessment were performed. Differences between neonates and children (patients older than 28 days) were assessed, and predictors of outcome were determined.
Results: Sixty-five cases of CSVT were reported. The incidence of paediatric CSVT in Switzerland was 0.558 per 100,000 per year. In neonates, the deep venous system was more often involved and parenchymal injuries were more common. Predictors of poor outcome were neonatal age (OR = 42.2; p = 0.001), parenchymal injuries in neuroimaging (OR = 20; p = 0.008) and the absence of anticoagulant treatment (OR = 12.6; p = 0.005). Most children showed global cognitive abilities within the normal range, but impairments in single cognitive subdomains were frequent.
Interpretation: Paediatric CSVT is rare. Its outcome is poor in neonates. Most children have good neurological outcomes, but some patients suffer from individual neuropsychological impairments.

59

Congenital Myastheni – a treatable neuromuscular disease

A. Klein[1], D. Beeson[2], M. Tröger[3], St. Robb[4]
[1]Neuropädiatrie, Universitäts Kinderspital, Zürich, Switzerland, [2]Radcliffe Hospitals, Oxford, United Kingdom, [3]Kantonsspital, Aarau, Switzerland, [4]Dubowitz Neuromuscular Centre, London, United Kingdom

Introduction: Congenital myasthenic syndromes are increasingly recognised as a differential diagnosis of congenital myopathies. As most respond to medication and some may lead to life threatening events this is an important differential diagnosis.
Methods: Case report
Results: We report a 10 year old girl, born at term after an uneventful pregnancy to non- consanguineous parents of Italian origin. Two maternal cousins died at the age of less than a week of a diaphragmatic hernia. First concerns were raised at the age of a few months because of poor head control in the prone position. She never crawled, bottom shuffled, walked at age 15 months. She was never able to run, had frequent falls and difficulties getting up from the floor. At the age of 4 years she was first investigated for a neuromuscular disease. On examination she had proximal and axial weakness in the antigravity range, no facial weakness and full eye movements. CK and lacate were normal. Muscle biopsy showed mild variation of fibre size, no signs of de- or regeneration, no increase of connective tissue and normal immunohistochemistry. On further follow up, she showed a slowly progressive weakness, predominantly proximal but also distal and axial, a minimal facial weakness, no ptosis or limitations of eye movements. Arm abduction and elevation was in the MRC 3- range, all other muscle groups were >MRC 3+. Muscle MRI of the thighs was normal. Because of the discrepancy of marked weakness compared to the mild findings on biopsy and on MRI a congenital myopathy seemed unlikely. On further questioning she described fluctuations of the weakness over weeks. Repeated Gowers manoeuvre showed fatigability. Repetitive stimulation of the accessory nerve showed a pathological decrement of 32%. Because the clinical findings were suggestive for a mutation in the DOK7 gene, we started salbutamol 3 x 2 mg. 2 weeks later she started to improve, which continued over the following months. Functional measurements showed a marked amelioration after 6 months. Molecular genetic analysis of DOK7 confirmed a frequently reported duplication c.1124_1127dupTGCC and mutation c.512G>A which has not previously been reported.
Conclusion: Congenital myasthenia should be considered in the differential diagnosis of myopathies, fluctuations and fatigability are often less obvious than in autoimmune myasthenia. Salbutamol is a good alternative to ephedrine with a good side effect profile and is available in Switzerland.

60

Isolated focal cerebellar lesions during development: Neurological and neuropsychological outcome

K. Wingeier[1], S. Bigi[1], M. El-Koussy[2], Th. Heinks-Maldonado[1], E. Boltshauser[3], M. Steinlin[1]
[1]University Children's Hospital, Inselspital, Bern, Switzerland, [2]University Hospital, Inselspital, Bern, Switzerland, [3]University Children's Hospital, Zurich, Switzerland

Introduction: The extent of influence of the cerebellum on developing cognitive functions is unknown. However, there are signs that it might play a crucial role. Consequently, the topic of cognitive disturbances after cerebellar lesions during development has become of increasing interest. The aim of the present study was to assess long-term sequelae after cerebellar lesions during childhood.
Methods: Eight participants with isolated focal hemorrhagic cerebellar stroke before the age of sixteen were recruited. All patients underwent a neurologic exam including the Zurich Neuromotor Assessment (ZNA), the International Cooperative Ataxia Rating Scale (ICARS) as well as an extensive neuropsychological battery assessing a broad range of cognitive functions. Quality of life and possible behaviour/emotional problems were assessed with different questionnaires.
Results: The results revealed adaptive fine motor problems (ZNA) and restricted oculomotor movements (ICARS). Conversely, no overall neuropsychological pattern could be identified except marginally reduced reaction times and susceptibility to interference. Furthermore, borderline results in semantic and phonological word fluency tasks were apparent. However, verbal performance and reading abilities were non-pathologic. The majority of the participants reported good quality of life without major physical restrictions or emotional disturbances.
Conclusions: In this patient group the presence of a cerebellar cognitive affective syndrome as frequently described in the literature cannot be confirmed. Nevertheless, individual neuropsychological impairments are present. Moreover, fine motor problems were common. Probably heterogeneity of age at stroke and exact lesion site (as well as its afferent and efferent connections to the cerebrum) may have led to interpersonal differences in neuropsychological outcome.

61

Language lateralisation correlates with verbal memory performance in children with focal epilepsy

R. Everts[1], S.A. Harvey[2], L.M. Lillywhite[3], J. Wrennall[4], D. Abbott[3], L. Gonzalez[1], G. Jackson[3], V. Anderson[1]
[1]Critical Care and Neuroscience, Murdoch Children's Research Institute, Melbourne, Australia, [2]Department of Neurology, The Royal Children's Hospital, Melbourne, Australia, [3]Brain Research Institute, Florey Neuroscience Institutes, Melbourne, Australia, [4]Department of Psychology, The Royal Children's Hospital, Melbourne, Australia

Introduction: Assessment of language dominance with functional magnetic resonance imaging (fMRI) and neuropsychological assessment is often used prior to neurosurgical interventions and is important in minimizing the risk of functional loss after surgery. The present study explores whether language lateralisation and cognitive performance are systematically related in young patients with focal epilepsy.
Methods: Language fMRI and neuropsychological data (language, visuo-spatial perception, memory) of 40 patients (7–18 years) with unilateral, refractory focal epilepsy in temporal and/or frontal areas of the left (n = 23) or right hemisphere (n = 17) were analysed. fMRI data of 18 healthy controls (7–18 years) served as a normative sample. A laterality index was computed to determine the lateralization of activation in three regions of interest (frontal, parietal, temporal).
Results: Atypical language lateralisation was demonstrated in 12/40 (30%) patients. A correlation between language lateralisation and verbal memory performance occurred in patients with left-sided epilepsy: bilateral or right-sided language lateralisation correlated with better verbal memory performance (Word Pairs Recall: frontal r = –0.4, p = .016 parietal r = –0.4, p = .043, temporal r = –0.4, p = .041). Verbal memory performance made the largest contribution to language lateralisation, whereas handedness and side of seizures did not contribute to the variance in language lateralisation.
Conclusion: This finding reflects the strong association between neocortical language and hippocampal memory regions in patients with left-sided epilepsy. Atypical language lateralisation is advantageous for verbal memory performance, presumably a result of a transfer of verbal memory function. In children with focal epilepsy, verbal memory performance provides a better idea of language lateralisation than handedness and side of epilepsy and lesion. Knowledge about the relationship between language lateralisation and verbal memory performance allows for a refined clinical interpretation of pre-surgical language fMRI and neuropsychological data.

62

Longitudinal neurodevelopmental evolution in patients with severe to profound static encephalopathy

G.P. Ramelli[1], U. Antonini[1], V. D'Apuzzo[1], R. Brunner[1]
[1]Ospedale San Giovanni, Bellinzona, Switzerland, [2]Istituto Provvida Madre, Balerna, Switzerland, [3]Istituto Provvida Madre, Balerna, Switzerland, [4]Universitätskinderklinik beider Basel, Basel, Switzerland

Introduction: Little information is currently available on the longitudinal neurodevelopmental evolution in patients with static encephalopathy and severe to profound cognitive dysfunction.
Methods: Between 1984 and 2005, patients with severe to profound static encephalopathy on care at the Istituto Provvida Madre underwent neuredevelopmental evaluation by means of the Munich functional Developmental Diagnostics test on an annual basis. Repeated multivariate analysis was used to assess the presence of longitudinal trends.
Results: 35 patients (18 female and 17 male subjects) underwent testing for at least 3 consecutive years. The underlying conditions were chromosomal disorders in 14, hypoxic-ischemic encephalopathy in 3, autism spectrum disorder in 3, brain malformations in 3, mitochondrial cytopathies in 2, epileptic encephalopathy in 1, congenital Cytomegalovirus infection in 1 and unknown in the remaining 8 cases. The median age of the patients at the time of initial testing was 6 years (range, 1.6–16), and the median follow-up from the time of the first testing was 4 years (range, 3–11). The median age at the most recent evaluation was 13 years (range, 5–18). Developmental evaluation of the 35 patients disclosed a linear maturation throughout the testing period of 1.0 to 2.0 months per year, whatever the underlying condition. Some minor differences were noted between the different task categories: gross motor skill (1.0-2.0 months per year), fine motor skill (2.0 months per year), perception (2.0 months per year), active language (1.0 months per year), passive language (2.0 months per year), social contact (1.0 months per year), autonomy (2.0 months per years).
Conclusions: These longitudinal observations in patients with severe to profound static encephalopathy demonstrate a linear maturation of 1.0 to 2.0 months per years, which is independent of the underlying etiology.

63

Mirror therapy in hemiparetic children: a pilot study

M. Jequier Gygax, P. Schneider, C.J. Newman
Unité de Neurologie et Neuroréhabilitation Pédiatrique, DMCP, CHUV, Lausanne, Switzerland

Objective: In mirror therapy, the mirror reflection of the non-paretic arm provides patients with the visual illusion of a functional paretic limb and modulates the abnormal proprioceptive input. Mirror therapy has been used in rehabilitation of hemiparesis after stroke. No study using mirror therapy has been conducted in cerebral palsy. In this pilot study we tested the effectiveness and practicability of the mirror therapy in a small group of hemiparetic children.
Methods: In a cross-over study, we measured strength and utilization of the paretic upper limb in ten children after 2x 2 weeks of bi-manual training with and without a mirror. We used handheld dynamometers to monitor the effects on grasping and pinch maximal strength, and a functional scale, the SHUEE (Shriner's Hospital Upper Extremity Evaluation) to analyze the spontaneous function and dynamic position. Using SPSS 16.0 we performed paired T-tests to compare outcomes of grasp, pinch strength and upper extremity utilization.
Results: We found that maximal grasp strength increased on average by 11% when testing was done behind the mirror (with mirror 5.60 ± 0.59 ppsi; without mirror 5.03 ± 0.56 ppsi; p = 0.037). Grasp strength was improved by the training (week

0: 4.25 ± 3.43 ppsi; week 4: 5.47 ± 2.54 ppsi; p = 0.035), but overall there was no significant difference between training with and without mirror. The improvement of strength was most important during the first 2 weeks of training (from 4.50 ± 3.54 to 5.89 ± 3.89 ppsi; p = 0.005), most significantly when using a mirror. For pinch bimanual training improved maximal strength by 31% (week 0: 2.95 ± 1.96 ppsi; week 4: 3.85 ± 2.53 ppsi; p = 0.038) independently of the use of a mirror, and most importantly after the first 2 weeks of training (p = 0.05). Dynamic positional analysis scores were significantly improved by the mirror therapy (pre-mirror DPA 67.9 ± 19.7%, post-mirror DPA 71.0 ± 20.3%; p = 0.05) and most importantly after the second 2 weeks of training.
Conclusion: This pilot study shows that mirror therapy improves strength in the hemiparetic hand and dynamic function of the hemiparetic arm. Interestingly there is a temporal factor influencing the effect of the training. Mirror therapy could be used in children considering appropriate training, which is discussed. Further and larger trials of mirror therapy are needed to further define short- and long-term benefits.

64

Normal cognitive functions in Joubert syndrome

A. Poretti[1], F. Dietrich Alber[1], F Brancati[2], B. Dallapiccola[2], E.M. Valente[2], E. Boltshauser[1]
[1]Pediatric Neurology, University Children's Hospital, Zürich, Switzerland, [2]CSS-Mendel Institute, Casa Sollievo della Sofferenza Hospital, Rome, Italy

Introduction: Developmental delay and/or cognitive impairment respectively are considered key features in Joubert Syndrome (JS). Impaired performance in several cognitive domains and affected language ability as well as behavioral and social problems are also well known in patients with JS. We report a young woman with JS and, exceptionally, normal intelligence and present the results of a detailed neuropsychological assessment.
Case reports: We report a 20-year-old woman with mild clinical signs of JS (minimal truncal ataxia and oculomotor apraxia) but typical neuroimaging findings (molar tooth sign, significant hypoplasia and dysplasia of the cerebellar vermis, and enlarged and unusually shaped fourth ventricle), normal full scale (IQ = 93), verbal (IQ = 93), and performance intelligence quotient (IQ = 94). Only minor difficulties in visual-spatial organization and in some executive functions could be detected. Her diagnosis was only reached following the diagnosis of JS in two brothers with severe cognitive impairment. Molecular investigation demonstrated a homozygous mutation in the INPP5E gene.
Conclusions: This exceptional observation (only one other case reported) confirms that normal cognitive functions are possible in JS. The pattern of neurocognitive deficits is partly reminiscent of the symptom profile of the cerebellar cognitive affective syndrome reported by Schmahmann and Sherman in acquired cerebellar lesions. The severe cognitive impairment of the two brothers despite the same genotype corroborates the well known intrafamilial variability and also allelic heterogeneity in JS. Therefore, in patients with very mild phenotype, the diagnosis may be missed without targeted neuroimaging.

65

Basilar artery occlusion in children: a relatively favorable outcome in a potentially life-threatening disease

B. Goeggel Simonetti[1], M. Gautschi[1], E. Boltshauser[2], T. Schmitt-Mechelke[3], M. Weissert[4], E. Wehrli[1], M. Steinlin[1]
[1]Neuropediatric Divisions, University Children's Hospitals Berne, and Zurich[2], Children's Hospitals Lucerne[3], and St. Gallen[4]

Introduction: Basilar artery occlusion is a rare, but potentially life threatening entity of pediatric stroke. Knowledge of its natural history, best treatment approaches and outcome is limited, leading to the analysis of this case series.
Methods: Data from the Swiss Neuropediatric Stroke Registry (SNPSR) were scanned for basilar artery occlusion diagnosed by brain imaging. The SNPSR is a prospective population-based study including children with stroke from birth to the age of 16 years living in Switzerland.
Results: Since the start of the SNPSR in 2000, 5 cases of basilar artery occlusion (out of 131 reported childhood strokes) have been recorded. Four were boys, age range was 4.5–13.9 years. At initial presentation, all patients suffered from impaired consciousness. Other symptoms included headache (4/5), gait disturbance (4/5), vomiting (4/5), slurred speech (2/5), and neuropsychological symptoms such as mood swings (1/5) or agitation (1/5). Etiology remained unknown in all cases. Possible trigger factors were preceding flu-like infections in 2 cases. Delay from onset of symptoms to diagnosis was 12 to 48 hours. Basilar occlusion was localized in the distal half of the basilar artery in all patients. Treatment consisted in systemic (1/5) or intraarterial (1/5) thrombolysis, heparinisation (2/5) and/or aspirin (3/5). Clinical outcome showed mild to moderate sequelae with residual motor, coordination and/or neuropsychological problems.
Conclusions: Basilar artery thrombosis is a rare condition in children. There is a considerable delay from onset of symptoms to diagnosis and treatment. Reducing the delay in treatment initiation might be a crucial factor in further improving outcome, which was relatively favorable in the children presented.

66

A missense mutation in the carboxypeptidase A6 gene linked to a recessive form of febrile seizures and temporal lobe epilepsy in a consanguineous Moroccan family

A. Salzmann[1], M. Guipponi[1], C. Lambercy[1], C. Buresi[1], D. Chaigne[2], A. Malafosse[1]
[1]University Hospitals of Geneva, Geneva, Switzerland, [2]Clinique Sainte-Odile, Strasbourg, France

Introduction: Febrile seizures (FS) are the most common form of childhood seizures. Genetic factors contribute significantly to the aetiology of FS. Rare familial forms exist and show an autosomal dominant inheritance with reduced penetrance.
Methods: Here, we report FS and temporal lobe epilepsy (TLE) in four out of seven siblings born to healthy Moroccan consanguineous parents. We hypothesized autosomal recessive inheritance of the trait and a founder mutation within a identical by descent (IBD) locus in this family. Genome-wide single nucleotide polymorphisms genotyping and copy number variations analysis was performed using Affymetrix and Agilent platforms, respectively.
Results: Combined linkage analysis and autozygosity mapping identified a unique IBD region of 9.6 Mb, flanked by SNPs rs17176439 and rs13249327, on human chromosome 8q12.1-q13.2. Copy number variations analysis did not reveal any genomic structural changes at the genome wide level. Systematic sequencing of the 38 genes published in Ensembl database (December 2007) and mapped within the linked interval revealed a homozygous missense mutation c.1025C>T of a highly conserved residue p.Ala270Val of the carboxypeptidase A6 gene (CPA6).
Conclusions: The present study suggests that CPA6 is genetically linked to autosomal recessive FS and TLE in a consanguineous family.

67

A new bedside test for gestures in stroke: The Apraxia Screen of TULIA (AST)

T.V. Vanbellingen[1], B.K. Kersten[4], A.V. Van de Winckel[3], M.B. Bellione[1], M.B. Bertschi[2], F.B. Baronti[1], R.M. Mürl[2], S.B. Bohlhalter[2]
[1]Klinik Bethesda, Tschugg, Switzerland, [2]Cognitive and Restorative Neurology, Bern, Switzerland, [3]Department of Rehabilitation Sciences, Leuven, Belgium, [4]Department of Psychology, Bern, Switzerland

Background and purpose: Apraxia in stroke patients may be overlooked in acute hospital settings as dexterous difficulties and impaired gestural communication are often attributed to the frequently co-existing sensorimotor deficits and aphasia. Early and quick detection of apraxia, using a valid and easy-to-use bedside test, may be relevant for functional outcome in stroke patients. The present study aimed to develop a new screening test for apraxia, called the Apraxia Screen of TULIA (AST), based on the comprehensive standardized test for upper limb apraxia (TULIA).
Methods: AST was developed in two phases. In Phase I an item reduction analysis of the TULIA (48 gestures) following the methods of classical test theory was performed based on a large population of stroke patients (n = 133) and healthy subjects (n = 50). Furthermore, the 6-point scoring method of TULIA was dichotomized to the score levels pass and fail. In Phase II validity of the resulting new scale AST was prospectively assessed in a new cohort of stroke patients (n = 31) by using Pearson's correlation analysis and binary classification display (apraxia yes, apraxia no) with the TULIA.
Results: Stepwise removal of items with low inter-rater reliability (4), ceiling effects (12), relatively lower internal consistency (15) and less content validity (5) resulted in the final scale of AST, reduced from 48 to 12 gestures, 7 in the imitation and 5 in the pantomime domain. Internal consistency was still high for the 12-items AST (Cronbach's alpha = 0.92). Validation of AST with the TULIA showed a remarkable diagnostic accuracy with high specificity, sensitivity and positive predictive value, both for the presence of apraxia and its severity.
Conclusions: AST offered a reliable and valid bedside test for gestures in stroke patients allowing a straightforward assessment of apraxia within a few minutes.

68

A positive side effect? The mechanism of action of the anti-epileptic drug Levetiracetam in the astroglial syncytium under inflammatory conditions

M.N. Stienen[1], N. Prochnow[1], A. Haghikia[2], D. Hinkerohe[3], P. Faustmann[1], R. Dermietzel[1]
[1]Dept. of Neuroanatomy and Molecular Brain Research, Bochum, Germany, [2]Dept. of Neurology, St. Josef-Hospital, Bochum, Germany, [3]Dept. of Neurology, Knappschaftskrankenhaus, Bochum-Langendreer, Germany

Astrocytes are increasingly associated to act as putative targets of affection in the pathogenesis of epilepsy and seizure induced tissue damage in the central nervous system. In the present study we investigated the influence of the anti-epileptic drug Levetiracetam (LEV; Keppra) on the evoked voltage gated current responses of astrocytes under acute inflammatory conditions in an astroglial syncytium in vitro. For this purpose primary glial cell cultures were prepared from brain hemispheres of postnatal wistar rats. To reach an (pro-) inflammatory state in culture, astrocytes were either cocultured with high amounts of microglia (M30%) or peripheral microglia was stimulated with the proinflammatory cytokine Interleukin1-fl (IL1-fl) for 2 hours prior to whole cell patch clamp recordings in the voltage clamp mode in vitro. Cocultures with low portions of microglia (M5%) served as controls and were basis for IL1-fl induction of an inflammatory state. Immunocytochemistry against ED1 was used for quantification of the microglial portions and evaluation of the state of activation. Electrophysiology revealed that LEV application during the inflammatory state shifted depolarized astrocytic membrane resting potentials back towards control values of non-inflammatory conditions. Mimicking inflammatory conditions, we were able to show a highly significant increase in the astrocytic inward rectifier mediated current response due to strong hyperpolarization (<= –80 mV) and an increased outward rectification at holding potentials >= –30 mV. This effect could be observed independently from the fact whether inflammation was induced by high levels of activated microglia or previous application of IL1-fl and remained absent in controls. Furthermore, expression of the anti-inflammatory cytokine Transforming growth factor-fl1 (TGF-fl1) could be proven to be upregulated in the presence of LEV. In summary, we suggest that the effect of LEV is mediated in two ways: first, via Kir-channel activation and second via an unspecific impact on outward rectifier in a TGF-fl1 operated way. Thus, LEV might serve as a tool to restore depolarized astrocytic membrane resting potentials during inflammation and provides a way to reduce excitation mediated Ca2+-wave spread and toxicity in glial tissues.

69

A sarcolemmal wounding assay to study membrane resealing in human cultured myoblasts

B.A. Azakir, B. Erne, M. Sinnreich
Neuromuscular Center, Department of Neurology, Basel, Switzerland

Background: The pathogenic basis for many muscular dystrophies is the inability of the muscle cell to maintain its sarcolemmal integrity, due to defective or deficient membrane associated structural proteins or components of the membrane repair machinery. An important protein implicated in this machinery is dysferlin. Mutations in dysferlin are a frequent cause for the recessively inherited limb girdle muscular dystrophies (LGMD), defining the common subtype of LGMD2B. Dysferlin is a large protein containing seven C2 domains, 2 DYSF domains and a transmembrane domain.
Objective: In order to study the function of individual dysferlin C2 domains, we have generated C2 domain deletion mutants of dysferlin and wish to study their membrane resealing capabilities. To achieve our objective, we developed an in vitro sarcolemmal resealing assay.
Methods: We used myoblasts from primary cultures of dysferlin deficient patients and control, transformed with E6 and E7 from HPV16. Sarcolemmal resealing kinetics were determined by measuring fluorescent dye uptake at defined, laser induced wound sites.
Results: We found a significant difference of resealing kinetics of laser induced sarcolemmal wounds in the presence versus the absence of calcium in normal myoblasts, reflecting the known calcium dependency of the resealing process. In the dysferlin deficient myoblasts, resealing did not occur, regardless of the presence or absence of calcium, confirming the membrane resealing deficiency demonstrated previously in mouse dysferlin deficient myofibers. Importantly, transfection of GFP-myc-dysferlin into dysferlin deficient myobalsts was able to restore the membrane resealing in presence of calcium.
Conclusion: This assay should be a valuable tool to measure sarcolemmal resealing capabilities of small molecular compounds or of recombinantly generated micro-dysferlin proteins in an attempt to develop therapies for dysferlin deficiency.

70

Adaptive gene expression changes in the lesioned striatum correlates with locomotor velocity in parkinsonian rats

C. Capper-Loup, A. Kaelin-Lang
Department of Neurology and Department of Clinical Research, Movement Disorders Center, Inselspital, Bern, Switzerland

In Parkinson's disease (PD), dopaminergic denervation produces an imbalance between direct and indirect pathways, leading to an inhibition of thalamocortical projections. This, in turns, causes bradykinesia or slowness of movement, a PD key symptom. However, bradykinesia only appears after a large striatal dopamine depletion and compensatory mechanisms probably delays the appearance of this symptom. The goal of our study was to analyze the role of direct and indirect pathways in these putative compensatory mechanisms. We used 6-hydroxydopamine (6-OHDA) PD rats and control animals. We measured the spontaneous locomotor behavior four weeks after the lesion and then proceed to in situ hybridization for markers of both striatal direct and indirect pathways. We also analyzed the correlation between behavior and gene expression. As expected, parkinsonian rats showed a lower velocity than control animals four weeks after the lesion. We observed a significant and positive correlation between velocity and both D1-class dopamine receptor (D1R) mRNA (direct pathway) as well as

enkephalin (ENK) mRNA (indirect pathway) in the lesioned striatum. We also found a significant and positive correlation between D1R mRNA and ENK mRNA. These correlations were only present in PD rats. Based on the classical basal ganglia model, we would expect that an increase of ENK expression in the indirect pathway induces an increase of bradykinesia and that direct and indirect pathways work in an opposite way, but we found the contrary with a synergy between both pathways. In conclusion, our results demonstrate strong mutual influences between both direct and indirect pathways, and spontaneous locomotor activity in parkinsonian rats; moreover both pathways work in synergy. We suggest that these mechanisms could play a role in compensatory mechanisms delaying appearance of bradykinesia in PD.

71

Amygdalo-hippocampal deep brain stimulation for temporal lobe epilepsy

C. Boëx[1], S. Vulliémoz[1], G. Folletti[2], L. Spinelli[1], A. Pegna[1], R. Tyrand[1], C. Staedler[2], A.O. Rossetti[2], E. Pralong[2], C. Pollo[2], M. Seeck[1]
[1]University Hospital of Geneva, Geneva, Switzerland, [2]Centre Hospitalier Universitaire Vaudois, Lausanne, Switzerland

Introduction: The objective of the study was to evaluate the effects of parameters (amplitude and configuration of stimulation; localization of the epileptogenic zone and of the electrode) of amygdalo-hippocampal deep brain stimulation (AH-DBS) in temporal lobe epilepsy (TLE).
Methods: Eight pharmacoresistant TLE patients, not candidates for ablative surgery, received chronic, DBS (130Hz, follow-up 12–74 months): two patients with hippocampal sclerosis (HS) and six patients with non lesional TLE (NLES). The effects of intensity (stepwise increases from 0(Off) to 2V) and of stimulus configuration (quadripolar, bipolar), on seizure frequency and neuropsychological performance were studied. The long-term outcomes were analysed in comparison to the localizations of the epileptogenic zones and of the electrodes.
Results: The two HS patients obtained a significant reduction (65–75%) of seizure frequency with high voltage bipolar DBS (at least 1V) or with quadripolar stimulation. Two of the six NLES patients became seizure-free, one of them without stimulation. Two NLES patients experienced a reduction of seizure frequency (65-70%); in one of both, the primary epileptogenic zone was later localized in the anterior pole of the temporal lobe. The remaining two NLES patients obtained no significant seizure reduction: in one of them, the mesial epileptogenic zone was identified as a secondary focus, in the other, the electrode was not located exactly in the mesial structures. Neuropsychological evaluation showed reversible memory impairment in two patients under strong stimulation only.
Conclusion: AH-DBS is a valuable treatment option for patients who suffer from drug-resistant TLE and who are not candidates for ablative surgery. A large zone of stimulation (high amplitude or quadripolar configuration) was needed in both HS patients. A weak stimulation and the microlesional effect were beneficial in two NLES patients. The proximity of the electrode to the primary epileptogenic zone, and the localization of this epileptogenic zone within the mesial structures, seem mandatory to the success of AH-DBS. Strong stimulations can impair memory functions that have to be carefully monitored.

72

Anticoagulation versus antiplatelets for carotid artery dissection – Cochrane Review (update)

S.T. Engelter, P.A. Lyrer
Department of Neurology and Stroke Unit, University Hospital Basel, Switzerland, Basel, Switzerland

Background: It is debated, whether anticoagulation or antiplatelets are superior in extracranial internal carotid artery dissection (eICAD), balancing risks and benefits of either approach.
Methods: We performed a systematic review applying the methodology of the Cochrane Collaboration. Randomised controlled trials (RCT), controlled trials and case studies (>3 patients), that reported on outcome stratified to the type of antithrombotic treatment were eligible for inclusion. Data were extracted independently by two reviewers. Primary outcomes were death (all causes) and death or disability. Secondary outcomes were (i) ischaemic stroke, (ii) symptomatic intracranial haemorrhage, and (iii) major extracranial haemorrhage. The first choice treatment was taken for analyses.
Results: No results from RCTs are currently available. Thirty-six case studies including 1284 patients were eligible for comparative analysis. There was no significant difference in the odds of death comparing antiplatelets with anticoagulants (Peto odds ratio [OR] 2.02, 95%-CI 0.62-6.60; p = 0.25). For "death or disability" the Peto OR of 1.77 (95%-CI 0.98–3.22; p = 0.06) suggested a strong trend in favour of anticoagulation. Ischaemic stroke happened in 1.9%. The Peto OR of 0.63 [95%-CI 0.21–1.86, p = 0.41] indicated no significant difference between both treatments. Symptomatic intracranial haemorrhages (0.8%) and major extracranial haemorrhages (1.6%) occurred only in the anticoagulation group. However, the Peto ORs (i.e., 0.24 [95%-CI 0.02–3.66]; 0.19[95%-CI of 0.02–1.48], respectively) indicated no significant difference between both treatment modalities.
Conclusions: The finding of a trend towards a benefit of anticoagulants (compared with antiplatelets) for "death or disability" is likely influenced by an allocation bias taking into account that anticoagulants had neither a favourable effect on stroke prevention nor on bleeding complications. In fact, there are – non-significant – trends for a less favourable effect of anticoagulants regarding bleeding complications. However, in the absence of RCT-based data no firm conclusions can be drawn. "Death or disability" is a worthwhile endpoint for RCTs.

73

Arc induction through motor learning in the primary motor cortex of rats

J.A. Hosp[1], S. Mann[1], B. Wegenast-Braun[2], M. Calhoun[2], A.R. Luft[1]
[1]Clinical Neurorehabilitation, Department of Neurology, University of Zürich, Zürich, Switzerland, [2]Department of Cellular Neurology, Hertie-Institute for Clinical Brain Research, University of Tübingen, Tübingen, Germany

Introduction: Although it is well known that motor learning depends on protein synthesis in primary motor cortex (M1) neurons (Luft et al., 2004), the identity of the activated genes and their appropriate proteins remains still poorly understood. Recently, induction of the protein Arc was observed in M1 of rats that learned a precise grasping task (Hanlon et al., 2009). Arc is encoded by the immediate early gene Arc/Arg3.1 and participates in various forms of neural plasticity. Nevertheless, it is not clear if this increased expression of Arc can be related to learning dependent changes or if it represents an epiphenomenon induced by environmental changes or enhanced activity of the trained forelimb.
Methods: Arc mRNA was visualized and quantified using a fluorescent in situ hybridization assay (FISH) for several conditions of a precise reaching task in rats: 1.) Skilled reaching task (SRT): a paradigm inducing motor learaning (precise grasping of a food pellet). 2.) Activity control group (ACT): a paradigm for enhanced movement activity of the forelimb without motor leraning. 3.) Priming: a paradigm to test environmental influences without enhanced forelimb activation or grasping. To display the steepest phase of the learning curve in the SRT group, animals were sacrificed at the second day of training. To maintain comparabilty between groups, animals of the ACT and Priming group were temporally matched to the rats of the SRT group. The application of the FISH technique allowed the visualization of Arc mRNA that was synthesized exclusively during the behavourial task.
Results: In a skilled reaching task (SRT), Arc mRNA levels in M1 of the trained hemisphere are increased by 50.9% ($p < 0.01$) when compared to the untrained hemisphere, by 91.9% ($p < 0.01$) when compared to the Priming group and by 46.9% ($p < 0.01$) when compared to the trained hemisphere of the activity control task (ACT) group. Furthermore, Arc mRNA levels in M1 are significantly correlated to the inter-session improvement of rats in the SRT group ($R = 0.63$; $p = 0.006$).
Conclusions: Alltogether, these results suggest that Arc expression in M1 is related to motor learning and cannot be only explained by environmental factors or increased usage of the trained forelimb during the task. Arc may be involved in formation and maintainance of long term potentiation (LTP) in M1, an essential mechanism for motor learning (Rioult-Pedotti et al., 2000).
References: Hanlon EC, et al. Effects of skilled training on sleep slow wave activity and cortical gene expression in the rat. Sleep. 2009;32:719–29. Luft AR, et al. Motor skill learning depends on protein synthesis in motor cortex after training. J Neurosci. 2004;24:6515–20. Rioult-Pedotti MS, et al. Learning-induced LTP in neocortex. Sience. 2000;290:533–6.

74

Assessment of pathologic synergies in stroke using the arm robot ARMin III

V. Klamroth-Marganska[2], M. Guidali[2], R. Riener[2]
[1]ETH, Zurich, Switzerland, [2]University Hospital Balgrist, Zurich, Switzerland

Introduction: Patients with hemiparetic stroke suffer from abnormal muscle co-activation patterns known in clinical rehabilitation as abnormal secondary torques or pathologic synergies. According to Brunnstrom, recovery after stroke is reflected by the patient's ability to move outside these pathological patterns. Robotics in neurological rehabilitation do not only offer a promising way to treat patients with impairments after stroke but also allow for accurate assessment of training efficacy. As the common clinical tests (e.g. Fugl-Meyer Assessment) are too imprecise to characterize specifically alterations in abnormal coupling between different joints, we used the arm robot ARMin III to measure the appearing torques in the affected upper limb of stroke patients.
Methods: ARMin III is an arm rehabilitation device developed at ETH Zurich in collaboration with the University Hospital Balgrist. It has an exoskeletal structure with seven actuated degrees of freedom. The patient is connected to the robot with cuffs on the upper arm and on the forearm. The device is adjustable to the patient's anatomy. Ten patients enrolled in a multicentre study for comparison of ARMin robot training and conventional therapy were assessed on the robot ARMin for pathological synergies. All patients hat suffered from ischemic stroke and were in the chronic stage (at least six months post-stroke). Isometric force measurements were conducted while all robot's degrees of freedom were locked. The patient was instructed to produce maximal shoulder abduction torques at three different shoulder abduction angles (50, 70 and 90 degrees) and the corresponding elbow flexion forces were measured. A torque estimation method via demanded motor current was used.
Results: Both, conventional therapy and robotic training evoked significant improvements following eight weeks of therapy (as measured on robot scales). All subjects showed positive effects regarding the strongest component of synergies: abnormal joint coupling between shoulder abduction and elbow flexion was getting smaller during the course of the therapy.
Conclusion: The therapy robot ARMin does not only provide a sensitive tool for rehabilitation treatment but also for rehabilitation assessment controlling and measuring therapeutic efficacy of both, robotic therapy and other rehabilitation techniques.

75

Asymmetry in slow wave activity and sleep spindles after acute cortical hemispheric stroke

R.P. Poryazova[1], R.H. Huber[2], R.K. Khatami[3], E.W. Werth[1], P.B. Brugger[1], C.B. Bassetti[4]
[1]University Hospital, Zurich, Switzerland, [2]University Children's Hospital, Zurich, Switzerland, [3]Sleep center, clinic Barmelweid, Bermelweid, Switzerland, [4]Neurocenter of southern Switzerland (EOC), Lugano, Switzerland

Introduction: Whereas thalamus is suggested to play a key role in the generation of sleep spindles, the role of the cerebral hemispheres has been rarely studied. A significant reduction in the power and coherence of sleep spindle frequency activity in EEG derivations recorded over the hemisphere ipsilateral to the lesion during the acute phase of stroke has been reported. Changes in slow wave activity have also been described. We aimed at investigating slow wave activity (SWA) and sleep spindles after cortical hemispheric and thalamic stroke and at comparing them to healthy controls.
Patients and methods: Nine patients, three with bilateral paramedian thalamic stroke (PMTS) and six with unilateral PMTS, seven patients with hemispheric cortical stroke (5 left and 2 right) and nine age and gender matched controls underwent high-density EEG (hd-EEG) examination with 128 electrodes during sleep. The recordings in all patients were performed within 10 days after stroke.
Results: Statistic nonparametric mapping showed a significant decrease in SWA and spindle frequency range (SFR) power over the affected hemisphere in comparison to the non-affected in a paramedian frontocentral region in the patients with hemispheric stroke, the decrease being more profound and over a much larger area for the SFR. Additionally an asymmetry index comparing the power in both SWA and SFR was calculated. Patients with hemispheric stroke showed a much higher asymmetry index for both SWA and SFR in comparison to patients with PMTS and to healthy controls. The asymmetry index in the hemispheric group was significantly higher for SFR in comparison to SWA. The asymmetry index did not differ between healthy controls and patients with PMTS.
Conclusion: SWA and SFR decrease after hemispheric cortical stroke over a paramedian frontotemporal region over the affected hemisphere. There is a significant asymmetry in SWA and SFR after hemispheric cortical stroke but not after paramedian thalamic stroke. These findings suggest that the cerebral hemispheres are important for the generation of both slow waves and sleep spindles.
Support: The study is supported by the Zurich Center for Integrative Human Physiology (ZIHP).

76

Blood flow dynamics in sensorimotor cortex correlate with motor skill recovery after ischemic stroke

Eugenio Abela[1], Andrea Federspiel[2], Roland Wiest[3], Tobias Kress[4], Matthias Sturzenegger[5], Christian Hess[5], Bruno Weder[1]
[1]Department of Neurology, Kantonsspital St. Gallen, St. Gallen, Switzerland, [2]Division of Psychiatric Neurophysiology, University Psychiatric Clinic, University of Bern, Bern, Switzerland, [3]Institute for Diagnostic and Interventional Neuroradiology, University Hospital Inselspital, Bern, Switzerland, [4]Department of Neurosurgery, Kantonsspital St. Gallen, St. Gallen, Switzerland, [5]Neurological University Department, University Hospital Inselspital, University of Bern, Bern, Switzerland

Introduction: Ischemic stroke is one of the leading causes for permanent disability in adult life. Despite improvements in acute stroke management, up t0 70% of stroke survivors suffer from permanent sensorimotor sequelae, impairment of skilled hand function being one of the most prevalent complaints. Neuropyhsiological predictors of motor skill recovery are still poorly understood; however, they may help to define subgroups of patients with different potential for beneficial outcome. Here, we prospectively examined cerebral blood flow in a group of stroke patients in the first nine months after stroke to delineate the hemodynamic basis of successful motor skill recovery.
Methods: We investigated skilled hand function and cerebral blood flow (CBF) with MRI in 12 patients with ischemic stroke to primary sensorimotor areas (8 lesions on the right hemisphere) and 12 age-matched healthy volunteers. Patients were assessed at 3 and 9 months after stroke, volunteers at two time points 3 weeks apart. Hand function was assessed with the Jebsen-Taylor Test (JTT), which measures manual skill with seven timed subtests that simulate everyday skills. Behavioural recovery was defined as JTT score reduction between examinations. Anatomical images and pulsed arterial spin labelling (PASL) sequences were acquired using a 3T MRI system. Anatomical scans consisted of one set of 3D T1-weighted images. PASL data were acquired as follows: gap between the labelling slab and proximal slice = 10 mm; labelling time 700 ms; post-labelling delay 1500 ms, TR = 4000 ms, TE = 15 ms, FOV = 230 × 230 mm^2, matrix size 64x64; six slices at a distance of 1.5 mm; slice thickness 6.0 mm. The anatomical scans were segmented and normalized using the unified segmentation algorithm in SPM5, which has shown robust results in patient populations. Mean CBF maps were reconstructed using in-house software for SPM5 running on Matlab. PASL time series were realigned to correct for motion artefacts, calculated CBF maps were co-registered with each participant's T1 image, normalized with the parameters obtained during segmentation, and then spatially smoothed with a 3D 10 mm FWHM Gaussian kernel. Patient images were flipped before statistical analysis, such that all lesions were on the right hemisphere. We computed two-sample t-tests between CBF maps of patients and controls for both time points. We applied linear regression to model the relationship between CBF and JTT score changes. To assess individual perfusion across recovery, CBF data were extracted from anatomical ROIs covering premotor and postcentral areas. Cytoarchitectonic probabilistic maps in SPM5 were applied for localisation.
Results: All patients performed the JTT faster at 9 months compared to 3 months post stroke ($t12 = 2.2$, $p = .04$). Six patients showed protracted recovery, whereas the other six had already attained relatively low JTT scores at 3 months. Compared to healthy volunteers, patients showed widespread hypoperfusion involving the affected sensorimotor cortices. This included the ispilesional premotor areas, and the contralesional cingulate motor areas at 3 months post-stroke ($t22 = 2.5$, $p < .01$). Linear regression revealed two clusters of CBF that were

significantly correlated with contralesional manual recovery between 3 and 9 months: an anterior cluster spanning premotor areas including the SMA (60% probability for cytoarchitectonic area 6), and a posterior cluster in the postcentral gyrus (40% probability for cytoarchitectonic area 3b). ROI analysis revealed that in the subgroup of protracted recovery, CBF changes in the cluster containing probabilistic area 3b correlated highly with behavioural recovery ($r = .84$, $p < .01$) (fig. 1), whereas only a moderate correlation was seen between CBF and behaviour of the same group in the anterior cluster ($r = .55$, $p < .01$).
Conclusions: Our behavioral data show a continuous recovery of hand function several months after stroke. Compared to controls, patients show areas of reduced CBF not only in the lesioned primary sensorimotor cortex, but also in secondary motor cortices, most notably cingulate motor areas and the ipsilesional premotor cortices. Of note, CBF changes within the ipsilesional sensorimotor loop (SMA/lateral premotor to primary somatosensory cortex) show a liner correlation with hand function scores. The highest correlation is seen within the primary somatosensory cortex (including probabilistic area 3b) for a subgroup of patients with protracted recovery, indicating that hemodynamic parameters within these regions are essential for restitution of skilled hand function.

77

Cellular abnormalities and differential gene expression in the brain of spontaneously hypertensive rats may cause cerebrovascular disease

M.-F. Ritz[1], F. Fluri[2], S. Engelter[2], N. Schaeren-Wiemers[1], C. Grond-Ginsbach[3], P. Lyrer[2]
[1]Neurobiology Laboratory, Basel, Switzerland, [2]Stroke Unit, Neurology Clinic, Basel, Switzerland, [3]Neurology, Heidelberg, Germany

Cerebral small vessel disease (VaD) is an important cause of stroke, cognitive decline and dementia. The pathology is associated with diffuse white matter abnormalities and small deep cerebral ischemic infarcts. Hypertension is one of the main risk for the disease, however, the cellular and molecular mechanisms involved in the development and progression of this condition are not yet fully understood. To identify potential players that may induce the disease, we performed cellular and gene expression analysis in the brain of Spontaneaously Hypertensive Rats (SHR) in comparison with the normotensive strain Wistar Kyoto (WKY) at various ages. Immunohistological analysis of the cortex and striatum of SHR revealed higher microvessel densities in both brain regions, but a reduced number of astrocytes. Moreover, signs of hypoxia-like conditions were observed in the brains of 9-month old SHR, that were absent in age-matched WKY. Gene expression study from the cortex of 2 and 9-month old SHR using DNA microarray technology showed that genes involved in energy and lipid metabolisms, mitochondrial respiratory chain, oxidative stress and hypoxia preconditioning were significantly differentially expressed compared to WKY. These results suggest that vascular dementia may be due to abnormal neurovascular units leading to hypoxia. The underexpression of genes belonging to cell metabolism and hypoxia preconditioning clearly demonstrated the unability of the SHR brains to tolerate high energy consumption and/or low oxygen conditions. This study gives some new insights into the pathomechanisms of small vessel disease, and may help targeting pathways for prevention and therapeutic strategies for patients at risk.

78

Characterization of lipid binding specificities of dysferlin's C2 domains

S. Di Fulvio[1], C. Therrien[2], S. Pickles[2], M. Sinnreich[1]
[1]Neuromuscular Center, Department of Neurology, Basel, Switzerland, [2]Montreal Neurological Institute, Montreal, Canada

Background: Mutations in the dysferlin gene lead to Limb Girdle Muscular Dystrophy type 2B (LGMD2B), Miyoshi Myopathy (MM) and distal anterior compartment myopathy. Dysferlin is a type II transmembrane protein with seven C2 domains and a DysF domain. Dysferlin is essential for membrane fusion events during skeletal muscle membrane repair, an important process that is currently poorly understood.
Objective: To better understand dysferlin's function, we sought to characterize the binding specificities of dysferlin's seven C2 domains to biologically relevant phospholipids and phosphoinositides that compose mammalian lipid membranes.
Methods: We have generated recombinant dysferlin C2-domain GST fusion proteins, as well as a GST C2A-domain synaptotagmin I fusion construct. Binding of fusion proteins to membranes blotted with biologically relevant lipids was assayed. Liposome centrifugation assays were performed to quantify the lipid protein binding.
Results: Using protein-lipid overlay assays and liposome centrifugation assays, we showed that dysferlin's C2A domain binds to phosphatidylserine (PS), phosphatidylinositol 4-phosphate (PIP) and phosphatidylinositol 4,5-bisphosphate (PIP2) in a calcium-dependent manner. Dysferlin's other C2 domains each bound PS in a weaker, calcium-independent manner.
Conclusion: The identified interactions between dysferlin and phospholipids may serve to fuse vesicular structures to the plasmamembrane during sarcolemmal repair.

79

Claudication of the lumbosacral plexus

F. Hatz, M. Sinnreich
Neuromuscular Center, Department of Neurology, Basel, Switzerland

Objective: To describe claudication of the lumbosacral plexus as a rare cause of reversible, exercise induced lower extremity sensori-motor deficits in a patient with high grade stenosis of both internal iliac arteries.
Methods and results: A 65 year old patient was addressed to our service for a 6 year history of exercise induced painful burning sensation and weakness in both lower extremities, occurring after walking for 50 meters. He underwent several lumbar operations due to lumbar spinal stenosis and percutaneous dilations of femoral arteries in both legs due to peripheral arterial occlusive disease, without improvement of symptoms. Clinical examination at rest showed no deficits with respect to force, sensation and reflexes in both lower extremities. Passive movements of both legs did not precipitate the symptoms. However, active flexion in either hip joints for 20 seconds triggered the painful sensation in the corresponding lower extremity, descending from the buttock into the leg, accompanied by weakness. After few minutes at rest, symptoms recovered entirely. Magnetic resonance angiography demonstrated absence of flow in the left internal iliac artery and a high grade stenosis of the right internal iliac artery, suggesting that claudication of the lumbosacral plexus was at the origin of the patient's symptoms. The patient is currently undergoing further angiologic work-up and treatment.
Conclusion: Claudication of lumbosacral plexus is a rare, potentially treatable cause for exercise induced pain and weakness in the lower extremities. This entity may be underdiagnosed.

80

Clinical and genetic analysis of 42 patients suspected for cadasil from lombardia gens registry

C. Valcarenghi[2], P. Baron[2], S. Lanfranconi[2], M. Sessa[3], G. Comi[3], G. Boncoraglio[4], E. Parati[4], P. Santoro[5], C. Ferrarese[5], C. Motto[6], R. Sterzi[6], G. Miceli[7], A. Pezzini[8], A. Padovani[8], S. Penco[1], S. Calzavara[3], P. Carrera[3], F. Taroni[4], C. Gellera[4], M. Grasso[10], E. Arbustini[10], M.T. Bassi[9], L. Obici[10], G. Merlini[10], S. Corti[2], G.P. Comi[2], M. Morbin[4], F. Tagliavini[4], G. Tadini[2], L. Candelise[2], A. Bersano[1]
[1]Neurocentro della Svizzera Italiana, Ospedale Civico, Lugano, Switzerland, [2]IRCCS Fondazione Ospedale Maggiore Policlinico, Mangiagalli e Regina Elena, Milano, Italy, [3]IRCCS Fondazione San Raffaele del Monte Tabor, Milano, Italy, [4]Fondazione IRCCS Istituto Neurologico Carlo Besta, Milano, Italy, [5]Azienda Ospedaliera San Gerardo, Monza, Italy, [6]Azienda Ospedaliera Niguarda Ca' Granda, Milano, Italy, [7]Istituto neurologico 'C.Mondino', Pavia, Italy, [8]Spedali Civili di Brescia, Clinica Neurologica e Neurologia Vascolare, Brescia, Italy, [9]Istituto Eugenio Medea, Bosisio Parini (Lecco), Italy, [10]IRCCS Policlinico San Matteo, Pavia, Italy

Backgroud/objective: CADASIL (Cerebral Autosomal Dominant Arteriopathy with Subcortical Infarcts and Leucoencephalopathy; OMIM#125310) is an autosomal dominant small arteries disease, mostly of brain, caused by mutations of the NOTCH3 gene on chromosome 19.The clinical phenotype is highly variable and is characterized by recurrent ischemic episodes, migraine with aura, mood disorders, cognitive deficits and seizures. Typical MRI features are diffuse and severe white matter changes

frequently extending to the anterior pole of the temporal lobe and lacunar infarcts. However given the extreme phenotypic variability and the small number of published series it is difficult to identify disease prevalence and specific clinical and MRI features suggestive for disease. The aim of this study is to validate the reliability of a diagnostic algorithm and to evaluate clinical features and genetic aspect of CADASIL highly suspected patients recruited by LOMBARDIA GENS project, a regional italian network investigating the prevalence of six monogenic diseases associated with stroke.
Patients/methods: 42 patients with suspected CADASIL were collected during two years project. For each patient demographic, clinical, familial history data and diagnostic criteria were registered using a standardised form and diagnostic algorithm.
Results: Genetic analysis showed the presence of causative mutations in three subjects (7%). Of the remaining cases, 26 were carriers of a polymorphism in exon 3 or 4 or an intronic mutation (62%) while twelve of them (29%) did not present any variant gene. Patients carrying causative mutations seem to have less cerebrovascular risk factors and a positive familiar history for cerebrovascular disease, in comparison to negative ones, whereas imaging were similar in the two groups. Notch3 polymorphisms and intronic mutations do not appear to generate significant phenotypic variations.
Discussion: Despite the small number of recruited patients hampers any significant conclusion, the proposed,diagnostic algorithm was demonstrated to be easy to use, reliable and sensible for CADASIL diagnosis. Since 7% of positive patients were found. Despite lack of risk factors and familial history were the most important differentiating factors, the extension of genetic analysis to all Notch3 exons will provide more accurate genotype-phenotype correlation. Skin biopsy will be critical to determinate whether polymorphisms or intronic mutations are associated to intermediate phenotypes or any vessel abnormalities like GOMS

81

Complete Healing of a Dissected Cervical Carotid Artery With Perfused False Lumen After Conservative Treatment

H. Sarikaya[1], K. Barath[1], R.W. Baumgartner[1]
[1]Neurology Department, Zurich, Switzerland,
[2]Institute of Neuroradiology, Zurich, Switzerland

In spontaneous dissection of the cervical internal carotid artery (sICAD), blood located in the false lumen is typically coagulated, which may account for the observation that sICAD does not rupture. We present the first sICAD patient with a perfused false lumen proven by color duplex ultrasound and magnetic resonance angiography. Treated conservatively with oral aspirin followed by warfarin, the dissected vessel healed completely without any complications.

82

Congenital myasthenic syndrome due to mutation in RAPSN

F. Hatz, H.R. Stöckli, M. Sinnreich
Neuromuscular Center, Department of Neurology, Basel, Switzerland

Objective: Congenital myasthenic syndromes are rare genetically determined disorders of the neuromuscular junction, manifesting predominantly in infancy. Anatomic localization of the neuromuscular transmission defect can be presynaptic, synaptic or postsynaptic. Identification of the molecular defect is important, as treatment options depend on the synaptic localization of the transmission defect. We describe an adult female patient with a postsynaptic congenital myasthenic syndrome due to mutations in the rapsyn (RAPSN) gene.
Methods and results: The patient was born with severe contractures of multiple articulations in upper and lower extremities (arthrogryposis multiplex). In early postnatal days she had cardio-pulmonary arrest requiring reanimation. Her sister died suddenly in infancy. The patient suffered since childhood from generalized weakness, which exacerbated under fever to such a degree that she would develop breathing and swallowing problems. Clinically she presented with a myopathic facies, contractures of finger joints, as well as fatiguable upper and lower extremities. Electrodiagnostic tests showed a neuromuscular transmission defect. Genetic analysis revealed a heterozygous mutation in the RASPN gene (N88K).
Conclusion: Congenital myasthenic syndromes are rare diseases, but should be suspected even in an adult patients with myopathic signs, fatiguability and bulbar symptoms. Sudden death in infancy is common for certain myasthenic syndromes, as was most probably the case in the patient's sister. Electrodiagnostic and genetic studies can help in securing the diagnosis.

83

Correlation of lesions MRI properties and attention deficits in early relapsing-remitting multiple sclerosis

S. Simioni[1], T. Kober[2], G. Krueger[3], M. Shevlyakova[4], P. Browaeys[5], J.-M. Annoni[6], R. Du Pasquier[1], R. Meuli[5], M. Schluep[1], C. Granziera[7]
[1]Department of Neurology, CHUV, Lausanne, Switzerland, [2]Laboratory for functional and metabolic imaging, Ecole Polytechnique Fédérale de Lausanne (EPFL), Lausanne, Switzerland, [3]Advanced Clinical Imaging Technology, Siemens Suisse SA - CIBM, Lausanne, Switzerland, [4]Chair of Applied Statistics, Ecole Polytechnique Fédérale de Lausanne (EPFL), Lausanne, Switzerland, [5]Department of Radiology, CHUV, Lausanne, Switzerland, [6]Department of Neurology, HUG, Geneva, Switzerland, [7]Brain and Mind Institute, Ecole Polytechnique Fédérale de Lausanne (EPFL), Lausanne, Switzerland

Introduction: Cognitive impairment affects 40–65% of multiple sclerosis (MS) patients, often since early stages of the disease. MRI has been extensively exploited to investigate the underlying physiopathological mechanisms but they still remain unclear. In this study, we aimed at characterizing and correlating the T1 relaxation times of cortical and sub-cortical lesions with cognitive deficits in a group of early relapsing-remitting (RR) MS patients.
Methods: Ten RRMS patients (age: 31.6 ± 4.7 y; disease duration: 3.8 ± 1.9 y; EDSS disability score: 1.8 ± 0.4) and 10 healthy volunteers (mean age: 31.2 ± 5.8 y) were included in the study. Participants underwent the Brief Repeatable Battery of Neuropsychological tests (BRB-N), Stockings of Cambridge, Trail Making Test (TMT), Boston Naming, Hooper Visual Organization Test and Rey-Osterrieth Complex Figure. Brain MRI was then performed at 3T (Magnetom Trio a Tim System, Siemens, Germany) using a 32-channel head coil. The imaging protocol included 3D sequences with 1x1x1.2 mm^3 resolution and 256x256x160 matrix (DIR, MPRAGE, MP2RAGE, FLAIR SPACE) and 2D Axial FLAIR (0.9x0.9x2.5 mm^3, 256x256x44 matrix). Lesion number, volume and T1 value were calculated in each contrast and in a merged mask representing the union of the lesions from all contrasts. T1 values of lesions were normalized with the mean T1 value in corresponding control regions of the healthy subjects. Parametric (t-tests) and non parametric (Spearman correlations) statistics were performed.
Results: Cortical and sub-cortical lesions count, T1 values and volume are reported in table 1. All RRMS patients showed cortical lesions (CLs), mainly CLs type I (CLs extending to the sub-cortical tissue). Patients also had lower performances in attention and information processing speed (TMT-A: $p = 0.01$; TMT-B: $p = 0.006$; PASAT from BRB-N: $p = 0.04$). The T1 values of CLs type I negatively correlated with the TMT-A score ($r = 0.78$, $p < 0.01$). The correlation between lesion volume and T1 value of CLs type I was insignificant, precluding an influence of partial volume effects on T1 values.

	total	DIR	FLAIR	MP2RAGE	MP-RAGE	SPACE
GM	8	18	8	12	10	14
WM	309	258	159	252	242	219
GM/WM	26	24	13	22	19	23
Σ	343	300	180	286	271	256

Table 1 A: Number of lesions recognised in the different MR sequences

	T1 (ms) of lesions (patients)	T1 (ms) of non-lesion tissue (patients)	T1 (ms) in control ROIs of healthy controls	Lesions' Volume (mm^3)
GM	1548±280	1390±31	1383±97	34.5±22.3
WM	1265±103	827±31	778±95	3981.9±4917.5
GM/WM	1521±161	1117±11	1087±100	396.6±461.8

Table 1 B: Inter-subject mean and standard deviation of the T1 relaxation times and volume

Conclusions: We report for the first time the presence and the T1 characteristics at 3T of CLs in early RRMS. CLs type I represent the most frequent CLs type in this cohort. Less attention deficits are concomitant with longer T1 values in CLs. Thus, long relaxation times might reflect a degree of tissue loss sufficient to stimulate compensatory mechanisms as those shown, in fMRI studies, to help maintaining attention performances in MS.

84

CT-Based IV Thrombolysis 3 to 4.5 Hours After Acute Ischemic Stroke in Clinical Practice

H. Sarikaya, P. Valko, A. Weck, D. Georgiadis, R.W. Baumgartner
Neurology Department, Zurich, Switzerland

Background: Outcome of stroke patients selected with cerebral computed tomography (CCT) for intravenous thrombolysis (IVT) administered in clinical routine from 3 to 4.5 hours after symptoms onset is not well investigated.
Objective: To compare the safety and clinical outcome of IVT in routine clinical praxis performed 181-270 minutes (late) and within 180 minutes (early) after onset of ischemic stroke in patients selected with CCT.
Design, Setting and Patients: A single-center prospective observational cohort study of consecutive patients with ischemic stroke undergoing CCT based IVT within 4.5 hours after symptom onset in a university hospital between March 1, 2002, and October 31, 2008.
Main Outcome Measures: The occurrence of symptomatic intracranial hemorrhage (sICH) within 36 hours after treatment, mortality and favorable outcome defined as a modified Rankin Scale score of 0-1 at 3 months.
Results: Of the 394 included patients, 100 were treated late. In this group, median baseline National Institutes of Health Stroke Scale (NIHSS) score was lower (9.5 vs 11.3, $p = 0.01$) and a longer median time-to-treatment (209 vs 142 minutes, $p < 0.0001$) than in the early group. The incidence of sICH (2.0% vs 2.4%, $p = 1.0$), death (9.0% vs 9.9%, $p = 1.0$) and favorable outcome (58.0% vs 51.5%, $p = 0.3$) were similar between the late and early cohorts. After adjustment for NIHSS score, no significant outcome differences were detectable between both groups.
Conclusion: These data suggest that IVT performed 181 to 270 minutes after symptoms onset in stroke patients selected with CCT is also beneficial in real-life clinical practice.

85

Data-driven approach to the topology of the iEEG functional network during epileptic seizures

F. Amor, C. Rummel, H. Gast, K. Schindler
Inselspital, Bern, Switzerland

Epileptic seizures are due to abnormal interactions between distributed brain areas. Critical parts of the underlying functional network may be surgical therapeutic targets and may be identified by graph theory that aims at characterizing local and global properties of the networks. To assess the functional topology, the network may be derived from the cross-correlation matrix of multi-site intra-cranial EEG recordings (iEEG). Classically, a unique threshold is used that constrains the topology by fixing a priori the average number of connections per node. Our new data-driven method dynamically evaluates a threshold for each pair of channels, thus allowing time varying. This approach is better suited to study seizure dynamics with an often dramatically changing number of functional links between distant sites. We investigated the iEEG of 5 patients suffering from pharmaco-resistant focal onset seizures. The zero-lag cross-correlation matrices were evaluated after filtering the signals in various frequency bands. We assessed the topologies of the underlying functional networks using our method, explored the time course of every seizure and every frequency band and selected the frequency bands where its range was appropriate for normalizing the graph measures between the regular and random cases. The spatio-temporal courses of local and global efficiency and nodal betweenness centrality were assessed. During the peri-ictal periods, time course was reproducible across the seizures of each patient, and differed across frequency bands. However, only in the beta-band values allowed proper normalization of the graph measures. In this frequency band, efficiency and betweenness centrality showed reproducible modifications of the networks topology characterizing seizure onset, seizure propagation and seizure termination. Using a data-driven instead of a unique threshold helps to restrict graph theoretical analysis to specific frequency bands and provides insights into the topology of epileptic functional networks during different seizure stages.

86

Decision making performances inmultiple sclerosis

J.M. Annoni
University hospital and medical school, Lausanne and Geneva, Switzerland

The purpose of this presentation is to discuss longitudinally, using the Iowa Gambling Task (IGT) and the weel of fortune, the dynamics of decision making capacity at a two-year interval in a group of patients with multiple sclerosis (MS) (n = 70) and minor neurological disability 2.5 at baseline). Cognition ≤(Expanded Disability Status Scale [EDSS] (memory, executive functions, attention), behavior, handicap and perceived health status will also be investigated. Standardized change scores ([score at retest-score at baseline]/standard deviation of baseline score) were computed. Results will that IGT performances decreased from baseline to retest. MS patients who worsen in the IGT are more likely to show a decreased perceived health status and emotional well-being. Relapsing rate, disability progression, cognitive and behavioral changes were not associated with decreased IGT performances. In conclusion, decline in decision making can appear as an isolated deficit in MS.

87

Differences of ischaemic posterior and anterior circulation strokes in 1449 consecutive patients

E. Rouge[1], B. Richoz[2], M. Faouzi[2], P. Michel[1]
[1]CHUV – UNIL, Lausanne, Switzerland, [2]Institute of Social and Preventive Medicine, Lausanne, Switzerland

Background: The current data comparing posterior and anterior circulation strokes with regards to clinical, etiological, radiological and outcome factors are conflicting. We searched for distinguishing features between both territories in 1628 consecutive acute ischemic stroke patients.
Methods: All consecutive patients with acute ischemic stroke admitted to a single stroke unit from January 2003 to July 2008 were included in a prospective registry. Territory of acute stroke was determined by a combination of neuroimaging (MRI and / CT / CTP) and clinical symptoms and signs. Patients with uncertain localisation and patients with simultaneous strokes in the anterior and posterior circulation were excluded from this analysis.
Results: Of a total of 1'628 patients, 466 (17.0%) had had posterior, 983 (56.8%) anterior, 136 (7.9%) unknown territory, and 43 (2.5%) simultaneous posterior and anterior territory stroke. Of 39 variables that were compared, 29 differed significantly in univariate analysis, including less dependency (OR = 0.50) and mortality (OR = 0.56) at 3 months in posterior stroke. In multivariate analysis (see table), male gender, lacunar mechanism, arterial dissection and endovascular recanalisation were more frequent in posterior stroke, whereas admission NIHSS, and IV-thrombolysis rate were lower. Significant acute arterial pathology (≥50% stenosis) was less frequently found on acute imaging in posterior stroke (OR = 0.33). Of 633 patients with significant arterial pathology, it was more frequently present intracranially in posterior (OR = 1.62) and extracranially in anterior stroke (OR = 0.87). In 610 patients where recanalisation was assessed at 24 hours, intracranial (OR = 0.26), extracranial (OR = 0.25) and overall recanalisation (OR = 0.34) was less frequent in the posterior circulation.
Conclusions: Acute posterior strokes are less severe and recover better, despite lower IV thrombolysis and recanalisation rates. They are more frequently due to lacunes and dissections and have less arterial pathology burden than anterior circulation strokes.

88

Drug screening for Myotonic dystrophy type 1 (DM1)

J. Kinter, M. Sinnreich
Neuromuscular Center, Department of Neurology, Basel, Switzerland

Objectives: To develop a screening assay for small molecular compounds for the treatment of myotonic dystrophy type 1.
Background: Myotonic dystrophy type 1 (DM1) is a genetic disorder caused by the expression of RNA species with expanded CUG triplet repeats causing toxicity through sequestration of splice factors. This results in mis-splicing of several pre-mRNAs leading to disease symptoms. Experimental evidence suggests that release of the sequestered splicing factor muscleblind-like 1 (MBNL1) might reverse certain aspects of DM1 pathology.
Methods: Ligand mediated conformational stabilization of proteins is a phenomenon in which substrates, inhibitors and cofactors provide enhanced stability to proteins upon binding. This phenomenon is based on the energetic coupling of the ligand-binding and protein-melting reactions. Using the fluorescent dye SYPRO Orange as a conformational indicator, thermal shift assay can be performed with various real time PCR platforms. Here we use for the first time the thermal shift assay to study RNA-protein interactions in an attempt to design a screening platform for the identification of small molecular weight compounds capable of interfering between expanded CUG repeats and a sequestered splice factor.
Results: Thermal shift analysis under various conditions revealed a robust and sensitive protocol to screen protein-RNA interactions between MBNL1 protein and CUG repeat RNA.
Conclusion: In an attempt to develop a screening assay for small molecular compounds for the treatment of DM1 we set up a novel screening system capable for high throughput screening.

89

Dysferlin interacts with alpha-tubulin in skeletal muscle

B.A. Azakir[1], S. Di Fulvio[1], B. Erne[1], C Therrien[2], M. Sinnreich[1]
[1]Neuromuscular Center, Department of Neurology, Basel, Switzerland, [2]Montreal Neurological Institute, Montreal, Canada

Background: Mutations in the dysferlin gene lead to Limb girdle muscular dystrophy type 2B (LGMD2B), Miyoshi Myopathy (MM) and distal anterior compartment myopathy. Dysferlin is a type II transmembrane protein containing seven C2 domains and two Dysf domains localized at the sarcolemma, the t-tubule system and to cytoplasmic vesicles. Dysferlin is an integral part of the skeletal muscle surface membrane repair machinery, but its mode of action is still poorly characterized.
Objective: Identifying dysferlin protein binding partners and understanding their role in dysferlin mediated membrane repair should shed light on the membrane repair mechanism and should be important for the development of therapeutic strategies for dysferlinopathies.
Methods: We used affinity purification followed by liquid chromatography/mass spectrometry on dysferlin pull down from mouse skeletal muscle tissue to identify novel dysferlin binding partners. Interaction of identified binding partners was confirmed by co-immunoprecipitation and confocal co-localization studies. Mapping of dysferlin domains involved in binding was performed by immunoprecipitation with individual C2 domain- GST fusion proteins.
Results: We have identified a large number of novel potential dysferlin protein binding partners. We were able to identify the few proteins that were previously shown to interact with dysferlin demonstrating the validity of the chosen approach. One of the identified partners was alpha-tubulin. We show by co-immunoprecipitation and pull down assays that dysferlin interacts with alpha-tubulin in vitro and in vivo. Dysferlin co-localized with alpha-tubulin close to the perinuclear region in myoblasts and along microtubules in myotubes. This interaction is mediated by dysferlin's C2A and C2B domain and is calcium independent.
Conclusion: We suggest that microtubules are implicated in dysferlin trafficking to the sarcolemma, a pathway that is currently poorly characterized for dysferlin.

90

EEG reactivity during hypothermia after cardiac arrest: a new outcome predictor

A.O. Rossetti[1], L.A. Urbano[1], P.W. Kaplan[2], M. Oddo[1]
[1]CHUV and UNIL, Lausanne, Switzerland, [2]Johns Hopkins Bayview Medical Center, Baltimore, United States

Introduction: Comatose survivors of cardiac arrest (CA) are increasingly treated by therapeutic hypothermia (TH). Continuous EEG (cEEG) is used to monitor brain function in ICU patients, but its value in patients with CA and TH is only beginning to be elucidated. The aim of this study was to examine whether cEEG during TH predicts outcome in these patients.
Methods: Between April 2009 and January 2010, consecutive comatose adults treated with TH after CA were prospectively included. We recorded demographical and pertinent clinical data; cEEG was performed during TH, under standard sedation, and EEG reactivity was tested at bedside. EEG, SSEP and clinical examinations were repeated after rewarming; decisions on ICU support interruption where taken without considering cEEG. Mortality at hospital discharge was the primary outcome; Glasgow-Pittsburgh Cerebral Performance Categories (CPC) at one month were also assessed. Owing to multiple comparisons, we considered $p < 0.0125$ as significant (Bonferroni).
Results: Among 31 consecutive patients, twenty-one received cEEG during TH and were analyzed. Mortality occurred in 9/21 (42.9%). Non-reactive cEEG background was observed in 6/9 (67%) non-survivors vs. 0/12 survivors ($p < 0.002$), prolonged discontinuous EEG activity (burst-suppression) in the same 6/9 (67%) non-survivors vs. 0/12 survivors ($p < 0.002$); sustained epileptiform abnormalities were seen in 4/9 (44%) non survivors (all with absent reactivity) vs. 0/12 survivors ($p = 0.021$). No patient with non-reactive or irritative EEG during TH improved at normothermia; epileptiform features were observed over the whole recording. Non-reactive cEEG and burst-suppression during TH had a positive predictive value of 100% (95%CI: 52%–100%) with a false positive rate of 0% (95%CI: 0%–26%) for mortality. Of the 12 survivors, one remained vegetative (CPC 4) at one month; 5 each had a CPC of 1 and 2, and one a CPC of 3.
Conclusion: Lack of EEG background reactivity and burst-suppression on cEEG during TH are robust early predictors of in-hospital mortality after CA.

91

Effect of repetitive arm cycling following Botulinum toxin for post-stroke spasticity as evident from fMRI

K. Diserens[1], D. Ruegg[2], R. Kleiser[3], S. Hyde[2], N. Perret[4], P. Vaudens[5], E. Fornari[6], F. Vingerhoets[7], R.J. Seitz[8]
[1]Department of Clinical Neurosciences, Unit for Early Neurorehabilitation, Centre Hospitalier Universitaire (CHUV), Lausanne, Switzerland, [2]Department of Medicine, Fribourg, Switzerland, [3]Brain Imaging Centre West, Jülich, Germany, [4]Neurological Centre Plein Soleil, Lausanne, Switzerland, [5]Reeducation Centre, Sion, Switzerland, [6]Department of Radiology, CIBM-Centre Hospitalier Vaudois (CHUV, Lausanne, Switzerland, [7]Department of Clinical Neurosciences, Neurology Service, Centre Hospitalier Universitaire Vaudois (CHUV) and University of Lausanne, Lausanne, Switzerland, [8]Department of Neurology, University Hospital Düsseldorf, Düsseldorf, Switzerland

Introduction: Investigations were performed to establish if repetitive arm cycling training enhances the anti-spastic effect of intramuscular botulinum toxin (BTX) injections in post-ischemic spastic hemiparesis. Effects on cerebral activation were evaluated by functional magnetic resonance imaging (fMRI).
Methods: Eight chronic spastic hemisyndrome patients (49 ±10 years) after middle cerebral artery infarction (5.5 ± 2.7 years) were investigated. BTX was injected in biceps and arm flexors into the affected arm twice, 6 months apart. Spasticity was assessed using the Ashworth scale and range of motion before and 3 months after BTX injections. Images were analyzed using Brain Voyager QX 1.8, and fMRI-signal changes were corrected for multiple comparisons (qFDR <0.05).
Results: During passive movements of affected and non-affected arms, fMRI-activity was increased bilaterally in sensorimotor cortex (MISI), secondary somatosensory areas (SII), and supplementary motor area predominantly in the contralesional hemisphere compared with rest. Following repetitive arm cycling, fMRI-activity increased further in MISI of the lesioned hemisphere and SII of the contralesional hemisphere. For patients with residual motor activity, treatment-

related fMRI-activity increases were associated with reduced spasticity; in completely plegic patients, there was no fMRI-activity change in SII but increased spasticity after training.
Conclusion: Increased activity in SII of contralesional hemisphere and in MISI of lesioned hemisphere reflect a treatment-induced effect in the paretic arm. It is hypothesised that the increased BOLD activity results from increased afferent information related to the anti-spastic BTX effect reinforced by training.

92

Effect of Vitamin D on Epstein-Barr (EBV)-specific CD8+ T cells in patients with early multiple sclerosis (MS)

A.P. Lysandropoulos, E. Jaquiery, S. Jilek, M. Canales, G. Pantaleo, M. Schluep, Ra Du Pasquier
CHUV, Lausanne, Switzerland

Background: Infection with EBV and a lack in vitamin D may be important environmental triggers of MS. 1,25-(OH)2D3 mediates a shift of antigen presenting cells (APC) and CD4+ T cells to a less inflammatory profile. Although CD8+ T cells do express the vitamin D receptor, a direct effect of 1,25(OH)2D3 on these cells has not been demonstrated until now. Since CD8+ T cells are important immune mediators of the inflammatory response in MS, we examined whether vitamin D directly affects the CD8+ T cell response, and more specifically if it modulates the EBV-specific CD8+ T cell response.
Material and methods: To explore whether the vitamin D status may influence the pattern of the EBV-specific CD8+ T cell response, PBMC of 10 patients with early MS and 10 healthy controls (HC) were stimulated with a pool of immunodominant 8-10 mer peptide epitopes known to elicit CD8+ T cell responses. PBMC were stimulated with this EBV CD8 peptide pool, medium (negative control) or anti-CD3/anti-CD28 beads (positive control). The following assays were performed: ELISPOT to assess the secrection of by T cells in general; cytometric beads array (CBA) and ELISA toγIFN- determine which cytokines were released by EBV-specific CD8+ T cells after six days of culture; and intracellular cytokine staining assay to determine by which subtype of T cells secreted given cytokines. To examine whether vitamin D could directly modulate CD8+ T cell immune responses, we depleted CD4+ T cells using negative selection.
Results: We found that pre-treatment of vitamin D had an anti-inflammatory action on both EBV-specific CD8+ T cells and on CD3/CD28-stimulated T cells: secretion of pro-inflammatory cytokines (IFN-gamma and TNF-alpha) was decreased, whereas secretion of anti-inflammatory cytokines (IL-5 and TGF-beta) was increased. At baseline, CD8+ T cells of early MS patients showed a higher secretion of TNF-alpha and lower secretion of IL-5. Addition of vitamin D did not restore the same levels of both cytokines as compared to HC. Vitamin D-pre-treated CD8+ T cells exhibited a decreased secretion of IFN-gamma and TNF-alpha, even after depletion of CD4+T cells from culture.
Conclusion: Vitamin D has a direct anti-inflammatory effect on CD8+ T cells independently from CD4+ T cells CD8+ T cells of patients with early MS are less responsive to the inflammatory effect of vitamin D than HC, pointing toward an intrinsic dysregulation of CD8+ T cells. The modulation of EBV-specific CD8+ T cells by vitamin D suggests that there may be interplay between these two major environmental factors of MS.
This study was supported by a grant from the Swiss National Foundation (PP00P3-124893), and by an unrestricted research grant from Bayer to RDP.

93

Effects of amygdalo-hippocampal stimulation on interictal epileptic discharges and synchronization

R. Tyrand[1], M. Seeck[1], L. Spinelli[1], E Pralong[2], S. Vulliémoz[1], G. Foletti[2], A.O. Rossetti[2], C. Pollo[2], C. Boëx[1]
[1]University Hospital Geneva, Geneva, Switzerland, [2]Centre Hospitalier Universitaire Vaudois, Lausanne, Switzerland

Introduction: The objective of the study was to assess the effects of pulse shape of high frequency deep brain stimulation (DBS) of the amygdalo-hippocampal complex (AH) on interictal epileptic discharge rates (IEDRs) and synchronization.
Methods: The effects of AH-DBS implemented with symmetrical versus asymmetrical biphasic and charge balanced pulses were evaluated in two different groups of patients: six patients with hippocampal sclerosis (HS) and six patients with non lesional (NLES) temporal lobe epilepsy. Synchronization of amygdalo-hippocampal and fronto-orbital intracranial EEG, ipsilateral to the epileptic focus, was computed.
Results: In HS patients, IEDRs were significantly reduced only with high frequency AH-DBS applied with symmetrical biphasic pulses. IEDRs were significantly reduced with high frequency AH-DBS in only two NLES patient, independently of pulse shape. If high frequency AH-DBS principally induced desynchronization, IEDRs and synchronization were not correlated.
Conclusions: The decrease of IEDRs suggest that high frequency AH-DBS could be efficient in HS patients if the stimulation was applied over a large zone through symmetrical biphasic pulses; in NLES patients, other individual characteristics might alter the efficacy of DBS like the localization of the epileptogenic zone and of the electrode. Comparison to long-term outcome suggests that IEDRs could be used as a predictor of chronic AH-DBS, whereas synchronization could not.

94

Effet de la fatigue physique sur la marche des hémiplégiques

A. Kassouha, L. Allet, I. Feldmann, A. Schnider
Hôpitaux Universitaires de Genève, Genève, Switzerland

Introduction: Chez les sujets hémiplégiques, les paramètres temporo spaciaux de la marche sont habituellement altérés, en particulier: la vitesse, la symétrie et la variabilité. Bien que la fatigue et la baisse de l'endurance soient des symptômes fréquents dans cette population, nous ne savons pas s'ils influencent ces paramètres.
Objectifs: Évaluer l'effet de la fatigue physique sur les paramètres de la marche dans des conditions simples et lors d'une double tâche.
Méthodes: 26 sujets hémiparétiques hospitalisés pour la rééducation suite à un accident vasculaire cérébral récent (73 ± 32 jours) et capables de marcher sans aide avec/sans moyen auxiliaire. Les paramètres de la marche ont été enregistrés à l'aide d'un tapis «GaitRite» de 7,2 m, au début et à la fin d'un circuit de marche sur un terrain plat. Le périmètre de ce circuit est déterminé quand l'effort devient difficile (5/10 sur l'échelle de Borg modifiée). L'enregistrement de la marche se fait à vitesse confortable avec et sans tâche cognitive de calcul mental.
Résultats: En fin de circuit la vitesse de marche augmente de 54,78 cm/sec (±20.24) à 58.96 cm/sec (±22,9) p = ,05. Cette augmentation est plus importante dans les conditions de double tâche, de 43,63 cm/sec (±17,21) à 49,62 cm/sec(±19,79) p = ,001. L'augmentation de la vitesse se fait par augmentation de la cadence et de la longueur de l'enjambée. L'asymétrie de longueur des pas augmente à la fatigue tant lors de la marche simple [de 5,34 cm (±3,92) à 6,52 cm (±4,90) p = ,05] que lors de la marche en double tâche [5,96 cm (±5,49) à 8,29 cm (±6,41) p = ,01]. Le coefficient de variabilité de longueur et de largeur des pas augmente lors de la marche en double tâche en fin de circuit. Ceci est significatif par rapport à la marche simple en fin de circuit et par rapport à la marche en double tâche au début p <,05.
Conclusion: L'augmentation inattendue de la vitesse de marche lors de la fatigue ne peut pas être interprétée comme une amélioration en raison de l'altération des autres paramètres. Il est important de prendre en compte l'état de fatigue physique lors d'un enregistrement de la marche.

95

Experience with intestinal infusion of levodopa plus carbidopa (Duodopa) in advanced idiopathic Parkinson's disease

H. Lisitchkina, J. Ide, D. Zutter
Neurorehaklinik HUMAINE, Zihlschlacht, Switzerland

In 11 out of 13 patients suffering from advanced idiopathic Parkinson's disease and with an unsatisfactory response to conventional therapies a treatment with intestinal infusion of levodopa plus carbidopa (Duodopa) was succesfully established. Overall a significant improvement could be achieved. There was a significant reduction of motor fluctuations with a clear increase of functional On. A marked improvement in the parameters of daily living were observed. Hallucinations and psychotic episodes have disappeared in most patients or were at least clearly diminished. There were not significant change of cognition. Several patients reported an improvement of sleep, depression and anxiety. Other non-motor symptoms showed no significant change.

96

Gait, as a new marker of Frontotemporal dementia

G Allali[1], B Dubois[2], F Assal[1], E. Lallart[3], L.C. de Souza[2], M. Bertoux[2], C. Annweiler[4], F.R. Herrmann[5], R. Levy[6], O. Beauchet[4]
[1]Department of Neurology, Geneva University Hospitals and University of Geneva, Geneva, Switzerland, [2]Federation of Neurology, La Salpêtrière Hospital, [3]CNRS UMR 7593, IFR Neurosciences Pitié-Salpêtrière, La Salpêtrière Hospital, [4]Department of Internal Medicine and Geriatrics, Angers University Hospital, Angers, France, [5]Department of Rehabilitation and Geriatrics, Geneva University Hospitals and University of Geneva, Geneva, Switzerland, [6]Hôpital Saint-Antoine, Service de Neurologie, Paris, France

Introduction: Gait and cognition are closely related in healthy older adults and demented subjects. The main diagnostic criteria of the behavioural variant of frontotemporal degeneration (bvFTD) include neurobehavioral and dysexecutive syndromes, but not gait changes although strong relationship between gait and prefrontal functions are increasingly recognized. The goal of this study was to compare gait variability between bvFTD, AD and healthy control and to describe the specificity of gait disorders in bvFTD using normal gait and gait during dual-tasking.
Methods: 19 subjects with bvFTD, 19 with AD and 22 healthy controls were included in this study. Mean values and coefficients of variation (CV) of temporal gait parameters while only walking and while walking and backward counting (dual tasking) were measured using the SMTECÆ-footswitch system.
Results: Stride time, mean value and CV, were significantly increased in both patient groups compared to healthy control during single task or walking alone ($p < 0.001$) and during dual tasking ($p < 0.001$). After adjusting for age, cognitive deficit, psychoactive drugs, sex and fall, only the bvFTD patient group was associated with an increase of CV of stride time during single walking ($p < 0.001$) and dual tasking ($p = 0.005$).
Conclusions: These data suggest that gait instability during single and dual tasking could represent an interesting marker for bvFTD. In clinical practice, such a diagnosis should be at least considered in any demented patient with gait instability.

97

Glucosamine-fullerenol – a nanotechnological approach in neuroprotection after experimental stroke

F. Fluri[1], E. Cam[1], D. Grünstein[3], S. Hong[3], P. Seeberger[3], B. Gao[1], C. Bassetti[1]
[1]Dep. of Neurology, University Hospital Zürich, Zürich, Switzerland, [2]Dep. of Neurology, University Hospital Basel, Basel, Switzerland, [3]Department of Biomolecular Systems, Max-Planck-Institute of Colloids and Interfaces, Potsdam, Germany, [4]Neurocenter (EOC) of Southern Switzerland, Lugano, Switzerland

Background: Fullerenol, a polyhydroxylated hollow sphere of 60 carbon atoms has been shown to possess antioxidant properties as well as other biological activities. Neuroprotective effects of water-soluble glucosamine-functionalized fullerenol (Glu-C60) in respect to infarct size were investigated in an animal model of transient cerebral ischemia.
Methods: 12 male spontaneously hypertensive rats (SHR) were subjected to transient middle cerebral artery occlusion (tMCAO) of 60 minutes using a silicone-coated filament. Immediately after reperfusion, either Glu-C60 in 0.9% NaCl (0.5 mg/kg) (n = 6) or 0.9% NaCl (n = 8) was administered intravenously. 24 hours after tMCAO the rats were euthanized and their brains were quickly removed. Infarct size was determined by image analysis (Image J) of 2,3,5-triphenyltetrazolium chloride (TTC)-stained coronal brain sections.
Results: In treated and control animals, infarct size was 136 ± 14 mm^3 and 242 ± 76 mm^3 respectively, after 24 hours. Reduction of infarct size in treated animals was 44% compared to the control group ($p = 0.011$).
Conclusion: Glu-C60 appears to reduce infarct size, probably due to its antioxidant properties. However, the exact mechanisms leading to a reduction of infarct size have to be evaluated in further studies.

98

I.V. – Thrombolysis as a Therapy for Ischemic Stroke, after previous Reversion of a present Oral Anticoagulation – 5 cases

L. Achtnichts, F. Fluri, Ph. Lyrer, St. Engelter
Department of Neurology, University Hospital Basel, Basel, Switzerland

Background: Atrial fibrillation (VHF) is a common cause of ischemic stroke. The prevalence of VHF increases with age. Oral anticoagulation with phenprocoumon is a proven preventive therapy of thromboembolic events. However, cerebral ischemia sometimes occurs even in cases with correctly, i.e. sufficiently administered oral anticoagulation. I.v.-thrombolysis with rt-PA within ≤4.5 hours after onset of symptoms has become a well-established therapy for ischemic stroke. According to different guidelines, an INR ≥1.5 (Europe) and ≥1.7 (US), is an exclusion criterion for the application of i.v.-thrombolysis. We report on 5 patients with clinically severe stroke syndromes who had stroke despite oral anticoagulation with INR >1.5 (mean 2.2). In 4 of the 5 of patients the effect of oral anticoagulation was undone with Prothromplex® NF(humane faktor II, VII, IX und X of the Prothrombin-Complex); following, i.v.-lysis with rt-PA was administered. One patient with an INR value of 1.6 was thrombolysed without a previous reversion of the oral anticoagulation. The patient data have been evaluated regarding the clinical course and complications (including intracranial hemorrhage).
Methods: The basic data (demographic variables, NIHSS, OCSP, stroke to needle and door to needle time), as well as data on clinical outcome (modified Ranking Scale – mRS – after 3 months, symptomatic intracranial hemorrhage – sICH) of the 5 patients were collected retrospectively from our stroke database and compared to those with INR <1.5 (n = 415).
Results and conclusions: On average, the 5 patients were 83.4 years old and had a mean initial NIHSS of 20 points. Compared to the average time in our clinic (mean 135 minutes), the “door to needle time” was 33 minutes longer. None of the patients with i.v.-thrombolysis after reversion of the anticoagulation had sICH. In the patient with INR of 1.6, who underwent thrombolysis without previous reversion, a sICB (NINDS-criteria) occurred. 3 of 5 patients died (malignant infarction). While one reached a “poor outcome” with mRS 4 after three months, one had a good recovery with mRS 1. Thus, in patients with reverted oral anticoagualtion before i.v. thrombolysis no intracranial bleeding occurred. Yet, no favorable clinical outcome could be noticed, either.

99

Impact of admission glucose and diabetes mellitus on recanalization and outcome after intra-arterial thrombolysis

M. Arnold[1], S. Mattle[1], A. Galimanis[1], L. Kappeler[1], U. Fischer[1], G.M. DeMarchis[1], J. Gralla[2], M.L. Mono[1], C. Brekenfeld[2], N. Meier[1], G. Schroth[2], H.P. Mattle[1]
[1]Department of Neurology, University Hospital, Inselspital, Bern, Bern, Switzerland, [2]Institute of Diagnostic and Interventional Neuroradiology, University Hospital, Inselspital, Bern, Bern, Switzerland

Background: Admission hyperglycemia predicts a worse outcome after intravenous thrombolysis (IVT) for ischemic stroke. Poor vessel recanalization and unfavourable outcome were reported in diabetics treated with IVT.
Methods: We analyzed 406 stroke patients treated with intra-arterial thrombolysis (IAT). The association of diabetes and admission glucose values with recanalization, outcome and mortality was determined. Outcome was measured using the modified Rankin scale (mRS) three months after IAT and categorized as favorable (mRS 0 to 2) or poor (mRS 3 to 6).
Results: There was no association between admission glucose values and vessel recanalization ($p = 0.296$), and recanalization did not differ between patients with and without diabetes ($p = 0.60$). Diabetics were more likely to have a poor outcome ($p = 0.0001$) and to be dead ($p = 0.011$) at 3 months. After multivariable analysis, there remained an independent relationship between diabetes and poor outcome ($p = 0.003$) and a trend towards a higher mortality in diabetics ($p = 0.06$). Moreover, higher age ($p = 0.002$), Charlson comorbidity index (CCI), ($p = 0.016$), NIHSS score ($p = 0.0001$) and leukocyte count ($p = 0.01$) were independent baseline predictors of poor outcome. Higher age ($p = 0.0011$), CCI ($p = 0.016$), baseline

NIHSS score (p = 0.0001), and cholesterol values (p = 0.009) predicted mortality. Higher glucose values showed a trend to poor outcome (p = 0.058) and were associated with higher mortality (p = 0.007) in univariate analyses. After multivariable analyses glucose was not associated with outcome (p = 0.33) or mortality (p = 0.47).
Conclusions: Diabetes was an independent predictor of poor outcome after IAT but not glucose values on admission. In contrast to IVT, vessel recanalization after IAT does not seem to be influenced by diabetes.

100

In patients with MS vaccine-triggered T cells appear in the peripheral circulation despite fingolimod-mediated S1P-receptor blockade

M. Mehling[1], P. Hilbert[2], S. Fritz[3], J. Kuhle[2], T. Klimkait[4], R. Lindberg[2], L. Kappos[2], C. Hess[3]
[1]University Hospital Basel, Department of Neurology and Immunobiology Laboratory, Basel, Switzerland, [2]University Hospital Basel, Department of Neurology and Clinical Neuroimmunology, Basel, Switzerland, [3]University Hospital Basel, Medical Outpatient Clinic and Immunobiology Laboratory, Basel, Switzerland, [4]University of Basel, Institute of Virology, Basel, Switzerland

Introduction: Lymphocytes have been shown to egress from secondary lymphoid organs (SLO) by migrating along a sphingosine 1-phosphate (S1P) gradient. The oral S1P receptor (S1PR)-agonist fingolimod -which has shown efficacy in the treatment of multiple sclerosis (MS)- blocks this egress, thereby reducing peripheral lymphocyte counts to 25–40% of baseline values. How this forced retention of lymph node-homing T cells in SLO impacts on the development of antigen-specific immune responses has not been characterized in humans. We aimed to characterize cellular and humoral immune responses to influenza vaccine in patients with MS with fingolimod-mediated sphingosine 1 phosphate receptor blockade and in healthy controls (HC).
Methods: Influenza-vaccine specific interferon-gamma secretion of T cells was measured by ELISpot technology. IgM and IgG against Influenza A and B was quantified by ELISA. Measurements were performed before vaccination and at days 7, 14 and 28 after vaccination. A patient diary and clinical assessments were used to monitor injection site reactions and general tolerability of the vaccine.
Results: On day 7 post vaccination a significant and comparable increase in the median frequency of influenza-specific T cells was observed in patients treated with fingolimod and in HC. On day 14 post vaccination this increase was maintained. Twenty-eight days after vaccination contraction to pre-vaccination levels was observed in both study-groups. By day 7 post vaccination concentrations of IgM anti-influenza A and anti-influenza B had increased significantly and comparably in both study groups, and remained increased at comparable levels day 28 after vaccination. Influenza A and influenza B IgG-seroprotection also increased comparably in both fingolimod-treated patients and in HC at day 7 and remained increased at days 14 and 28 post vaccination. Rates of injection site reactions and general vaccine-associated symptoms were similar in both study groups.
Conclusion: These results indicate that S1PR-dependent SLO-egress in humans is differentially regulated among recently antigen-triggered and bulk T cells, providing -together with the quantitatively unimpaired vaccine-specific humoral response- an immunological explanation for few infectious complications despite severe lymphopenia in fingolimod-treated individuals.

101

Interference with gesture production by transient inhibition over left ventral premotor cortex: A Theta Burst Stimulation study

S. Bohlhalter[1], M. Bertschi[1], T. Vanbellingen[2], P. Wurtz[3], D. Cazzoli[3], T. Nyffeler[1], C.W. Hess[3], R. Müri[1]
[1]Department of Cognitive and Restorative Neurology, Inselspital, Bern, Switzerland, [2]Klinik Bethesda, Tschugg, Switzerland, [3]Perception and Eye Movement Laboratory, Inselspital, Bern, Switzerland

Introduction: The traditional view of a predominant posterior parietal representation of gestures has been recently challenged by neuroimaging studies demonstrating that pantomime tool use and gesture discrimination may critically depend on ventral premotor function. The aim of the present work was therefore to investigate the effect of transient disruption of these brain sites by inhibitory continuous theta burst stimulation (cTBS) on gesture production and recognition.
Methods: 14 right-handed healthy subjects (8 women, age range 25–39) participated in the study. cTBS was applied over left ventral premotor cortex (vPMC) and left posterior parietal cortex (PPC) versus baseline (BSL) using a repeated measures design with 1 week intervals between the 3 sessions. Gesture production was assessed off-line within 15 minutes after cTBS using a recently developed test of upper limb apraxia (TULIA). The TULIA includes 2 domains (pantomime and imitation) and 3 semantic categories (meaningless, communicative and tool-related gestures). Based on its highly sensitive scoring method the TULIA test shows no ceiling effect. TULIA scores were determined by a blinded rater based on video recordings. Following the TULIA, gesture recognition was evaluated by modified postural knowledge test (PKT). In the PKT subjects had to select pictures of correct gesture postures on a computer screen. PKT performance was measured by recording score rates and reaction times.
Results: cTBS of the left vPMC significantly lowered total TULIA scores when compared to BSL. The effect was even more prominent when contrasted with cTBS of the left PPC. Further analysis at domain and semantic level of TULIA revealed that both differences were explained by significant effects on pantomime and tool use gestures. However, cTBS over either stimulation site had no influence on imitation scores of TULIA or measures of gestural recognition in PKT.
Conclusion: The interference of cTBS over left vPMC with gesture production points to the critical role this brain region has in the control of gestures, particularly if they are pantomimed and related to tool use.

102

Intra-arterial Thrombolysis For Acute Ischemic Stroke In Octogenarians

M.L. Mono[1], A. Kohler[1], M. Arnold[1], A, Galimanis[1], U. Fischer[1], C. Brekenfeld[2], J. Gralla[2], G. Schroth[2], H.P. Mattle[1], K. Nedeltchev[1]
[1]Department of neurology, Inselspital, Bern, Switzerland, [2]Department of Neuroradiology, Inselspital, Bern, Switzerland

Introduction: It is unclear whether octogenarians with acute ischemic stroke derive benefit from intra-arterial thrombolysis (IAT). The aim of the present study was to compare baseline characteristics, clinical outcome and complications of patients aged ≥80 with those of patients aged <80 years.
Methods: 39 patients aged ≥ 80 years and 410 patients aged <80 years were treated with IAT at a single center. The modified Rankin scale (mRS) score was used to assess clinical outcome at 3 months.
Results: There was a female preponderance among the old patients (70% vs. 44%, P = 0.003). Octogenarians were more likely to have hypertension (82% vs. 59%, P = 0.007) but less likely to be smokers (3% vs. 26%, P = 0.002). Stroke severity, location of the vessel occlusion, and time from symptom onset to IAT did not differ between the groups. Good recanalization (TIMI 2-3) was equally frequent in octogenarians and younger patients (61% vs. 66%, p = 0.43). The rates of symptomatic intracerebral hemorrhage (sICH) were 5% in each group (p = 0.81). Favorable clinical outcome (mRS <2) was less frequent among octogenarians (23% vs. 51%, P = 0.001), and mortality was higher (38% vs. 20%, P = 0.02).
Conclusion: Compared with younger patients, octogenarians did not have an increased risk of sICH after IAT. Although favorable outcome was less frequent and mortality was higher, IAT appeared to be safe inpatient aged ≥80 years. It is reasonable to include octogenarians in randomized controlled trials to assess the balance of risk and benefit of IAT in this patient group.

103

Iron infusion in Restless Legs Syndrome in Pregnancy

A. Bloch[1], A. Krafft[1], A. Hübner[1], M. Raimondi[2], E. Werth[1], R. Zimmermann[1], C.L. Bassetti[2]
[1]University Hospital, Zürich, Switzerland, [2]Neurocenter of Southern Switzerland, Lugano, Switzerland

Background: In a recent prospective study we recently found a 9% prevalence of Restless Legs Syndrome (RLS) in pregnancy. Severe RLS with iron deficiency was more common

in the 7th and 8th months of pregnancy and had profound effects on fatigue, sleepiness and sleep quality (A. Hübner, unpublished). Anectdotal reports suggests the possibility of iron supplementation as therapeutic option of RLS in pregnancy.
Objective: To assess the effect of an infusion of ferric carboxymaltose on RLS in pregnant women with RLS and iron deficiency.
Patients and methods: Pregnant women in the third trimester of pregnancy with moderate to severe RLS with iron deficiency (ferritin <35 ug/l) or anemia (<11 g/dl) are enrolled in this open-label non-controlled study. Depending on Hb, Iron substitution is performed with an infusion of 500–900 mg of ferric carboxymaltose. Assessment of the effect of treatment is be done by actigraphy for periodic limb movements in sleep (before and one week after therapy), questionnaires (International RLS Study group questionnaire, fatigue severity scale, Epworth Sleepiness Scale, Pittsburgh sleep quality index) and blood tests (iron, ferritin, CRP) at the screening visit, the therapy visit, 3, 7, 14 and 28 days after therapy as well as 2 weeks (questionnaires only) and 6 weeks after delivery.
Results: So far three patients have been enrolled and treated with ferric carboxymaltose. All three reported a marked decrease in RLS-symptoms from the first night after infusion and showed a decrease of the IRLSSG score of 48%, 59% and 61% respectively. One patient has already had a post therapy actigraphy and showed a decrease of PLMS of 72% in night 1, 61% in night 2 and 9% in night 3.
Conclusions: Preliminary results of this ongoing project sugget that iron infusion may have a positive effect on RLS during pregnancy when associated with iron deficiency (ferritin <35 ug/l) or anemia .
Supported by: Vifor

104

IV Thrombolysis in Posterior Circulation Stroke – a multicenter observational study

H. Sarikaya[1], S. Engelter[2], P. Lyrer[2], M. Arnold[3], H. Mattle[3], D. Georgiadis[1], R.W. Baumgartner[1]
[1]Neurology Department, Zurich, Switzerland, [2]Neurology Department, Basel, Switzerland, [3]Neurology Department, Berne, Switzerland

Background: Intravenous thrombolysis (IVT) is an approved treatment for posterior (PCS) and anterior (ACS) circulation stroke. Although the mechanism of stroke and clinical outcome differ between PCS and ACS, no randomized-controlled trial has investigated whether IVT is beneficial in PCS or clinical outcome differs between these two stroke groups. We aimed to compare the safety and clinical outcome of IVT applied to patients with PCS and ACS in routine clinical praxis.
Methods: Prospectively collected data of 883 consecutive acute stroke patients treated with IVT at three stroke centers in Switzerland between June 1998 and December 2008 were analyzed. Presenting characteristics, symptomatic intracranial hemorrhage (sICH), mortality and favorable outcome (modified Rankin scale 0 or 1) at 3 months were compared between patients with ACS and PCS.
Results: Compared to patients with ACS (n = 788, 89%), those with PCS (n = 95, 11%) were younger (mean age 63 vs. 67 years, p = 0.01), had a lower mean baseline National Institute of Health score (9 vs. 12, p <0.001) and more often a favorable outcome (66 vs. 47%, p <0.001), and suffered less sICH (0 vs. 5%, p = 0.03). Mortality was similar in the two groups (PCS, 9%; ACS, 13%; p = 0.32). After adjustment for baseline characteristics, favorable outcome (p = 0.62) was similar in PCS and ACS, whereas patients with PCS tended to have less sICH (p = 0.07).
Conclusion: The data of this multicenter observational study suggest that the rate of sICH and clinical outcome after IVT for posterior and anterior circulation stroke are comparable in real-life clinical practice.

105

Late clinical improvement despite persistent autoantibodies in anti-N-Methyl-D-aspartate-receptor antibody limbic encephalitis

D. Zutter[1], G. Kägi[2], H. Gast[3], A. Fontana[4], CL. Bassetti[5]
[1]Neurorehaklinik HUMAINE, Zihlschlacht, Switzerland, [2]Neurologische Klinik, Kantonsspital, St. Gallen, Switzerland, [3]Neurologische Klinik, Inselspital, Bern, Switzerland, [4]Institut für Experimentelle Immunologie, USZ, Zürich, Switzerland, [5]Neurocenter of Southern Switzerland, Lugano, Switzerland

Background: Since 2007 over 200 patients with anti N-Methyl-D-Aspartate-Receptor (NMDAR) encephalitis were reported. Data on treatment response are scarse.
Patients and methods: Two patients with anti-NMDAR encephalitis and delayed/partial response to treatment are presented.
Results: Patient 1: This 36-year-old female presents with insomnia, visual disturbances, multifocal seizures, and finally coma. On repeated examinations a pleocytosis of 40–79 cells and normal brain MRI are found. An extensive diagnostic work up remains negative. After 5 1/2 months of intensive care treatment transfer to a rehabilitation unit in a awake but unaware state. Eight months after disease onset anti-NMDAR antibodies are found in serum and liquor. Immunotherapy with high dose steroids, endoxan, and later rituximab leads to a gradual neurological improvement. Three monthes later the patient exhibits purposeful movements, simple speach, independent eating, and recognition of family members. She is able to walk with assistance. Anti-NMDAR antibodies remain high in serum. Patient 2: This 40-year-old female presents with psychotic symptoms, catatonic syndrome, multifocal dyskinesias, seizures and finally coma. On repeated examinations a pleocytosis of max. 23 cells and a normal brain MRI are found. Anti-NMDAR antibodies are presented in serum and liquor. A teratoma of the right ovary is found and removed. After 2 weeks of intensive care treatment transfer to a rehabilitation unit in a awake but unaware state with continuous multifocal dyskinesias. Six weeks after disease onset immutherapy with high dose steroids and endoxan leads to a rapid neurological improvement within days. One year later the patient exhibits moderate cognitive deficits (amnesia, inattention, visuospatial disorientation, frontal lobe syndrome) and a REM sleep behaviour disorder. Anti-NMDAR antibodies persist in serum.
Conclusion: Anti-NMDAR encephalitis should be considered in the differential diagnosis of encephalitis complicated by psychosis, epilepsy, and movement disorders. Immunotherapy can lead to neurological improvement even months after disease onset. The absence of a decline of anti-NMDAR antibodies questions their role in the pathogenesis of the disease.

106

LINGO1 and LINGO2 variants are associated with essential tremor and Parkinson disease

Wider[1], Vilarino-Guell[2], A. Ross[2], Jasinska-Myga[2], Kachergus[2], A. Cobb[2], I. Soto-Ortolaza[2], Heckman[2], Behrouz[2], M. Testa[3], K. Wszolek[2], J. Uitti[2], Jankovic[4], D. Louis[5], N. Clark[5], Rajput[6], Vingerhoets[1], J. Farrer[2]
[1]HUV, Lausanne, Switzerland, [2]Mayo Clinic, Jacksonville, United States, [3]Emory University, Atlanta, United States, [4]Baylor College, Houston, United States, [5]Columbia University, New York, United States, [6]University of Saskatchewan, Saskatoon, Canada

Introduction: Genetic variation in the leucine rich repeat and Ig domain containing 1 gene (LINGO1) was recently associated with an increased risk of developing essential tremor (ET) and Parkinson disease (PD).
Methods: Herein, we performed a comprehensive study of LINGO1 and its paralog LINGO2 in ET and PD, by sequencing both genes in patients (ET, n = 95; PD, n = 96), and by examining haplotype-tagging single-nucleotide polymorphisms (tSNPs) in a multi-center North American series of patients (ET, n = 1247; PD, n = 633) and controls (n = 642).
Results: The sequencing study identified six novel coding variants in LINGO1 (S4C, V107M, A277T, R423R, G537A, D610D) and three in LINGO2 (D135D, P217P, V565V), however segregation analysis did not support pathogenicity. The association study employed 16 tSNPs at the LINGO1 locus and 21 at the LINGO2 locus. One variant in LINGO1 (rs9652490), previously implicated in ET and PD, displayed evidence of an association with ET (odds ratio – OR = 0.63; P = 0.026) and PD

(OR = 0.54; P = 0.016). Additionally, four other tSNPs in LINGO1 and one in LINGO2 were associated with ET, and one tSNP in LINGO2 associated with PD (P <0.05). Further analysis identified one tSNP in LINGO1 and two in LINGO2 which influenced age at onset of ET, and two tSNPs in LINGO1 which altered age at onset of PD (P <0.05).
Conclusions: Our results support a role for LINGO1 and LINGO2 in determining risk for and perhaps age at onset of ET and PD. Further studies are warranted to confirm these findings and to determine the pathogenic mechanisms involved.

107

Localisation of the primary somatosensory cortex with electric source imaging of mechanical evoked potentials

A. M. Lascano, F. Grouiller, M. Genetti, L. Spinelli, M. Seeck, K. Schaller, C. M. Michel
Neurology and Neurosurgery Clinics, Department of Clinical Neurosciences, University Hospital and University of Geneva, Geneva, Switzerland

We examined the feasibility of imaging the primary hand sensory cortex with electric source imaging (ESI) of the somatosensory evoked potentials (SEP) after pneumatic mechanical stimulation of the finger. We recorded 256-channel SEP from 27 healthy volunteers, applied a distributed inverse solution, and performed statistical parametric mapping in the inverse space to define the location and the timing of significant activity in the brain. We also recorded intracranial SEP in 4 epileptic patients with the same stimulation parameters as well as fMRI in 10 subjects who also had ESI, 3 of them with simultaneous EEG-fMRI. We found a very stable focal initial activation of the postcentral gyrus with ESI and a temporal propagation to precentral, frontal, and parietal areas. The localization of the sensory cortex was confirmed by fMRI. The sequential activation was also seen in the intracranial recordings. These results suggest that ESI of pneumatic somatosensory stimulation is a precise non-invasive method for mapping of the primary sensory cortex and for studying the intracortical connections between sensory and motor brain areas.

108

Marked clinical and electrophysiological response to fluoxetine treatment in congenital slow channel myasthenic syndrome

A.K. Payer[1], A. Abicht[2], M. Sinnreich[1], D. Fischer[1]
[1]Center for Neuromuscular Disorders, Dept. of Neurology, USB, Basel, Switzerland, [2]Medizinisch Genetisches Zentrum, München, Germany, [3]Dept. of Neuropädiatrics, UKBB, Basel, Switzerland

Objective: To describe a patient with a new mutation in the alpha subunit of acetylcholine receptor (AChR) with clinical and electrophysiological hallmarks of a slow-channel myasthenic syndrome (SCCMS), responsive to fluoxetine treatment.
Background: SCCMS is due to a genetically determined kinetic abnormality of the AChR at the neuromuscular junction leading to its prolonged open state. Fluoxetine has a non-depolarizing blocking activity of nicotinic AChRs and has been used as treatment for SCCMS.
Methods: Clinical examination, nerve conduction studies, repetitive nerve stimulation at varied frequencies before and after treatment with fluoxetine were performed on a 44 year old patient with suspected SCCMS. Sequence analysis of the alpha-subunit of AChR according to standard protocol.
Results: A 44 year old woman had progressive muscle weakness, being hypotonic as an infant with delayed acquisition of motor milestones. At age 16 she stopped playing piano due to weakness of finger extensors. Later, upper limb girdle weakness developed. At presentation she had bilateral ptosis, external ophthalmoparesis, a myopathic facies, neck extensor weakness, proximal upper extremity weakness and finger extensor weakness. Motor nerve conductions studies revealed a double compound muscle action potential (repetitive R-CMAP) of the ulnar CMAP. Low frequency repetitive stimulation of ulnar, spinal accessory, and facial nerves showed a CMAP decrement greater than 10% in all nerves analysed, which worsened at higher frequencies (5 Hz, 10 Hz) and also after administration of an acetylcholinesterase inhibitor (Pyridostigmin). The diagnosis of SCCMS was suspected. She had a marked treatment response to fluoxetine, 80 mg/day. After 2 months, she experienced marked improvement of proximal muscle strength, but persistent ptosis and ophthalmoparesis. Repetitive nerve stimulation on fluoxetine showed a normalization of the decrement in ulnar and spinal accessory nerves, and the R-CMAP disappeared. Genetic analysis of AChR revealed a new c.959G>T (GGA>GTA), p.GLy320Val mutation within the alpha subunit. Analyses of further healthy family members to prove pathogenicity of the mutation are ongoing.
Conclusion: We suggest initiating treatment in SCCMS when the clinical and electrophysiological findings are characteristic.

109

Motor recovery after experimental ischemic stroke does not depend on protein synthesis in motor cortex

M. Schubring-Giese, B. Hertler, C.O. Atiemo, A.R. Luft
Neurology, University of Zurich, Zurich, Switzerland

Introduction: Motor recovery after an ischemic stroke is commonly assumed to involve brain mechanisms that also enable movement learning in the healthy. One of these mechanisms is neural plasticity that requires the expression of genes and proteins to mediate lasting modifications to neural network function and structure. We have previsouly shown that learning a novel motor skill requires intact protein synthesis in primary motor cortex (M1) (Luft et al. J Neurosci 2004, 24:6515). Here, we hypothesized that the same would be true for motor recovery after an M1 stroke.
Methods: Three groups of rats were subjected to 7 days of training a forelimb reaching skill. Two groups received a ~2 mm photothrombotic lesion in the forelimb representation contralateral to limb used for reaching. Sham animals (n = 5) were operated but not lesioned. Stroke rats were injected with the protein synthesis inhibitor anisomycin at two injection points inside normal tissue along the lesion's edge (n = 7) or vehicle (n = 6) after post-lesion training sessions 2 and 3 (days 4 and 5 after stroke). Sham rats also received ANI injections. Recovery training was continued until session 10.
Results: All groups learned the reaching skill achieving similar pre-lesion performance levels (p >0.5). Lesioned rats showed a marked reaching deficit in comparison with sham (performance loss 90%, p = 0.001). ANI had no effect on recovery (p = 0.4) or performance of sham animals. Motor recovery after an M1 lesion does not require protein synthesis in the periinfarct tissue.
Conclusion: This finding points to substantial differences in the mechanisms that mediate motor recovery and learning.

110

Natural evolution of white and grey matter infarction between 24 and 72 hours after transient middle cerebral artery occlusion in spontaneously hypertensive rats

F. Fluri[1], E. Cam[1], B. Gao[1], C. Bassetti[1]
[1]Dep. of Neurology, University Hospital Zürich, Zürich, Switzerland, [2]Dep. of Neurology, University Hospital Basel, Basel, Switzerland, [3]Neurocenter (EOC) of Southern Switzerland, Lugano, Switzerland

Background: In rats, 10–15% of brain volume is white matter (WM), whereas the proportion in human brain is about 42%. Most of the neuroprotectants were investigated in rats and thus the focus on their efficacy laid on grey matter (GM) but only little attention was paid to WM effects. However, before evaluating WM protection by neuroprotectants, natural infarct evolution of WM and GM has to be determined in an animal model of brain ischemia.
Methods: Male spontaneously hypertensive rats (SHR) underwent transient middle cerebral artery occlusion (tMCAO) of 60 minutes using a silicone-coated filament. 24 and 72 hours respectively after tMCAO, MR imaging (T2-weighted) was performed to detect brain infarct. Infarct size was determined by image analysis (Image J) of the T2-weighted scans.
Results: 24 hours after tMCAO, the size of the whole infarction (WM and GM) as well as of GM and WM infarction was 217 ± 71 mm^3, 159 ± 58 mm^3 and 59 ± 16 mm^3 respectively and increased to 296 ± 71 mm^3, 221 ± 58 mm^3 and 75 ± 14 mm^3 respectively. Between 24 and 72 hours after tMCAO, infarction in GM increased 13% more than in WM (p = 0.3).
Conclusion: In this study, there was a trend of a larger increase of GM infarction between 24 and 72 hours compared to WM infarction. This finding may indicate a greater vulnerability of WM than GM in SHR.

111

New ischaemic brain lesions on MRI after stenting or endarterectomy for symptomatic carotid stenosis: a substudy of the International Carotid Stenting Study (ICSS)

L.H. Bonati[1], L.J. Jongen[6], S. Haller[2], H.Z. Flach[8], J. Dobson[9], P.J. Nederkoorn[1], S. Macdonald[11], P. Gaines[12], A. Waajier[6], P. Stierli[3], R. Jäger[4], P.A. Lyrer[1], L.J. Kappelle[7], S.G. Wetzel[2], A. van der Lugt[8], W.P. Mali[6], M.M. Brown[5], H.B. van der Worp[7], S.T. Engelter[1]

[1]Department of Neurology and Stroke Unit, University Hospital Basel, Basel, Switzerland, [2]Department of Radiology, University Hospital Basel, Basel, Switzerland, [3]Vascular Surgical Center, University Hospital Basel, Basel, Switzerland, [4]Academic Neuroradiological Unit, UCL Institute of Neurology, London, United Kingdom, [5]Department of Brain Repair and Rehabilitation, UCL Institute of Neurology, London, United Kingdom, [6]Department of Radiology, University Medical Center Utrecht, Utrecht, Netherlands, [7]Department of Neurology, Rudolf Magnus Institute of Neuroscience, University Medical Center Utrecht, Utrecht, Netherlands, [8]Department of Radiology, Erasmus Medical Center, Rotterdam, Netherlands, [9]Department of Epidemiology and Population Health, London School of Hygiene and Tropical Medicine, London, United Kingdom, [10]Department of Neurology, Adacemic Medical Center Amsterdam, Amsterdam, Netherlands, [11]Department of Radiology, Freeman Hospital, Newcastle-upon-Tyne, United Kingdom, [12]Sheffield Vascular Institute, Northern General Hospital, Sheffield, United Kingdom

Background: The International Carotid Stenting Study (ICSS) of stenting and endarterectomy for symptomatic carotid stenosis found a higher incidence of stroke within 30 days of stenting compared with endarterectomy. We aimed to compare the rate of ischaemic brain injury detectable on MRI between the two groups.
Methods: Patients with recently symptomatic carotid artery stenosis enrolled in ICSS were randomly assigned in a 1:1 ratio to receive carotid artery stenting or endarterectomy. Of 50 centres in ICSS, seven took part in the MRI substudy. The protocol specified that MRI was done 1–7 days before treatment, 1–3 days after treatment (post-treatment scan), and 27–33 days after treatment. Scans were analysed by two or three investigators who were masked to treatment. The primary endpoint was the presence of at least one new ischaemic brain lesion on diffusion-weighted imaging (DWI) on the post-treatment scan. Analysis was per protocol. This is a substudy of a registered trial, ISRCTN 25337470.
Results: 231 patients (124 in the stenting group and 107 in the endarterectomy group) had MRI before and after treatment. 62 (50%) of 124 patients in the stenting group and 18 (17%) of 107 patients in the endarterectomy group had at least one new DWI lesion detected on post-treatment scans done a median of 1 day after treatment (adjusted odds ratio [OR] 5.21, 95% CI 2.78–9.79; p <0.0001). At 1 month, there were changes on fluid-attenuated inversion recovery sequences in 28 (33%) of 86 patients in the stenting group and six (8%) of 75 in the endarterectomy group (adjusted OR 5.93, 95% CI 2.25–15.62; p = 0.0003). In patients treated at a centre with a policy of using cerebral protection devices, 37 (73%) of 51 in the stenting group and eight (17%) of 46 in the endarterectomy group had at least one new DWI lesion on post-treatment scans (adjusted OR 12.20, 95% CI 4.53–32.84), whereas in those treated at a centre with a policy of unprotected stenting, 25 (34%) of 73 patients in the stenting group and ten (16%) of 61 in the endarterectomy group had new lesions on DWI (adjusted OR 2.70, 1.16–6.24; interaction p = 0.019).
Conclusion: About three times more patients in the stenting group than in the endarterectomy group had new ischaemic lesions on DWI on post-treatment scans. The difference in clinical stroke risk in ICSS is therefore unlikely to have been caused by ascertainment bias. Protection devices did not seem to be effective in preventing cerebral ischaemia during stenting. DWI might serve as a surrogate outcome measure in future trials of carotid interventions.

112

Novel Twinkle mutation associated with macular degeneration

V. Mihaylova[1], A. Schaller[2], J. Bremer[1], J. Petersen[1], K. Landau[3], H. Jung[1]

[1]Department of Neurology, University Hospital, Zurich, Switzerland, [2]Department of Human Genetics, University Hospital, Bern, Switzerland, [3]Department of Ophthalmology, University Hospital, Zurich, Switzerland

Introduction: Mitochondrial disorders are a group of heterogeneous diseases characterized by defects of the oxidative phosphorylation and presenting with a variety of manifestations most frequently with neurological syndromes. Mitochondrial diseases can be caused by genetic defects in mitochondrial DNA or in nuclear genes. Heterozygous mutations in Twinkle have been reported to cause autosomal dominant progressive external ophthalmoplegia accompanied sometimes by other symptoms. Here we report on a 70-year-old patient with a late onset of polyneuropathy, sensorineural hearing loss, diabetes mellitus and macular degeneration.
Methods: Detailed neurological, neuro-otological, neuro-ophthalmical examinations, EMG, nerve conduction studies, muscle and nerve biopsy, ECG, echocardiography, CSF examination, laboratory investigations and molecular genetic testing were performed.
Results: By direct sequencing of C10orf2 (encoding for Twinkle) a novel nonsense mutation was found heterozygously in our patient (p.R217X).
Conclusion: We report an association of macular degeneration with Twinkle mutations. Our report expands the phenotypic spectrum of Twinkle mutations and provides further evidence of mitochondrial dysfunction in the pathogenesis of age-related macular degeneration.

113

Novel valosin containing protein mutation in a Swiss family with hereditary inclusion body myopathy, paget's disease of the bone and dementia

A.K. Peyer[1], J. Kinter[1], St. Frank[2], P. Fuhr[1], A. Fischmannx, St. Kneifel[4], S. Thomann[1], P. Camano[5], M. Sinnreich[1], S. Renaud[1]

[1]Center for Neuromuscular Disorders, University Hospital Basel, Basel, Switzerland, [2]Insitute of Pathology, University Hospital Basel, Basel, Switzerland, [3]Department of Radiology, University Hospital Basel, Basel, Switzerland, [4]Department of Nuclear Medicine, Basel, Switzerland, [5]Unidad Experimental, Hospital Donostia, San Sebastian, Spain

Background: VCP is an evolutionary highly conserved member of the superfamily of ATPases associated with various cellular activities. Mutations in VCP cause autosomal dominant IBMPFD. Only 14 disease causing mutations in VCP have been described in few families world-wide so far.
Method: History, clinical examination, myopathological findings, radiological data of muscle and bone as well as molecular findings of affected members from a large Swiss family are presented.
Results: Six family members were affected in three generations. Cardinal signs were late onset progressive muscle weakness, leading to wheel chair dependance by age 55. One patient had scintigraphic evidence of Paget's disease of the bone, and another suffered from early onset dementia. Electromyographic examination showed neurogenic and myopathic findings. MR and CT scans of the lower trunk and limbs revealed atrophy and fatty replacement of the axial muscles, as well as extensors and flexors of the thigh. Histological sections of skeletal muscle showed findings consistent with inclusion body myopathy. Sequence analysis of the VCP gene revealed a novel heterozygous mutation (A828T, I206F). This mutation was not present in 100 control chromosomes. The mutation lies in an evolutionary conserved region in close proximity to the ATP binding pocket of VCP.
Conclusion: We report a novel pathogenic dominant VCP allele in a Swiss family leading to IBMPFD.

114

On the origin of the language related N400s: an ERP waveform and source localisation analysis

A. Khateb[1], A.J. Pegna[2], T. Landis[2], M.S. Mouthon[2], J.M. Annoni[2]
[1]The Edmond J. Safra Brain Research Center for the Study of Learning Disabilities, Faculty of Education, University of Haifa, Haifa, Israel, [2]Lab. of Experimental Neuropsychology and Neuropsychology Unit, Neurology department, Geneva University Hospitals and Faculty of Medicine, Geneva, Switzerland

The event-related potential (ERP) N400 component, initially described in the sentence context due to semantic incongruities, was subsequently observed although with varying latencies in lexical decision, semantic judgement (of words, images and pictures), rhyme detection and repetition priming tasks. Firstly linked to the semantically-induced N400, the cognitive nature and the cerebral origins of N400-like responses have repeatedly been questioned. In this study, we analysed N400 effects in 22 right-handed subjects performing three different language tasks. In the semantic word categorisation task, subjects decided whether or not word pairs presented sequentially were semantically related (SR) or not (SU). In the rhyme detection task, they decided whether words in each pair were phonologically related (PR, i.e. rhymed) or not (PU). In the image judgement task, they decided whether two sequentially presented images were categorically related (IR) or not (IU). In each task, the comparison of ERPs to unrelated vs related conditions using point-wise t-tests confirmed the presence of significant differences during the N400 time window. The individual analysis of the difference waves (Unrelated minus Related ERPs) showed that the N400 was stronger in amplitude and earlier in latency in the IU than in SU and PU. However, the topographic maps computed on the peak of the mean wave difference were strikingly highly correlated over the three tasks. Similarly, source localisation showed a bilaterally distributed network including in all tasks the middle and superior temporal gyrus. In view of these similarities, it is suggested that N400s index the "mismatch" that arises in various cognitively primed contexts.

115

Outcome of Acute Isolated Posterior Cerebral Artery Occlusion after Intra-arterial Thrombolysis

N. Meier[1], U. Fischer[1], O. Findling[1], C. Brekenfeld[2], M. El-Koussy[2], G.M. De Marchis[1], M.L. Mono[1], J. Gralla[2], K. Nedeltchev[1], H.P. Mattle[1], G. Schroth[2], M. Arnold[1]
[1]Dpt. of Neurology, Inselspital, University Hospital Bern and University of Bern, Bern, Switzerland, [2]Dpt. of Neuroradiology, Inselspital, University Hospital Bern and University of Bern, Bern, Switzerland

Introduction: Posterior cerebral artery (PCA) strokes may lead to a variety of neurological and neuropsychological symptoms. To date, there are only limited data on intra-arterial thrombolysis (IAT) for acute isolated PCA occlusion. We aimed to evaluate recanalization rate, outcome and quality of life in patients who undergo IAT for isolated PCA occlusion.
Methods: Prospective collection and analysis of 8 patients with short-term (3 months) and long-term (median 35 months) outcome including Stroke Specific Quality of Life (SSQOL).
Results: From January 2000 to September 2009, 3 women and 5 men (median age 64 years, range 44–79 years) underwent IAT for acute isolated PCA occlusion. Median National Institute of Health Stroke Scale (NIHSS) score on admission was 9 (range 2–17). All patients presented with dense visual field defects and variable additional symptoms. Median time to treatment was 5.7 hours, and median Urokinase dose was 750'000 IU. Recanalization was complete in 2 patients, partial in 2, minimal in 1, and was not achieved in 3 patients. Recanalization tended to be better when the microcatheter could be placed in or close to the thrombus. No patient suffered major complications during and after IAT, and 3-months outcome was favourable (modified Rankin scale score 0–2) in 75% of patients. Median NIHSS score decreased to 1.5. At long-term follow-up, neuropsychological domains were more severely impaired than other neurologic functions.
Conclusions: Our experience shows that IAT is a feasible and probably efficacious treatment for patients with isolated PCA occlusions. We did not observe any major complication after IAT.

116

Outcome of stroke patients with versus without pharmacological augmentation of rehabilitation

S.T. Engelter[1], M. Frank[1], P.A. Lyrer[2], M. Conzelmann[1]
[1]Felix Platter-Spital, Neurorehabilitation, Basel, Switzerland, [2]Depart. of Neurology and Stroke Unit University Hospital, Basel, Switzerland

Background: Based on experimental studies, pharmacological augmentation (PA) of stroke rehabilitation might be reasonable. Whether PA is beneficial in clinical practice is unclear, as most studies have small sample sizes, narrow inclusion criteria, or methodological shortcomings.
Methods: We performed a prospective, explorative study about the use of PA in addition to regular rehabilitative therapies in a stroke-rehabilitation unit. Over 20 months, we systematically observed (a) the utilization rate of PA, (b) putative side effects, and (c) the functional outcome of patients with versus without PA (non-PA). Outcome was quantified by delta FIM; the increase in abilities in activities of daily living during in-hospital rehabilitation as measured with the "Functional Independence Measure" (FIM). The decision to use PA was made by the treating physicians and required the consent of patients/relatives.
Results: 97 of 249 (39%) patients (mean 73 years) had PA. L-Dopa was used in 29%, SSRI in 21%, and acetylcholinesterase inhibitors in 17%. In 12 patients PA was associated with delirium (n = 5), gastrointestinal symptoms (n = 4), electrolyte disorders (n = 2), or incontinence (n = 1). PA-patients did not differ from non-PA patients in age (72.7 vs 73.1 years, p = 0.78), gender (58% vs 52% males p = 0.37) und stroke type (ischemia 84.5% vs 81.4% p = 0.62). However, compared with non-PA patients, PA-patients were more severely affected at entry (NIH Stroke Scale Score 8.4 ± 6.5 vs 5.5 ± 5.5; p <0.001; FIM total 60.7 ± 28.6 vs 73.6 ± 32.8; p = 0.02). At discharge the PA-group had a higher mean delta FIM as compared with non-PA-patients (21.8 ± 17.4 vs 16.3 ± 18.9; p = 0.02).
Conclusion: Pharmacological augmentation of stroke rehabilitation was used frequently. It was associated with a better outcome. L-Dopa had the highest utilisation rate. Most patients tolerated the treatment well. Thus, there is scope for benefit of this approach. A large controlled-randomized trial is justified.

117

PFO May Be Causal For The First Stroke But Unrelated To Subsequent Ischemic Events

M.-L. Mono
Department of Neurology, Inselspital, Bern, Switzerland

Introduction: Studies with very long follow-up are still scarce in patients with cryptogenic stroke and patent foramen ovale (PFO). We assessed the risk of stroke recurrence under antithrombotic treatment during a mean follow-up of 8.1 years. In patients with recurrent ischemic events, we sought to determine competitive stroke causes that had emerged since the index event.
Methods: 159 158 patients with cryptogenic stroke and PFO received aspirin (48%), clopidogrel (2%) or oral anticoagulants ((50%). Structured telephone interview and a written survey were used to obtain information on recurrent ischemic events (stroke or TIA) and the adherence to antithrombotic treatment. In case of a suspected recurrent event, we reviewed all available medical records related to the event.
Results: Mean age was 50.751 (SD 13.513) years. The event leading to the diagnosis of a PFO was a TIA in 23%, a stroke in 76%, and an amaurosis fugax in 1%. In 28%, the index stroke or TIA was preceded by at least one cerebrovascular event. During a mean follow up of 8.1 (SD 4.7) years, 31 (19.6%) patients had a recurrent cerebrovascular event (11 strokes and 20 TIAs). The average annual rate of recurrent stroke was 1,3% and that of recurrent stroke and TIA 3.5%. The risk of recurrent stroke and TIA was significantly increased in hypertensive patients (p = 0.028) and in those with previous cerebrovascular events (p = 0.005). Etiologic workup revealed a competitive cause for 12 recurrent events (39%): large artery disease (10%), small artery disease (6%), cardioembolism (13%), cerebral vasculitis (3%), and antiphospholipid antibody syndrome (6%). Nineteen recurrent events (61%) were cryptogenic.
Conclusion: The risk of stroke recurrence in PFO patients on antithrombotic treatment remains low over a long follow-up period. Competitive etiologies are identified for more than a third of recurrent ischemic events putting the causal role of PFO into perspective.

118

Rapid cerebral amyloid binding by Abeta antibody infused into APP transgenic mouse models of AD

D.T. Winkler[1], D. Abramowski[3], S. Danner[3], M. Zurini[3], P. Paganetti[3], M. Tolnay[2], M. Staufenbiel[3]
[1]Department of Neurology, University Hospital Basel, Basel, Switzerland, [2]Institute of Pathology, University Hospital Basel, Basel, Switzerland, [3]Novartis Institutes for Biomedical Research, Basel, Switzerland

Introduction: Alzheimer's disease (AD) constitutes the most prevalent form of dementia. Extensive evidence suggests that aggregation of the amyloid-β (Aβ) peptide plays a central role in AD pathogenesis. Antibody mediated reduction of cerebral Aβ aggregation has been achieved in different transgenic mouse lines and rapidly transferred into the clinics. Yet, the mechanisms of Aβ immunotherapy remain only partly understood.
Methods: We studied mechanisms of Aβ immunotherapy for Alzheimer's disease in human APPSwedish and APPwild-type transgenic mice. Plasma, brain tissue and cerebrospinal fluid were analyzed by Western blotting, Mesoscale electrochemoluminescence immunassays and histology, respectively, subsequent to intravenous infusion of an N-terminal antibody β1 into young and aged APP transgenic mice.
Results: Following intravenous Aβ antibody treatment, plasma Aβ increased rapidly reaching significantly higher levels in preplaque compared to plaque bearing mice (APP23: 5.9-fold increase vs. 13.2-fold, ANOVA p <0.001; APP51: 5.9-fold vs. 9.7-fold, ANOVA p <0.005). Assuming that injected β1-antibodies completely blocked plasma Aβ degradation during the initial phase, the increase allowed estimating the half-life of plasma Aβ40 as 4.6 min. Cerebral and CSF Aβ remained unchanged. Strikingly, Aβ antibodies exhibited strong transient cerebral amyloid plaque binding rapidly after intravenous administration in a subset of animals with more severe cerebrovascular amyloid.
Conclusions: We conclude that the plasma Aβ increase subsequent to passive immunization is not directly reflecting cerebral amyloid removal but can be attributed to stabilization of plasma. Nevertheless, the lower increase of plasma Aβ in aged mice may be indirectly diagnostic for cerebral plaque formation. Importantly, intravenously administered antibodies can rapidly bind to parenchymal plaques, potentially facilitated by vascular amyloid mediated damage of the blood brain barrier.

119

Recurrent TIAs and arterial pathology, but not ABCD2 or perfusion imaging predict early deterioration or recurrence after TIA or minor stroke

G.J. Grujic, F.M. Faouzi, A.C. Aubert, O.C. Odier, M.P. Michel CHUV, Lausanne, Switzerland

Background: Patients with TIA or minor stroke are at risk of clinical deterioration and recurrent strokes, especially during the first 7 days. ABCD2 score severity and the presence of DWI lesions have been associated with further events. The present study aims to additional parameters that could improve a short term prognostic model.
Methods: All patients admitted to our stroke unit between 01/2003 and 4) hemispheric ≤12/2008 with acute hemispheric TIA or minor (NIHSS stroke ("MS") undergoing acute arterial imaging (mainly CT-angiography) were prospectively registered. Hemispheric TIA/MS was determined en clinical grounds (presence of focal cognitive and/or visual field deficits). The end-point was defined as recurrence or deterioration (≥4 points on NIHSS) within 7 days after the first event. A wide battery of demographic, epidemiological, clinical and radiological data including acute CT-perfusion (CTP) was analysed as potential predictors using logistic regression.
Results: Of the 443 patients (224 TIAs and 219 MS), the end-point occurred in 41 patients (9.3%). In multivariable analysis, TIA rather than MS (OR = 2.94, p = 0.004), additional previous ischemic cerebrovascular event (OR =2.53, p = 0.01, more pronounced if within 7 days), motor signs (OR = 2.793, p = 0.02), and arterial pathology on acute imaging (OR = 3.64, p <0.001), were significant predictors of the end-point, but not ABCD2 score (OR = 1.03, p = 0.80). CTP was not predictive in a subgroup of 311 patients (43.7% with TIA and 56.4% with MS) of which 28 (9.0%) had R/W (OR = 1.21p = 0.65). Good outcome at 3 months (mRS 0-1) was predicted by lower ABCD2 scores (OR = 0.28, p = 0.001), absence of early deterioration (OR = 0.23, p <0.001), initial TIA rather than MS (OR = 1.61, p = 0.09) and younger age (OR = 0.97, p <0.001).
Conclusions: Although ABCD2 predicted 3 months outcome in patients with hemispheric TIA or minor stroke, it failed to predict early deterioration or recurrence. Presence of CTP abnormalities was not predictive for early or late outcome. Patients with additional recent ischemic events and acute arterial pathology were at highest early risk and need urgent evaluation and management.

120

Sex-Based Differences in Basilar Artery Occlusion: Secondary Analysis of the Treatment and outcome of acute basilar artery occlusion in the Basilar Artery International Cooperation Study (BASICS)

M. Arnold[1], U. Fischer[1], A. Compter[2], J. Gralla[3], O. Findling[1], H.P. Mattle[1], L.J. Kappelle[2], D. Tanne[4], W. Schonewille[5], A. Algra[1]
[1]Department of Neurology, Inselspital, University of Bern, Bern, Switzerland, [2]Department of Neurology, University Medical Centre Utrecht and Rudolf Magnus Institute of neurosciences, Utrecht, Netherlands, [3]Institute of Diagnostic and Interventional Neuroradiology, Inselspital, University of Bern, Bern, Switzerland, [4]Stroke Center, Department of Neurology, Chaim Sheba Medical Center and Tel Aviv University, Tel-Hashomer,, Tel Aviv, Israel, [5]Department of Neurology, St. Antonius Hospital, Nieuwegein, Netherlands, [6]Julius Center for Health Sciences and Primary Care, University Medical Center, Utrecht, Netherlands

Background: Previous studies suggested a different response to intravenous thrombolysis (IVT) and intra-arterial thrombolysis (IAT) between men and women with anterior circulation stroke. We studied differences according to gender in patients with acute basilar artery occlusion (BAO) who participated in the Basilar Artery International Cooperation Study (BASICS).
Methods: We compared men and women treated with antithrombotic treatment (AT) alone; IVT or combined IVT-IAT (cIVT-IAT); and IAT. Adjusted risk ratios (aRR) were calculated for poor clinical outcome (modified Rankin Scale score of 4 to 6) and mortality at one month and for insufficient vessel recanalization.
Results: Of 389 male and 226 female patients, 181 received AT alone, 120 IVT (n = 79) or cIVT-IAT (n = 41), and 287 IAT. In the AT group 68 of 111 (61%) men and 47 of 70 (67%) women had a poor outcome (aRR 0.96, 95% CI 0.75–1.24), in the IVT/cIVT-IAT group 47 of 77 (61%) men and 24 of 43 (56%) women (aRR 1.19, 95% CI 0.89–1.60), and in the IAT group 142 of 185 (77%) men and 71 of 102 (70%) women (aRR 1.01, 95% CI 0.88–1.17). Mortality was not different between men and women neither in the AT group (aRR 0.80, 95% CI 0.55-1.16), nor in the IVT/cIVT-IAT group (aRR 1.11, 95% CI 0.72–1.73), nor in the IAT group (aRR 1.01, 95% CI 0.75–1.36). Insufficient recanalization after cIVT-IAT or IAT was similar in men and women (23% vs. 22%; aRR 0.92, 95% CI 0.58–1.46).
Conclusions: In patients with acute BAO no significant gender differences for functional outcome and recanalization were observed.

121

Short-term outcome after stenting versus endarterectomy for symptomatic carotid stenosis: prospective individual patient data meta-analysis of three randomised trials in the Carotid Stenting Trialists Collaboration

L.H. Bonati[1], J. Dobson[11], G. Fraedrich[6], W.P. Mali[4], G. Chatellier[10], H. Zeumer[7], A. Branchereau[9], P.A. Ringleb[5], J.L. Mas[8], A. Algra[2], M.M. Brown[3]
[1]Department of Neurology and Stroke Unit, University Hospital Basel, Basel, Switzerland, [2]Department of Neurology and Julius Center, University Medical Center Utrecht, Utrecht, Netherlands, [3]Department of Brain Repair and Rehabilitation, UCL Institute of Neurology, London, United Kingdom, [4]Department of Radiology, University Medical Center Utrecht, Utrecht, Netherlands, [5]Neurologische Klinik, Universitätsklinikum Heidelberg, Heidelberg, Germany, [6]Department of Vascular Surgery, Medical University, Innsbruck, Austria, [7]Department of Diagnostic & Interventional Neuroradiology, University Hospital Hamburg-Eppendorf, Hamburg, Germany, [8]Service de Neurologie, Unité Neuro-Vasculaire, Centre R. Garcin, Hôpital Sainte-Anne, Paris, France, [9]Service de chirurgie vasculaire, Hôpital Timone Adultes, Marseille, France, [10]Clinical Research Unit, Hôpital Européen Georges Pompidou, Paris, France, [11]Department of Epidemiology and Population Health, London School of Hygiene and Tropical Medicine, London, United Kingdom

Background: Recent randomised controlled trials (RCTs) have shown a higher short-term risk of stroke associated with stenting (CAS) compared with endarterectomy (CEA) for the treatment of symptomatic carotid stenosis. However, trials were underpowered to investigate whether CAS may be a safe alternative to CEA in specific patient subgroups. We therefore performed a prospective individual patient data meta-analysis of three RCTs.
Methods: individual data from all 3433 patients with symptomatic carotid stenosis randomised in the contributing trials were pooled and analysed with fixed-effect binomial regression models adjusted for source trial. The primary outcome event was any stroke or death. The analysis by intention-to-treat (ITT) included all patients and outcome events occurring between randomisation and 120 days thereafter. The per-protocol (PP) analysis was restricted to patients receiving the allocated treatment and events occurring within 30 days after treatment.
Results: In the first 120 days after randomisation, any stroke or death occurred significantly more often in the CAS group (153/1725 [8.9%]) than in the CEA group (98/1708 [5.7%], risk ratio (RR) 1.54, [95% confidence interval 1.21, 1.97], p = 0.0004). Of all tested subgroup variables, only age significantly modified the treatment effect: in patients <70 years old (the median age), the estimated 120 day stroke or death risk was 5.8% in CAS and 5.8% in CEA (RR 1.00 [0.68–1.47]); in patients 70 years or older, there was an estimated twofold increase in risk with CAS over CEA (11.9% versus 5.7%, RR 2.09 [1.51–2.89], interaction p = 0.0038). The Interaction with age was also significant in the PP analysis.
Conclusions: Stenting should be avoided in older patients with symptomatic carotid stenosis, but may be a safe alternative to endarterectomy in younger patients. However, determination of the efficacy and ultimate balance between the two procedures requires further data on long-term stroke recurrence.

122

Similar Global N-acetylaspartate Concentration in Clinically Benign and Non-Benign Multiple Sclerosis Patients with more than 15 Years of Disease Duration

L. Achtnichts[1], O. Gonen[2], D. Rigotti[2], J.S. Babb[2], Y. Naegelin[1], K. Bendtfeld[1], J. Hirsch[1], M. Amann[1], R.I. Grossman [2], L. Kappos[1], A. Gass[1]
[1]University Hospital Basel, Basel, Switzerland, [2]New York University School of Medicine, New York, United States

Objective: To investigate whether multiple sclerosis (MS) patients with a clinically benign disease course show overall neural integrity, reflected by the preservation of the MR marker N-acetylaspartate (NAA), and higher NAA concentrations than in MS patients with similar disease duration but more pronounced disability.
Methods: T1 and T2 lesion loads and fractional brain parenchymal volume (fBPV) were determined on structural MRI and whole brain NAA concentration (WBNAA) was obtained from proton MR spectroscopy in: (i) 24 (20F) benign MS patients 50.9 ± 10.5 years old (mean ± standard deviation), of 23.1 ± 7.2 years disease duration from first symptom and Expanded Disability Status Scale (EDSS) score of 2.1 ± 0.7; (ii) 30 non-benign patients (19F) 53.6 ± 9.0 years old, 22.9 ± 5.8 years disease duration and 4.7 ± 1.0 EDSS; and (iii) 17 controls (9F) 34.0 ± 6.0 years old.
Results: The T1 hypointense lesion load of the non-benign patients: 4.1 ± 5.4 cm^3, was significantly higher than the 2.1 ± 2.2 cm^3 of the benign (p = 0.029), but their T2 hyperintense lesion volumes: 8.4 ± 8.0 cm3 and 6.2 ± 5.5 cm3, respectively, were indistinguishable (p'0.1). The controls' fBPV (86.2 ± 3.3%) was significantly higher than in both, the benign (76.4 ± 6.7%) or the non-benign patients (76.2 ± 8.4%) (p'0.0001). The controls WBNAA ' (12.2 ± 2.3 mM) was significantly higher than in the benign (10.5 ± 2.4 mM, p = 0.03) and non-benign patients (9.7 ± 2.2 mM, p = 0.002) with no significant difference between the 2 patient groups (p'0.2).
Conclusions: This study stresses similarly to other MRI measures that a clinically benign MS course is not directly associated with less pathology load than in more disabled MS phenotypes. This low association of MRS and clinical findings is likely to be due to the interference of other mechanisms such as brain plasticity or the relative sparing of clinically eloquent brain regions. Approved by authors.

123

Sleep disordered breathing in TIA/ischemic Stroke: effects on short- and long-term outcome and CPAP treatment efficacy: an open, observational, clinical, multicentre trial with a randomized arm – SAS CARE study

C.W. Cereda[1], A. Azzola[4], C. Baumann[9], F. Bornatico[1], A. Ciccone[6], ML. Dell'Acqua[1], NT. Economou[1], ttle Fischer[2], A. Gallino[5], S. Gyoerik[5], M. Gugger[3], R. Kathami[8], L. Lavie[7], P. Lavie[7], C. Limoni[1], A. Luft[9], J. Mathis[2], H. Mattle[2], L. Nobili[8], S. Ott[3], L. Petrini[1], M. Pons[4], J. Schneider[9], E. Werth[9], C.L. Bassetti[1]
[1]Neurocenter (EOC) of Southern Switzerland, Lugano, Switzerland, [2]Neurology, University Hospital, Bern, Switzerland, [3]Pneumology, University, Bern, Switzerland, [4]Pneumology, Ospedale Civico, Lugano, Switzerland, [5]Internal Medicine, Ospedale San Giovanni, Bellinzona, Switzerland, [6]Neurology, Niguarda Hospital, Milano, Switzerland, [7]Sleep Center, University of Haifa, Haifa, Israel, [8]Sleep Center, Barmelweid, Aarau, Switzerland, [9]Neurology, University Hospital, Zürich, Switzerland

Introduction: Sleep Disordered Breathing (SDB) represents a risk factor for cardiovascular morbidity, mortality and is frequent in patients with transient ischemic attacks and ischemic stroke (acute cerebrovascular events, ACE). Clinical studies suggest that 1) SDB negatively affects short-term and long-term clinical and vascular outcome after ACE 2) Continuous positive airway pressure (CPAP) treatment reverses the detrimental cardiovascular consequences of SDB. The effect of CPAP in patients with SDB and ACE remains poorly known and was assessed only in small or non-randomized trials.
Objective: The SAS CARE 1 study is planned to verify if SDB has a detrimental 3 months effect on cardiovascular functions and markers after ACE; The SAS CARE 2 study is designed to address if treatment of SDB with CPAP reduces the combined rate of mortality, stroke, cardiovascular events (myocardial infarction/revascularisation/instable angina/ hospitalisation for heart insufficiency) over a 24 months period in patients after ACE.
Methods: SAS CARE 1 (n = 200, start: April 2010) is an open, observational trial in patients with ACE admitted in a Stroke Unit. Three months after the ACE vascular parameters and markers (blood pressure, heart rate variability, endothelial function – peripheral arterial tonometry investigated by ENDO PAT 2000, and specific humoral factors) will be assessed and correlated to the apnoea-hypopnea index (AHI). SAS CARE 2 (preliminary phase n = 200, final aim n = 1000) is an open, randomised, 5-arm parallel group, observational, partially interventional, controlled study in patients with ACE within the last 90 days or previously screened in SAS CARE 1. After baseline assessments the patients will be classified according to their AHI in four arms: Non-SDB patients (AHI <10), patients with central SDB, patients with moderate-severe obstructive and sleepy SDB (AHI ≥20, ESS score ≥10), and patients with moderate-severe obstructive and non-sleepy SDB (AHI ≥20, ESS score <10). All patients with moderate-severe obstructive and sleepy SDB (AHI ≥20, ESS score ≥10) will receive CPAP treatment. Patients with moderate-severe obstructive and non-sleepy SDB (AHI ≥20, ESS score <10) will be randomised to receive CPAP treatment or not.
Results: The SAS CARE study is planned to start in May 2010. Conclusion: The SAS CARE study will add to our understanding of the clinical implications of SDB in patients with ACE and the feasibility/efficacy of CPAP treatment in selected patients with ACE and SDB.

124

Stroke complicating left ventricular noncompaction: case reports, review and management

J.M. Pignat[1], B. Leeman[1], H. Muller[1], M. Payot[2], R. Meuli[2], A. Schnider[1], J. Bogousslavsky[3], M. Reichhart[2]
[1]HCUGE, Geneva, Switzerland, [2]CHUV, Lausanne, Switzerland, [3]Clinique Valmont-Genolier, Glion-sur-Montreux, Switzerland

Introduction: Left ventricular noncompaction (LVNC) is a rare cardiomyopathy in which interruption of the endomyocardial development leads to ventricular trabeculations and recesses. Although such ventricular malformation is expected to be emboligenic, recent studies have observed only a low incidence of stroke. Besides, a causal link between LVNC and stroke occurrence could so far not be established, which raises questions with regards to recurrence risk prospection. Based on a literature review and additional case reports, we aim to systematize the global management of LVNC with a special emphasis on stroke prevention.

Method: We performed a systematic literature search on PubMed for studies and case reports (twelve) related to LVNC and cardio-embolic events. Four additional cases are reported. The A-S-C-O stroke classification is used to propose guidelines for secondary prevention.
Results: As there are not more strokes in LVNC per se than in control groups, therapeutic anticoagulation (TA) is not indicated for primary prevention, but patients suffering from concomitant emboligenic disorders, including heart diseases or thrombophilia, form high-risk subgroups for which TA becomes justified. Secondary prevention is case dependent. TA seems to be indicated in LVNC unless an alternate aetiology, which needs platelet antiaggregant or statin treatment rather than TA to prevent stroke recurrence, is explicitly identified. In this case, LVNC involvement and TA are challenged.
Conclusion: LVNC per se is not a main stroke risk factor but primary and secondary preventions should be explicitly considered depending on the comorbidities. Further studies are necessary to elucidate the role of LVNC in the pathogenesis of stroke.

125

The Bern Stroke Project. Outcome of acute ischaemic stroke in the Canton of Bern, Switzerland, in 2008

U. Fischer[1], M.L. Mono[1], M. Zwahlen[2], K. Nedeltchev[1], M. Arnold[1], A. Galimanis[1], O. Findling[1], N. Meier[1], C. Brekenfeld[3], J. Gralla[3], G. Schroth[3], H.P. Mattle[1]
[1]Department of Neurology, University of Bern, Bern, Switzerland, [2]Social and Preventive Medicine, University of Bern, Bern, Switzerland, [3]Neuroradiology, University of Bern, Bern, Switzerland

Introduction: Data on outcome of patients with acute ischaemic stroke (AIS) in large populations are scarce.
Methods: We prospectively assessed demographic data, management, outcome and its' predictors of all consecutive AIS patients during 12 months admitted to the 18 primary care hospitals of the canton of Bern (969'299 inhabitants). Blinded follow-up was obtained 3 months after AIS by telephone interview. The primary outcome was case-fatality and favourable clinical outcome (modified Rankin scale (mRS) </= 2) at 3 months. We further analysed predictors of length of hospital stay using linear regression and cumulative mortality and favourable outcome at 3 months using logistic regression.
Results: From December 2007 to December 2008 807 AIS patients were included (45% women; mean age: 72.3 years). Median NIHSS on admission was 5 (0-40). Thrombolysis was performed in 107 of 807 patients (13%). Age >/= 75 years ($p < 0.0031$) and NIHSS >/= 10 ($p = 0.0043$) were independently associated with a longer hospital stay, whereas inhospital dead ($p < 0.0001$) and thrombolysis ($p = 0.0073$) shortened length of hospitalisation. Cumulative mortality at three months was 20%. Age >/= 85 years ($p<0.0312$), NIHSS >/=12 ($p = 0.0062$) and comorbid conditions ($p = 0.002$) were independent predictors of mortality. At 3 months 50.9% of patients had a favourable outcome with age <75 years ($p < 0.001$), male sex ($p = 0.0025$), NIHSS <10 ($p < 0.001$), absence of diabetes ($p = 0.0224$) and lower Charlson comorbidity index (CCI), ($p = 0.0035$) and thrombolysis ($p = 0.0108$) as independent favourable predictors.
Conclusions: Thirteen percent of consecutive AIS patients admitted to Bernese hospitals underwent thrombolysis. Age <75 years, lesser stroke severity, absence of diabetes, lower CCI, male sex and thrombolysis independently predicted favourable outcome in this large population.

126

The cerebellum interacts with the network for action observation

A.A. Sokolov[1], M. Erb[2], A. Gharabaghi[3], W. Grodd[2], M.S. Tatagiba[1], M.A. Pavlova[4]
[1]Department of Neurosurgery, University of Tübingen Medical School, Tübingen, Germany, [2]Section for Experimental MR of the Central Nervous System, Department of Neuroradiology, University of Tübingen Medical School, Tübingen, Germany, [3]Neuroprosthetics Research Group, Werner Reichardt Centre for Integrative Neuroscience, University of Tübingen Medical School, Tübingen, Germany, [4]Department of Pediatric Neurology and Child Development, Children's Hospital, and MEG Center, Institute of Medical Psychology and Behavioral Neurobiology, University of Tübingen Medical School, Tübingen, Germany

Introduction: Recent brain imaging findings suggest cerebellar involvement in action observation, but the data are controversial. Since the cerebellum and the cerebral hemispheres are contralaterally interconnected and the right parieto-temporal cortices are of particular importance for visual processing of body motion, we hypothesized engagement of the left cerebellum in action observation. For proving this assumption, we combined lesional and functional magnetic resonance imaging (fMRI) approaches.
Methods: For the lesion study, eight patients with tumors to the left lateral or medial cerebellum and eight healthy matched controls were recruited. They had to detect a point-light walker simultaneously camouflaged by a mask. Lesion volumetry analysis was performed on structural MRI scans by using MRIcro software and Statistical Parametric Mapping (SPM2). In the fMRI study, thirteen healthy participants performed a one-back repetition task with an unmasked point-light walker and a spatially scrambled control display. Pre-processing and analysis of fMRI data were conducted with SPM8b.
Results: While lesion volume does not differ significantly between the two patient groups (Mann-Whitney test, U = 7.5, n.s.), visual sensitivity to body motion is impaired in patients with tumors to the left lateral ($\chi^2 = 11.44$, $P < 0.01$), but not the left medial cerebellum ($\chi^2 = 1.95$, n.s.), as compared to controls. Accordingly, the whole-brain fMRI analysis in healthy individuals reveals robust responses to biological motion in the left lateral cerebellum ($p < 0.05$, FWE-corrected). Dynamic causal modelling shows reciprocal interaction between the left lateral cerebellar lobule Crus I and the right superior temporal sulcus (mean endogenous connectivity parameters: 0.55 ± 0.15 for Crus I to STS, and 0.51 ± 0.18 for STS to Crus I).
Conclusions: For the first time, these findings indicate communication between the left lateral cerebellum and the right STS, a key structure of the neural circuitry underpinning visual processing of body motion. The outcome of this study has broad implications for basic and clinical neuroscience. The data will help to further develop neurological and neuropsychological management of infratentorial infarctions, to understand the mechanisms underlying neuropsychiatric conditions associated with cerebellar abnormalities, such as autistic spectrum disorders or schizophrenia, and to improve strategies for posterior fossa neurosurgery in regard to cognitive functions.

127

The frequency dependent filter behaviour of the cerebrovascular system in migraine

M. Müller[1], M. Marziniak[1]
[1]Department of Neurology, Kantonsspital Lucerne, Lucerne, Switzerland, [2]Department of Neurology, University of Münster, Münster, Germany

Introduction: In recent years, the frequency dependent behaviour of the cerebrovascular system to respond to blood pressure changes is considered a filter system. In patients with stroke or with traumatic brain injury this filter system showed characteristic changes. In migraine, several functional systems are involved in a migraine attack: the trigeminovascular system, the autonomic nervous system, and the cerebrovascular system. By using transfer function estimations between blood pressure (BP) and blood velocity (V) in the middle cerebral artery, as assessed by transcranial Doppler ultrasound, the cerebrovascular system may show a completely different linear filter behaviour. We investigated whether the filter characteristics phase shift and gain normalize in migraineurs under a treatment with triptans.
Methods: 33 healthy subjects [18 male, 15 female, mean age ± SD, 36 ± 13 years (range 14–71 years)] served as controls. 14 women (mean age ± SD, 42 ± 5 years) with frequent menstrual migraine attacks were perimenstrually treated with frovatriptan; 8 responded to the therapy with an attack reduction of 50% or more, 6 did not respond. All 14 women were investigated by means of simultaneous recordings of BP and V, and calculations of transfer function estimations. The first investigation was performed prior to medication, the second after taking frovatriptan for a mean of 5 ± 2 days. Additionally, three migraineurs underwent continuous BP and V recordings over a period of 2 hours after 10 minute baseline recordings and thereafter the subcutaneous application of 6 mg sumatriptan. The two hours recordings were divided into 10 minutes intervals; for each interval the transfer function estimations were calculated and compared to the baseline period.

Results: Compared to controls, the migraineurs exhibited a severely disturbed behaviour in terms of phase shift and gain. Compared to their corresponding baseline investigation phase shift and gain remained unchanged in the sumatriptan group and even in the responder group of frovatriptan.
Conclusion: In migraine the filter behaviour of the cerebrovascular system seems basically disturbed and will not be normalized by the used triptans. References: Müller M, et al. Changes in linear dynamics of cerebrovascular system after severe traumatic brain injury. Stroke. 2003;34:1197–202. Giller CA and Müller M. Linearity and non-linearity in cerebral hemodynamics. Med Eng Phys. 2003;25:633–46.

128

The role of cognitive functioning in the process of decision making in patients with multiple sclerosis

S. Simioni[1], J.-M. Annoni[2], M. Gschwind[3], P. Vuilleumier[3], M. Schluep[1]
[1]Service of Neurology, CHUV, Lausanne, Switzerland, [2]Service of Neurology, HUG, Geneva, Switzerland, [3]Department of Neuroscience, Faculty of Medicine, University of Geneva, Geneva, Switzerland

Introduction: A deficit in decision making (DM) related to a decreased emotional arousal was reported in patients with multiple sclerosis (MS) using tasks assessing DM under ambiguity (i.e. where subjects have to figure out the game rules implicitly, by using the feedbacks they get after choices). By contrast, DM under risk evaluation (i.e. where relevant information and explicit rules are given) has never been studied in MS.
Methods: Eighty patients with relapsing-remitting (RR) MS (age: 36.1 ± 7.7 y; disease duration: 5.1 ± 3.3 y; EDSS disability score: 1.9 ± 0.5) and 40 healthy volunteers were enrolled in the study. We used the Cambridge Gamble Task (CGT) to measure DM under risk. A row of 10 boxes (red or blue with a ratio varying across trials) was presented on a computer screen. Participants had to guess whether a yellow token was hidden in a red or blue box and gamble points on their choice. A winning choice was rewarded by the total of points gambled, whereas a losing choice was punished by subtracting gambled points from the capital. Risk taking, Quality of DM, Deliberation time, Risk adjustment, Delay aversion and Overall proportion bet were measured. Participants also underwent the Brief Repeatable Battery of Neuropsychological Tests (BRB-N: Selective Reminding Test [SRT], 10/36 Spatial Recall Test, Paced Auditory Serial Addition Test [PASAT], Symbol Digit Modalities Test [SDMT], Word List Generation test [WLG]), and the Stockings of Cambridge (SOC). Non parametric statistics were performed.
Results: In the CGT, RRMS patients showed higher deliberation times ($p = 0.0002$) and poorer quality of DM ($p = 0.009$) than controls, whereas risk taking was comparable. They also obtained lower scores in tasks assessing verbal learning (SRT: $p = 0.002$), attention/processing speed (SDMT: $p = 0.0003$; PASAT: $p = 0.06$) and executive functions (SOC-latency: $p = 0.001$; SOC-correct trials: $p = 0.02$; WLG: $p = 0.01$). In RRMS patients, CGT deliberation times negatively correlated with attention measures (SDMT: $r = –0.3$, $p = 0.008$; PASAT: $r = –0.3$, $p = 0.008$). By contrast, CGT quality of DM negatively correlated with executive functioning (SOC-latency: $r = –0.3$, $p = 0.02$).
Conclusions: Quality of DM is impaired in RRMS patients, whereas risk taking is not increased. Concomitantly, deficits in attention and executive functioning are detected. These cognitive deficits might reflect a fronto-sub-cortical dysfunction responsible for decreased DM competence. In MS, deficits in DM also depend on cognitive functioning.

129

Transient Ischemic Attack versus Mimic-Frequency, clinical characteristics and outcome

M. Amort[1], F. Fluri[1], J. Schäfer[2], F. Weisskopf[1], M. Katan[1], A. Burow[1], H.C. Bucher[2], L. Bonati[1], P.A. Lyrer[1], S.T. Engelter[1]
[1]Stroke Unit and Department of Neurology, Basel, Switzerland, [2]Institute for Clinical Epidemiology and Biostatistics, Basel, Switzerland

Background: In some patients transient focal neurological symptoms are not attributable to a transient ischemic attack (TIA). This entity might be labeled "TIA-mimic". The needs with respect to diagnostic and therapeutic measures differ widely between mimic and TIA patients. It would be clinically useful to have features which are helpful to distinguish both entities in the emergency situation.
Methods: We determined frequency, clinical characteristics and outcome events (Stroke, TIA, myocardial infarction (MI), death within 90 days) of mimic versus TIA patients. Data of a prospective, single-university center TIA study cohort were used.
Results: Fifty-five of 303 patients (18.2%) were TIA mimics. Epileptic seizures (26/55; 47%) and migraine attacks (12/55; 22%) were the most common diagnosis among mimics. Pure hemisensory loss (odds ratio [OR] 2.9; 95%-confidence interval [CI] 1.29–6.35, padjusted for multiple testing = 0.048) was more frequent in mimics than in TIA patients. Unilateral paresis was significantly less prevalent in mimics (OR 0.29; CI 0.14–0.57, padjusted = 0.001) than in TIA patients. The frequency of aphasia was nearly identical in TIA- (21.4%) and in mimic patients (21.8%). Dysarthria was present as often in TIA patients (20.6%) as in mimics (12.7%; padjusted for multiple testing = 0.25). The duration of symptoms did not differ between TIA (178.5 ± 332 minutes) and mimic patients (203.4 ± 341.2 minutes, $p = 0.63$). The mean blood pressure measured at admission was nearly identical among TIA (systolic 157 ± 35.8 mm Hg, diastolic 85 ± 20.3 mm Hg) and mimic patients (systolic 158 ± 23.2 mm Hg, $p > 0.8$; diastolic 87± 14.3 mm Hg 3, $p > 0.4$). At 90 days, none of the mimics, but 35 TIA patients (14%; 13 strokes, 19 TIA, 3 MI) had outcome events.
Conclusion: Among putative TIA patients in the emergency department, hemisensory symptoms indicated mimics, while hemiparesis suggested TIAs. Language or speech abnormalities and blood pressure values did not differentiate between both entities. The absence of outcome events within 3 months among the mimics indicated a better prognosis.

130

Transient pure word-blindness due to functional disconnection

M. Gschwind[1], S. Arzy[2], M.D. Martory[1], T. Landis[1], P. Vuilleumier[1], G. Allali[1]
[1]Departement of Neurology, University Hospital and Departement of Neuroscience, University of Geneva, Geneve, Switzerland, [2]Department of Neurology, Hadassah Hebrew University Hospital, Jerusalem, Israel

Introduction: "Word-blindness" is characterized by the loss of the ability to read and understand written scripts, although spontaneous writing and all other speech faculties are intact (Grüsser & Landis 1991). A very rare variant is "pure word blindness" or "alexia without agraphia and without hemianopia" which has been related to structural lesions disconnecting the projection from visual cortex to language areas, while sparing the geniculocalcarine pathway (Dejerine 1892, Epelbaum 2008).
Methods: Here we report the case of a patient with pure word-blindness, in which a multimodal approach was used to investigate the neural basis of her transient symptomatology. The patient was a 78 year-old right-handed woman, who while reading a newspaper suddenly noticed that the letters were "floating", making reading impossible. Her past medical history included a left temporo-occipital stroke two years before presentation (with hemianopia, achromatopsia, memory troubles), that had completely recovered. Neurological examination on admission revealed an inability to read both whole words and letter by letter. No hemianopia or any sensorimotor deficits were detected. Neuropsychological evaluation showed that other language and visual functions were intact. While the patient was able to spontaneously write long sentences, she could not copy even single words. Her symptoms progressively improved and a complete recovery was achieved 48 hours after admission.
Results: Standard brain MRI during the acute phase and three days later showed an old left temporo-occipital ischemic lesion, but no evidence for acute ischemia. Standard EEG and transcranial Doppler were also normal. However, Diffusion Tensor MRI and Tractography revealed a significant decrease in volume and fiber integrity of the left inferior longitudinal fasciculus (ILF) as compared with her right ILF and with a healthy control subject. No asymmetry was found in the arcuate fasciculus and callosal connections. After recovery, functional MRI revealed preserved activation of the visual word form area (VWFA) and Wernicke's area. Finally, the comparison of EEG signals recorded during alexia and after recovery revealed a significant decrease in beta power (8–13 Hz) in the left occipito-temporal cortex.
Conclusion: This patient, although presenting an old temporo-occipital lesion, had no word-blindness before and after the episode. While she presumably suffered from a chronically

damaged left ILF, fMRI revealed a normal functioning of VWFA and Wernicke's area. It is only during her transient episode of word-blindness that electrophysiological alteration was found in the left temporo-occipital cortex for the beta band, suggesting a temporary functional disconnection or decoupling between visual and language areas, explaining the impressive clinical symptoms of the patient.

131

Visual hallucinations in dementia with Lewy bodies: a multichannel visual evoked potential approach

G. Allali[1], M. Genetti[2], M. Seeck[1], C.M. Michel[2], F. Assal[1]
[1]Department of Neurology, Geneva University Hospitals and University of Geneva, Geneva, Switzerland, [2]Functional Brain Mapping Laboratory, University Medical Center & Dept of Clinical Neurosciences, University Hospital Geneva, Geneva, Switzerland

Introduction: Dementia with Lewy bodies (DLB) and Alzheimer's disease (AD) are two common forms of dementia in elderly people. In addition to cognitive impairments, fluctuating attention and extrapyramidal signs, recurrent visual hallucinations are the core clinical features of DLB and seem to be one of the best clinical predictor of DLB. Hypometabolism in the occipital cortex found in such DLB patients has been involved in etiopathogenesis of visual hallucinations and involvement of visual pathways has been suggested. Yet, few electrophysiological data have studied the origin of these visual symptoms. The goal of this study was to compare high resolution visual evoked potentials (VEP) between DLB and AD patients.
Methods: 256-channel VEP were recorded in 3 DLB subjects with visual hallucinations and 3 AD subjects without these visual symptoms. Full-field pattern-reversal stimuli were delivered to each eye separately. In addition to waveform analyses, we investigated differences in the spatio-temporal scalp configuration (topography) between the groups across time. EEG was continuously recorded at a sampling rate of 1 kHz without filter. Epochs were selected from 50 ms before to 450 ms after visual stimulations and were band-pass filtered between 1 and 30 Hz.
Results: Waveform analyses revealed differences after the P100, from 120 ms to 250 ms post stimulus onset (p-value for minimum 5 ms <0.01). Comparison between groups showed differences over the occipital and frontal electrodes around 200 ms post stimulus onset with a higher amplitude in the DLB group ($p < 0.01$). This was reflected in the spatio-temporal segmentation procedure by 2 distinct topographies between 195 to 270 ms ($p < 0.05$ for the Global Explain Variance and the total number of time frames of appearance) which double-dissociated DLB and AD patients.
Conclusions: These preliminary results suggest that those differences in the processing of elementary visual information at the level of the visual cortex and in frontal regions between AD and DLB patients fit with recent models of recurrent visual hallucinations that combine deficits in object perception and attentional binding.

132

Visual object agnosia: when a ball is an orange and vice versa

R. Ptak, M. Di Pietro, E. Robert, A. Schnider
[1]Service de Neurorééducation, Hôpitaux Universitaires de Genève, Genève, Switzerland

Introduction: Patients with associative visual agnosia fail to recognize the identity of visually presented objects despite preserved semantic knowledge. Current accounts of the disorder postulate subtle visual impairments, a deficit of form integration, or a semantic deficit confined to visual information.
Methods: Here we present a patient with associative visual agnosia following a stroke affecting the left inferior temporal lobe, who showed striking errors when identifying pictures of objects, animals, or faces. Damage was confined to the fusiform, lingual and inferior occipital gyrus.
Results: The patient identified only 46% of 260 visually presented line drawings, compared to 95% correct responses to verbal description of the same items. He produced satisfactory copies of objects that he was unable to identify. When asked to point to an object presented together with a visual and a semantic distracter, his performance was flawless. However, when asked to decide which of three objects belonged to the same category (e.g. two fruits), he was biased toward choosing the two visually similar objects (e.g. an orange and a ball). In addition, when asked to indicate whether an array of objects contained a given item (e.g. a button), he often chose a visual distracter (e.g. a wheel), but rarely a semantic or neutral distracter.
Conclusions: The results indicate that misidentifications of our patient are based on global visual similarity between the target picture and the distracter. We suggest that in our patient a picture activates representations of different objects sharing the same form, which explains his large number of visual errors. The misidentifications of our patient can thus be understood in terms of a visual classification deficit.

133

Whole-brain structural connectivity in patients with focal epilepsy studied with magnetic resonance diffusion spectrum imaging (DSI)

S. Vulliémoz[1], A. Lemkaddem[2], L. Cammoun[2], T. Kober[2], R.M. Meuli[3], F. Lazeyras[1], C.M. Michel[1], J.P. Thiran[2], M. Seeck[1]
[1]Hôpitaux Universitaires et Faculté de Médecine, Genève, Switzerland, [2]Ecole Polytechnique Fédérale, Lausanne, Switzerland, [3]Centre hospitalier Universitaire Vaudois, Lausanne, Switzerland

Introduction: In patients with focal epilepsy, diffusion MRI often reveals structural changes extending beyond visible lesions or show structural abnormalities even when the clinical scans are normal. Magnetic Resonance Tractography, based on diffusion tensor imaging, allows non-invasive mapping of white matter tracts in vivo. Recently, Diffusion Spectrum Imaging (DSI), based on an increased number of diffusion directions and intensities, has improved the sensitivity of tractography, notably with respect to the problem of fibre crossing and recent development allow acquisition times compatible with clinical application.
Methods: We used DSI tractography and parcellation of the grey matter in regions of interest to build whole-brain connectivity matrices describing the mutual connections between cortical regions at different spatial resolutions in patients with focal epilepsy and healthy controls. The combination with other imaging modalities (EEG source imaging, isotope imaging, simultaneous EEG-fMRI) localising cortical regions corresponding to the irritative zone (IZ) or seizure onset zone (OZ) allows to reconstruct tracts of interest to map the connectivity of the IZ/OZ, as well as physiological closeby tracts subserving normal neurological/cognitive functions.
Results: We here present our preliminary results on patients with lesional and cryptogenic epilepsy showing that this new analysis strategy allows investigating focal connectivity changes at a whole-brain level with unprecedented sensitivity.
Conclusion: Whole-brain imaging of structural connectivity in patients with epilepsy opens new avenues for understanding epileptic networks and for clinical management of candidates for epilepsy surgery.

134

Perception of timing in Parkinson's Disease

Eveline Geiser[1], Alain Kaelin-Lang[2]
[1]Massachusetts Institute of Technology, Department for Brian and Cognitive Sciences, [2]University Hospital Bern, Neurology

Introduction: Parkinson disease (PD) is diagnosed on the basis of the classical motor trias (bradykinesia, rigidity, and resting tremor). Recently, a lack of internal timekeeping mechanisms has been suggested in PD-patients resulting in higher variability and inaccuracy of patients compared to controls in motor tasks, thus, resulting in impaired timing PRODUCTION. In PD-patients the cells in the substantia nigra pars compacta projecting to posterior putamen are most severely affected by neurodegeneration, thus leading to more severe dopaminergic depletion in the posterior putamen and subsequently reduced projection to the ventrolateral thalamus and supplementary motor area (SMA). Notably, these anatomical structures depleted of dopamine in PD-patients, have been found to be involved in timing perception in healthy individuals. The present study aimed to investigate timing PERCEPTION in PD-patients. Particularly, we aimed to test the ability of PD patients to discriminate between regular and irregular auditory cueing.
Methods: PD-patients were presented with metrical and non-metrical auditory rhythms of different time scales and metrical hierarchies in a metrical decision task. Their performance was measured before and after the L-Dopa test. As a control condition a reaction time task was equally included. Reaction time in the metrical decision task was controlled for motor

reaction time changes before and after the L-Dopa test. Discrimination rate was analyzed by calculating d-prime.
Results: Preliminary data suggest that L-Dopa alters performance and reaction time in the meter decision task in PD patients.
Conclusion: We conclude that the cortico-striatal pathway is crucial in auditory regularity perception explaining the sensitivity of PD-patients to external auditory pulse perception. These mechanisms seem to be modulated by L-Dopa therapy. Finally, PD patients could serve as a model to investigate the neurophysiological correlates of time perception.

135

Recovery-prediction of upper limb function in cervical spinal cord injury: stratification by ulnar somatosensory evoked potentials

Martin Schubert, Fabian Kuhn, Pascal Halder, Martina Spiess, Armin Curt, EM-SCI Study group

Introduction: Early prediction of functional outcome of hand function in tetraplegic patients is crucial for an adequate planning of the rehabilitation process. It is known from earlier studies that somatosensory evoked potentials remain invariant during functional recovery after spinal cord injury (SCI) 1. It was therefore aimed to describe the one-year time course of ulnar nerve stimulated somatosensory potentials (uSEP) after cervical SCI, its relation to neurological and functional parameters, and its use for a stratified outcome prediction of hand function.
Methods: In 356 patients uSEP, standardized assessments of light touch and a protocol to assess spinal cord independence measure (SCIM) 2 comprising a score to assess hand function were evaluated repeatedly throughout the first year after cervical SCI.
Results: In 32% uSEP were abolished and could never be recorded during the year after injury. In 40% uSEP were recorded in every assessment whereof 12% showed delayed latencies at initial examination with significant shortening by 2 ms over 6 months. Thus, despite the significant shortening of delayed uSEP latencies this change was small and not in a clinically relevant range. In 15% re-occurring potentials were observed while 12% were inconsistently recordable. Initial neurological and functional scores were different for each of these groups while the rates of sensory recovery and functional improvement did not vary between groups but increased in parallel.
Conclusions: uSEP in cervical SCI yield invariant assessment of sensory tract integrity which can be obtained in a majority of cervical SCI early after the injury. Recordability of uSEP and classification by latency and amplitude criteria therefore qualify as objective and independent stratification marker for an early prediction of sensory and hand function recovery. This detailed description of uSEP in a large cohort of cervical SCI patients confirms a lack of significant repair in upper limb sensory tracts during one year post injury. It is suggested that uSEP in cervical SCI can be used early after trauma to objectively classify severity of cord injury and make a first prognosis of hand function outcome.
1) Curt A, Dietz V. Electrophysiological recordings in patients with spinal cord injury: significance for predicting outcome. Spinal Cord. 1999;37:157–65.
2) Catz A, et al. The Catz-Itzkovich SCIM: a revised version of the Spinal Cord Independence Measure. Disabil Rehabil. 2001;23:263–8.

136

A Method for Imaging Elusive Deep Brain Nuclei at 3 Tesla Multimodal MRI

T. Lönnfors-Weitzel[1], T. Weitzel[3], C. Kiefer[1], T. Krause[3], A. Stibal[2], A Kaelin-Lang[4], C Ozdoba[1]
[1]Institute of Interventional and Diagnostic Neuroradiology, University of Bern, University Hospital of Bern, Inselspital, Bern, Switzerland, [2]Department of Neurosurgery, University of Bern, University Hospital of Bern, Inselspital,, Bern, Switzerland, [3]Department of Nuclearmedicine, University of Bern, University Hospital of Bern, Inselspital, Bern, Switzerland, [4]Department of Neurology, University of Bern, University Hospital of Bern, Inselspital, Bern, Switzerland

Objective: Thalamic, mesencephalic and pontine nuclei represent a challenging group of brain structures for brain imaging. They are involved in a multitude of clinical syndromes and are increasingly being targeted in therapeutic interventions with deep brain stimulation, most prominently Nucleus ventrointermedius (VIM) in thalamus and subthalamic nucleus (STN) in mesenzephalon in context of movement disorders. Pontine nuclei, (i.e. pedunculo pontine nucleus, (PPN)) are an exception as a target in Europe, but are increasingly a point of interest in modulation of movement, hearing and degeneration. Until recently identification of potential targets relied on atlas based coordinates. Our aim is to visualize elements in motor loops involved in many movement disorders and other clinical syndromes.
Methods: All imaging was performed at 3 Tesla (Trio, Siemens Medical Solutions, Erlangen, Germany). Multimodal datasets were constructed from MR submodalities (sometimes called multispectral MR) based on acquisition and coregistration of a set of different isotropic 3D Images. For delineation of deep brain nuclei a set of 7 MR submodalities was chosen, including PD, T1, T2 and T2-FLAIR images spanning a broad range of parameters. By using an independent component analysis based Hotelling transformation the number of dimensions of the multimodal dataset was reduced to 5. In the resulting dataset each voxel is represented by a 5-dimensional feature vector. Based on said feature vectors a degree of similiarity was defined. Voxels with different degree of cortical matter (nuclei) were systematically chosen. Visualization is performed by coloring all voxels according to their similiarity to the chosen voxel. In case the chosen voxel represents part of a nucleus the whole nucleus is delineated including all other nuclei sharing similar features. All nuclei were referred to Schaltenbrand and Wahren anatomical atlas and to Salamon Neuroanatomy Web-atlas.
Results: All above mentioned nuclei could be identified in all subjects in multimodal maps and some in T2. I.e. the pedunculopontine nucleus was identified on the suszeptibility weighted images and in maps acquired by multimodal analysis.
Conclusions: Highfield MRI is a potent method for identification of subtle anatomical structures and can be used to heighten accuracy of targeting in animal models. Should these structures become relevant to human therapies in functional neurosurgery, these methods can be applied.

137

Acute Basilar Artery Occlusion Treated With Intra-Arterial Thrombolysis – Clinical and MRI Predictors Of Clinical Outcome

M. El-Koussy[1], A. Karameshev[1], H.P. Mattle[2], G. Schroth[1], J. Gralla[1], C. Brekenfeld[1], ML. Mono[2], K. Nedeltchev[3], M. Arnold[2]
[1]Dept. Neuroradiology, Univ. Bern, Bern, Switzerland, [2]Dept. Neurology, Univ. Bern, Bern, Switzerland, [3]Dept. Neurology, Triemli Hospital, Zurich, Switzerland

Introduction: Basilar artery occlusion (BAO) is a potentially fatal clinical condition. Intra-arterial thrombolysis (IAT) for BAO improves the prognosis. The extent of early ischemic damage on pre-treatment diffusion-weighted MR-imaging (DWI) can predict the clinical outcome in BAO and influence the response to IAT. The predictive value of previously published DWI-scoring systems has not been compared yet. We studied the MRI and predictors of clinical outcome, e.g. NIH-Stroke-Scale (NIHSS), Glasgow-Coma-Scale (GCS).
Methods: Patients with acute BAO were treated with IAT at our Stroke Unit within 12h after symptom onset. Pre-treatment MRI-scans as well as a clinical follow-ups were performed. Three recently published DWI-scoring systems were compared. In addition, a modified scoring system was proposed.
Results: Thirty-six patients (13 women, 23 men; mean age 60, SD15) were included. The median NIHSS-score on admission was 17. The mean time-to-treat was 5.6 h after onset of symptoms. Recanalisation after IAT was achieved in 26 patients (72%). The outcome at three months was good (mRS 0-3) in 19 (52.8%) and poor (mRS 4-6) in 17 (47.2%) patients. There was

no significant correlation between the time-to-treat, recanalisation rate and the clinical outcome. Significant baseline predictors were the NIHSS on admission and GCS. All four DWI-scoring systems significantly correlated with the clinical outcome. The multivariate analysis revealed that the herein proposed DWI-score was a more reliable predictor of functional outcome (P = 0.004).
Conclusion: DWI is a strong predictor for clinical outcome in BAO treated by IAT. The proposed DWI-scoring is a simplified, clinically-weighted scoring system slightly outperformed the previously published scoring systems. Still, the therapeutic decision must be discussed in an interdisciplinary team, including neurologists, and must be guided by the clinical status of the patient.

138

Angiocentric Glioma: A Case Report and Comparison of Imaging findings

C. Amaxopoulou[1], A Pangalu[1], R.A. Kockro[2], H. Dohmen-Scheufler[3], A. Valavanis[1]
[1]Department of Neuroradiology, University Hospital Zürich, Zürich, Switzerland, [2]Department of Neurosurgery, University Hospital Zürich, Zürich, Switzerland, [3]Department of Neuropathology, University Hospital Zürich, Zürich, Switzerland

Introduction: In 2007 the World Health Organization renewed the classification of tumors of the Central Nervous System: Angiocentric glioma was established as a new clinicopathological entity of brain tumors. We present the first case of angiocentric glioma in our institution and overview the current literature of reported cases particularly related to imaging findings.
Methods: We report of a nine year old child with angiocentric glioma suffering from persistent seizures which could not be controlled with medical treatment. We evaluated the MRI and CT findings as well as the histopathologic features in context with the current literature.
Results: In this case CT presented a hypodense, non-enhancing lesion of the left mesial temporal lobe. On MR imaging the lesion was non-enhancing and hypointense on T1. It was hyperintense on fluid-attenuated inversion recovery and T2. Microscopically the tumor consisted of monomorphous, bipolar tumor cells with a conspicuous perivascular arrangement in terms of pseudorossetes. The tumor cells were positive reactive for vimentin and glial fibrillary acidic protein and showed epithelial membrane antigene positive “dot like” reactions. Initially a sub-total tumor resection was performed followed by gross total resection due to persistent seizures. On the first follow-up three months after surgery the patient was seizure free and without neurological deficits.
Conclusions: We compared our findings with 26 cases in the literature. Seizures were reported the most frequent symptom. Findings on CT and MR imaging were identical to the case reported here. In all but one of the reported cases, complete resection resulted in a long term seizure- and recurrence-free outcome. Complete surgical resection should be the primary goal of treatment in this histological entity.

139

Application of drug-eluting stents for the treatment of symptomatic intracranial stenosis: Preliminary results

J. Abu-Isa, P. Mordasini, C. Brekenfeld, U. Fischer, M. Arnold, M.L. Mono, D. Do, J. Gralla, G. Schroth
Inselspital, Bern, Switzerland

Introduction: Intracranial stenting for treatment of symptomatic intracranial stenosis is a relatively novel approach but has been widely applied in the recent years. Although the procedural-related complication rate is low the early in-stent re-stenosis rate of these dedicated “bare metal stents” is a matter of concern in the delicate intracranial anatomical setting. Although low re-stenosis rates have been shown for drug-eluting stents in the cardiovascular field, no data on the intracranial application is available.
Methods: Between 2003 and 2009 eleven patients (7 male, 4 female, mean age 57.7 years) were treated with drug-eluting stents (Xience, Endeavor, Promus) for symptomatic intracranial stenosis. Follow-up was performed using trans-cranial ultrasound (TCD), magnetic resonance imaging (MRI) and angiography (DSA). Location of target lesion was the intracranial internal carotid artery (ICA) in three cases, vertebral artery (VA) in three cases, medial cerebral artery (MCA) in three cases and the basilar artery (BA) in two cases.
Results: The application of the stents was feasible in all cases. Mean follow-up interval was 13.6 months including 10 patients (one patient developed a post-interventional fatal cerebral hyperperfusion syndrome). In nine patients follow-up did not show relevant re-stenosis. In one case of an MCA stenosis TCD revealed asymptomatic (50%) re-stenosis after 3.5 years.
Conclusion: The application of drug-eluting stents in the treatment of symptomatic intracranial stenosis is technically feasible. The re-stenosis rate in this small group of patients is very low and indicates a positive effect of the drug-eluting stent on pathomechanism of intracranial in-stent re-stenosis.

140

Assessment of cerebral blood flow by selective vessel encoding arterial spin labeling: Ready to challenge angiography?

R. Wiest[1], M. Hauf[1], J. Gralla[1], K. Jann[2], G. Schroth[1], H. Mattle[3], JJ. Wang[4], A. Federspiel[1]
[1]Neuroradiology, Inselspital Bern, Switzerland, [2]Psychiatric Neurophysiology, Psychiatric University Hospital Bern, Switzerland, [3]Neurology, Inselspital Bern, Switzerland, [4]Neurology and Neuroradiology, University of Pennsylvania, United States

Introduction: Arterial Spin Labeling (ASL) is a quickly developing technique with a wide range of applications in the field of neuroradiology and neurology. ASL is noninvasive, fast and provides a quantified measure of blood flow in units of ml/100 g/min. Recent advances in ASL have permitted noninvasive evaluation of vascular territories to investigate perfusion deficits and collateral blood flow.
Methods: We have tested selective vessel-encoded ASL in ten patients with extra- and intracranial occlusive disease (seven patients with carotid artery (CA) stenosis and three patients with middle cerebral artery (MCA) stenosis. The method was paralleled by non invasive MR-angiography and Digital Subtraction Angiography (DSA). Imaging was performed on a Siemens 3T Trio scanner (Siemens, Erlangen, Germany). Tagging duration was 1375 ms for the tagging pulse train. The post labeling delay was 1000 ms and TR/TE was 3000 ms/52 ms. A total of 20 images were acquired for a set of six cycles. Analysis and computation of selective ASL maps were performed using self written Matlab programs (MathWorks, Inc., Natick, USA).
Results: Mean CBF showed a 40% decrease in the affected hemisphere supplied by the stenotic carotid artery (37.7 ml/100 g/min vs. 22.6 ml/100 g/min). In patients with MCA stenosis there was a 31% decrease compared to the contralateral hemisphere (26 ml/100g/min vs. 18 ml/100g/min). In three patients that underwent internal carotid artery stenting mean CBF in the affected hemisphere increased by 29% (from 25 ml/100 g/min to 35 ml/100 g/min) after treatment with marked extension of the supplied vascular territory. Visual analysis of the CBF map in 7 untreated patients allowed a discrimination of 1) the territorial supply of the middle and anterior cerebral artery and 2) anterior cross flow to the affected hemisphere in accordance with DSA. Discrimination between anterior and posterior circulation supply was conclusive only in two patients with CA stenosis compared with DSA.
Conclusion: Vessel-encoded ASL may be currently used to map the anterior cerebrovascular territories, anastomoses and treatment response of patients with cerebrovascular disease non-invasively. The discrimination of the anterior and posterior circulation, however, is still a challenging issue due to confounding labeling effects at the carotid level during basilar artery tagging. In contrast, angiography must be considered as the “unchallenged” gold standard up to now.
This work has been partially granted by the SNF Grant (SPUM) 33CM30-124114 Impact of qualitative MR perfusion imaging on the management of patients with carotid artery disease.

141

Cerebral microbleeds and iron deposition in deep grey matter based on SWI discriminate stable versus progressive mild cognitive impairment (MCI)

Sven Haller[1], A. Bartsch[4], Duy Nguyen[1], C. Rodriguez[2], J. Emch[2], G. Gold[3], K.O. Lovblad[1], P. Giannakopoulos[2]
[1]Neuroradiology, Geneva, Switzerland, [2]Division of Old Age Psychiatry, Department of Psychiatry, Geneva, Switzerland, [3]Department of Rehabilitation and Geriatrics, Geneva, Switzerland, [4]Neuroradiology, Heidelberg, Germany

Introduction: We investigated whether stable versus progressive mild cognitive impairment (sMCI, pMCI) subjects can be discriminated based on cerebral microbleeds and iron deposition in deep grey matter.
Methods: Susceptibility weighted imaging (SWI) was assessed at baseline in 35 healthy controls (HC) and 69 MCI subjects. At follow-up after one year, 40 MCI subjects remained stable (sMCI), while 27 MCI progressed (pMCI), 2 subjects were lost upon follow-up. Cerebral microbleeds were visually analyzed by two experienced neuroradiologists in consensus. Iron deposition in deep grey matter was assessed in a voxel based morphometry (VBM) like voxel-wise statistical analysis after non-linear spatial registration.
Results: The number of microbleeds was significantly higher in MCI compared to HC ($p < 0.01$), yet there were no significant differences in respect to this parameter between sMCI and pMCI. Iron concentration increased in MCI compared to HC in right pallidum ($p < 0.01$) and right substantia nigra ($p < 0.01$) but significantly decreased in right red nucleus ($p < 0.05$). Again, no significant differences were present according to this analysis between sMCI and pMCI. However, when using a support vector machine (SVM) classifier, we were able to discriminate MCI versus HC (accuracy 83.55%) and sMCI versus pMCI (accuracy 85.26%).
Conclusions: The observed differences in cerebral microbleeds and iron deposition in deep grey matter are neuroimaging surrogate markers of the degenerative process in MCI and discriminate between MCI and HC. Discrimination between sMCI and pMCI is possible only when applying advanced multi vector pattern analysis, a branch of machine learning.

142

Cerebrovascular Reserve Capacity (CVR) measurements in patients with steno-occlusive arterial disease using Arterial Spin Labeling (ASL)

M. Hauf[1], F. Kellner-Weldon[1], K. Jann[2], R. Wiest[1], A. Federspiel[2], G. Schroth[1]
[1]Institute of Diagnostic and Interventional Neuroradiology, Inselspital, University of Bern, Bern, Switzerland, [2]Department of Psychiatric Neurophysiology, University Hospital of Psychiatry, Bern, Switzerland

Introduction: In cerebrovascular disease the individual risk of stroke recurrence is influenced by the risk of thromboembolism and hemodynamic compromise of the brain parenchyma. Cerebral hemodynamics can be studied by CVR. Currently, CVR is routinely investigated with Transcranial Doppler Ultrasound (TCD). TCD, however is limited due to the inability to quantify cerebral perfusion and poor spatial resolution. Positron emission tomography, the gold standard of brain perfusion imaging, is expensive, routinely unavailable for clinical use and carries the risk of radiation exposure. ASL provides the opportunity to perform whole brain perfusion imaging providing a quantified measure of blood flow.
Methods: Seventeen patients (6 f; age range 15–73 yrs) with steno-occlusive disease of the carotid (n = 14) or the middle cerebral artery (MCA; n = 3) were investigated with pseudo continuous ASL (pCASL) (TR 4000 ms, 16 slices, label time 1.72s, post labeling delay 1.5 s) to measure CBF at rest and during a vasodilatory stimulus of 5% CO2. CBF maps were calculated using a self-written MATLAB program. CBF values in the cortical territory of the MCA were extracted using MRIcroR.
Results: To determine normal values we calculated CBF values of 16 MCA territories without upstream steno-occlusive disease. The mean CBF at rest was 59.6 ml/100 g/min (SD 12.1). A correlation between resting state CBF values and the resting state endtidal Co2 (ETCo2) (Pearson's r = 0.43) and age (Pearson's r = –0.57) were observed. During a vasodilatory stimulus CBF increased in the MCA territories by 17.1 ml/100 g/min (SD 10.4), or 2.4 ml/ΔETCo2/100g/min (SD 1.56). In 6 MCA territories with an upstream stenosis of 70–90% CBF values increased by 2.04 ml/ΔETCo2/100g/min (SD 1.41), and in 9 MCA territories with un upstream stenosis ≥90% by 0.14 ml/ΔETCo2/100g/min (SD 1.14).
Conclusion: Preliminary data show the feasibility of CVR measurements with ASL in steno-occlusive disease to provide non-invasive CBF and CVR values covering the whole brain parenchyma. CVR is markedly reduced in patients with arterial stenosis ≥90%, but not in patients with a stenosis of 70–90%. The variance of the data reflects CVR dependency on stenosis grade as well as on collateral flow. The CBF values at rest depend on age and the endogenous level of ETCo2. These findings have to be considered in the interpretation of the data, particularly in bilateral steno-occlusive arterial disease. This work has been granted by the SNF Grant (SPUM) 33CM30-124114.

143

Classification of MS-Lesions using Dynamic Histogram Analysis (DHA)

J. Slotboom, R. Verma, M. El-Koussy, R. Wiest
Institute for Diagnostic and Interventional Neuroradiology, Bern, Switzerland

Introduction: MRI is a cornerstone in the diagnosis and follow-up of multiple sclerosis (MS). Standard imaging protocols for disease monitoring include FLAIR, T2- and T1-weighted image series before and after contrast agent (Gd-DTPA) administration. Active MS lesions show Gd-uptake due to disruption of the blood-brain barrier (BBB), whereas chronic lesions usually do not enhance. Routine imaging protocols discriminate enhancing and non-enhancing lesions, but do not take into account the amount of leakiness as a function of time. Here, we propose a novel strategy to assess white matter lesions and normal appearing white matter (NAWM) by application of fast EPI-based DSCE-MR-imaging.
Methods: Five female patients (age 31–65 years, mean age 38.2 years), four with relapsing-remitting MS, one with hyperacute MS were studied with DHA. DHA analyses perfusion histogram parameters as a function of time, i.e. the time dependent contrast uptake in the brain tissue before, during and after Gd-DTPA administration. The contrast of the difference-images between baseline and bolus passage depends on the concentration in the blood vessel, causing a positively increased difference signal, and BBB disruption causing a negative difference signal due to T1-shortening.
Results: Two patients displayed with active lesions, three patients showed no active lesions on contrast enhanced T1 images. Despite the small number patients, the histogram center parameter showed significant difference during the reperfusion phase of –1.6 a.u. for non active lesions, versus –45.9 a.u. ($p < 0.05$) for active lesions. During this phase the histogram center parameter of all MS lesions (–16.4 a.u.) was compared to normal appearing white matter (11.2 a.u.) resulting in a significant difference between the two tissue types ($p < 0.03$). The hyperacute lesion showed extreme fast contrast enhancement within 20 seconds after bolus application, resulting in strong negative histogram center parameter of –78.0; the other enhancing lesion of –13.8. Chronic MS-lesions did not show this behaviour. No significant difference in the width parameter has been observed in this small patient group.
Conclusion: DHA enables to study time dependent enhancement behaviour of MS-lesions, which might be helpful in making further sub-classifications of active MS-lesions based on the magnitude of BBB disruption. It further allows to study subtle perfusion alterations of NAWM.

144

Computer Simulation of Thromboaspiration as Used in Interventional Neuroradiology for the Treatment of Acute Stroke

J. Slotboom, P. Mordasini, C. Brekenfeld, J. Gralla, G. Schroth
Institute for Diagnostic and Interventional Neuroradiology, Bern, Switzerland

Introduction: In the interventional treatment of acute stroke, thromboaspiration is a technique which is increasingly often used. If the stroke is caused by relatively soft thrombotic material, the clot can be removed by means of thrombo-aspiration using aspiration catheters. The success of the intervention depends on the applied vacuum, the physical dimensions of the catheter and the visco-elastic properties of the blood and the clot. Many different aspiration catheters are available on the market. The aim of this study was to create a simple simulation model that computes the flow of a blood/clot mixture through catheter system. The physical dimensions of nine different commercially available (aspiration) catheters were used to simulate their expected aspiration performance.
Methods: The relation between pressure difference between the tip and the base of a catheter (assuming a cylindrical shape) and laminar flow can be approximated by Poisseulles' equation and is the quotient of a constant named flow resistance and the pressure difference. The flow resistance is proportional to the length of the catheter and the viscosity of the transported fluid and inverse proportional to the radius of the fourth power.

Poisseulles' equation was integrated numerically by of fourth order Runge-Kutta method. The input parameters of the program are the inner diameter and length of the catheter, the viscosities of blood and clot material, the pressure of the vacuum, the mean arterial blood pressure, and the clot volume that needs to be aspirated.
Results: Assuming a total clot volume of 2.5 ml and a vacuum pressure of 100 mbar and an mean blood pressure of 140 mm Hg, clot viscosity of 12500 mPa.s (worst case, i.e. literature value for clot formed under low shear stress conditions), blood viscosity of 4 mPa.s the total aspiration time ranged from 16.6 seconds to 913.7 seconds for the tested catheter geometries. There is a very strong dependence on the radius of the aspiration catheter. Catheters with an as thin as possible wall which completely fill the occluded blood vessel turned out to aspirate clots most efficiently allowing for the fastest recanalization.
Conclusion: A simulation program was developed which simulated a mixed viscosity flow of clot and blood through an aspiration catheter. There is a strong dependence of the obtained recanalization times on the physical dimensions of the investigated commercial aspiration catheters.

145

DTI neuroimaging parameters provide highly accurate prediction of rapid cognitive decline in mild cognitive impairment

S. Haller[1], D. Nguyen[1], C. Rodriguez[2], J. Emch[2], G. Gold[3], A. Bartsch[4], K.O. Lovblad[1], P. Giannakopoulos[2]
[1]Neuroradiology, Geneva, Switzerland, [2]Division of Old Age Psychiatry, Department of Psychiatry, Geneva, Switzerland, [3]Department of Rehabilitation and Geriatrics, Geneva, Switzerland, [4]Neuroradiology, Heidelberg, Germany

Introduction: Most previous studies aiming to establish structural neuroimaging predictors of dementia in mild cognitive impairment (MCI) focused on gray matter changes. Recently, diffusion tensor imaging (DTI) studies revealed the presence of group differences in fractional anisotropy (FA) between MCI and healthy controls. To date, no longitudinal study assessed the utility of DTI in the individual prediction of MCI rapid cognitive decline.
Methods: We report the results of a DTI analysis in 35 healthy controls (HC) and 69 MCI community-dwelling individuals who were neuropsychologically followed-up after one year. FA was analyzed in Tract-Based Spatial Statistics (TBSS). In addition to the group comparisons, we analyzed individual classification accuracy implementing support vector machines (SVM), a branch of machine learning.
Results: There were significantly higher FA values in HC compared to MCI cases in the ventral part of the corpus callosum and the right temporal and frontal white matter pathways including the inferior longitudinal and uncinate fasciculi, as well as the parahippocampal white matter. There were no supra-threshold differences for the voxel-wise comparisons between stable MCI and progressive MCI cases using strict correction for multiple comparisons. At the individual level, SVM classification accuracies were 91.4% for the distinction between MCI and HC and 98.4% for that between stable MCI and progressive MCI.
Conclusions: In the light of these observations, the DTI FA may become an applicable and clinically useful tool for the individual classification of stable versus progressive MCI.

146

Fallbericht: Kleiner Schlaganfall mit grosser Ursache

C. Zubler[1], T. Aymard[2], S. Bohlhalter[3], M. Arnold[3], J. Gralla[1]
[1]Neuroradiologie, DRNN, Inselspital Bern, Bern, Switzerland, [2]Universitätsklinik für Herz- und Gefässchirurgie, Inselspital Bern, Bern, Switzerland, [3]Universitätsklinik für Neurologie, Inselspital Bern, Bern, Switzerland

Einführung: Zuweisung einer 43 Jahre alten Patientin zur Thrombolyse mit Verdacht auf akuten zerebrovaskulären Insult (CVI) bei Status nach Kollaps mit anschliessender Schwäche des linken Armes. Im neurologischen Status zeigte sich ein sensomotorisches, armbetontes Hemi-Syndrom links (Kraftgrad M4, National Institute of Stroke Scale Score (NIHSS) 2). Die Blutdruckwerte waren mit 90/65 mm Hg grenzwertig erniedrigt. In der Magnetresonanztomographie (MRT) zeigten sich bilaterale, frische embolische Ischämien zerebellär beidseits und im Stromgebiet der Arteria cerebri media rechts; normale intrakranielle Gefässe; die Halsgefässe in der 3D-Rekonstruktion erschienen zunächst unauffällig; die Einzelschichten hingegen wiesen auf eine Dissektion der Aorta ascendens mit Ausdehnung in die supraaortalen Gefässe hin, welche sich in der Computertomographie (CT) bestätigte.
Diskussion: In der Schweiz erleiden schätzungsweise 16 000 Menschen pro Jahr einen CVI, es ist national die dritthäufigste Todesursache. Eine schnelle Behandlung ist entscheidend, da die etablierten Therapien (intravenöse (i.v.) und intraarterielle (i.a.) Thrombolyse) zeitlich begrenzt sind (4,5 h resp. 6 h) und zum Anderen sich die Erfolgsaussichten der Therapie mit der Zeit deutlich verschlechtern. Somit findet jede Form der Abklärung unter erheblichem Zeitdruck statt. Oft wird auf eine zeitraubende Bildgebung verzichtet. In einigen Zentren wird die i.v. Lyse-Therapie bei eindeutigen klinischen Symptomen und fehlenden Kontraindikationen nach Anfertigung eines Nativ-Schädel-CTs begonnen. In unserem Fall mit Typ A Aortendissektion und bereits bestehender Perikardtamponade hätte eine medikamentöse Fibrinolyse fatale Folgen gehabt. Die akute Aortendissektion Typ A ist eine sehr selten beschriebene Differentialdiagnose beim akuten Hirninfarkt mit einer Inzidenz von 0,5–3/100000 pro Jahr. Die Mortalität und Morbidität der Aortendissektion ist hoch und steigt mit dem Zeitintervall zwischen Auftreten und Diagnosestellung stark an. Der Einbezug der Halsgefässe in die Bildgebung ist lediglich mit einem minimalen Zeitaufwand verbunden und dient in unserem Zentrum zur Entscheidungsfindung ob primär eine i.a. oder i.v. Thrombolyse durchgeführt werden soll. Der vorliegende Fall zeigt, dass eine erweiterte Bildgebung Patienten mit oligosymptomatischer Aortendissektion vor folgenschweren Entscheidungen wie der i.v. Thrombolyse, welche eine absolute Kontraindikation darstellen bewahren kann.

147

In vivo quantification of fat in muscular tissue using two-point Dixon technique and T2 relaxation time measurements

O. Scheidegger[1], A.C. Nirkko[2], C. Kiefer[1]
[1]Institute for Diagnostic and Interventional Neuroradiology, Inselspital, Bern, Switzerland, [2]Department of Neurology, Inselspital, Bern, Switzerland

Introduction: Neuromuscular disorders eventually lead to fibro-fatty infiltration, and disease progression as well as benefits from therapy are difficult to assess objectively. Magnetic resonance (MR) imaging is a non-invasive tool which allows acquisition of multiple tissue parameters at a high spatial resolution. Here, we assess two different MR techniques for fat quantification in muscles.
Methods: MR imaging was performed in the human calf using a clinical 3 T MR scanner and a 15 channel, circularly polarized knee coil. 1) Spectral imaging was performed using a gradient-echo sequence (TR 20 ms), where the chemical shift difference between water and fat was encoded into images with different echo times (TE 2.45/3.675 ms) and post-processed using the Dixon technique. 2) Eight echoes were collected during readout of a multi spin echo sequence (TR 2250 ms, TE 12, 24, 36, 48, 60, 72, 84, and 96 ms), which allowed a bi-exponential fit (Levenberg-Marquardt) of the signal decay using the corresponding T2 relaxation times of muscle and fat tissue as starting values. Signal histogram analysis of subcutaneous fat (SF), tibial anterior muscle (TA), and gastrocnemius muscle (GM) were performed, as well as calculation of T2 relaxation times and fat volume fraction using both techniques.
Results: Histograms of GM and TA were similar, but different to SF. T2 relaxation times were 39 ± 4 ms (TA), 38 +/- 2 ms (GM), and 116 ± 12 ms (SF). Fat volume fraction were 0.07 ± 0.01 (TA), 0.07 ± 0.01 (GM), and 1.00 ± 0.05 (SF) using the Dixon technique. Fat volume fraction were 0.20 ± 0.05 (TA), 0.18 ± 0.04 (GM), and 1.00 ± 0.01 (SF) using the bi-exponential fit of T2 signal decay.
Conclusions: The two-point Dixon technique and the determination of fat fraction using T2 relaxation times were used for in vivo quantification of fat content in muscle tissue. In healthy volunteers, the latter technique yielded slightly elevated values compared to the Dixon technique. The Dixon technique uses pi-phase-shift and subtraction of complex valued images for encoding the signal of fat and water protons, whereas a model assumption is used for the separation of fat and muscle tissue using T2 relaxation times. Due to this, adequate separation of fat and muscle tissue might be impaired when additional tissue changes (e.g. fibrous transformation) alter T2 relaxation times. The Dixon technique is therefore more suitable for quantification of fat content.

148

Interactive Tool for Computer Aided Multiple Sclerosis-Lesion Counting in MR-images and Volumetry

J. Slotboom[1], Y. Burren[1], C. Kiefer[1], M. Zbinden[1], C.P. Kamm[2], H. Mattle[2], R. Wiest[1], G. Schroth[1], M. El. Koussy[1]
[1]Institute for Diagnostic and Interventional Neuroradiology, Bern, Switzerland, [2]Neurology, Bern, Switzerland

Introduction: MRI is the technique of choice for the diagnosis and monitoring of multiple sclerosis. MRI not only allows the detection of the totally affected brain tissue from T2-weighted MR-images, but also allows the discrimination of old lesions from new active lesions from contrast enhanced MR-images. Traditionally the number of MS-lesions is used as indicator of disease progression, which are "manually" counted by the neuroradiologist. Manual lesion counting may seem to be a very straightforward and simple procedure, but in practice, this turns out to be not the case; especially lesion counting from T2-weighted images. There are several reasons for this. The first reason is that there are no clear rules on how to count the MS-lesions exactly. More specifically: what is the minimum size of a MS-lesion to be counted? how to count multiple small lesions which are closely together? Also highly problematic are MS-lesions which are visible in more than one adjacent images, especially in the case of multiple closely together located lesions. These questions will be answered by every neuroradiologist in a different fashion.
Method: The aim of the study was to develop an algorithm for computer aided MS-lesion counting and volumetry. The application was completely written in JAVA and allows for the analysis of image data in the DICOM format. The evaluation takes the following steps.
1. Image data loading.
2. Graphical definition of prototype lesion tissue by the neuroradiologist, i.e. the neuroradiologist simply marks one or more lesions.
3. Automatic segmentation based on the defined prototype MS-lesion tissue (mouse click).
4. Refinement step: manual sub-selection of found lesions (if necessary) by means of mouse-clicking on those image sub-segments.
5. Automatic lesion number counting and volumetry by one single mouse click.
6. Storage of total lesion count and volumetry.
Results: A fully working application has been developed and the method was tested on a collective of 64 patients. The application counts connected lesions visible in multiple adjacent slices correctly. Lesion volume values obtained from MS-patients are very realistic, statistical tests passed successfully. Due to the fact that no minimum lesion volume can be defined, the number of lesions obtained by the application is larger than the manually obtained lesion counts. Improvements in the lesion counting algorithms are currently under investigation.
Conclusion: The study showed that computer aided MS-lesion counting and volumetry is feasible and will help to improve the quality of monitoring MS-disease progression in future.

149

In-vivo evaluation of a combined flow restoration and mechanical thrombectomy device in a swine model of acute vessel occlusion

P. Mordasini[1], J. Gralla[1], G. Schroth[1], U. Fischer[2], M. Arnold[2], C. Brekenfeld[1]
[1]Institute of Interventional and Diagnostic Neuroradiology, Inselspital, Bern, Switzerland, [2]Department of Neurology, Inselspital, Bern, Switzerland

Background and Purpose: The purpose of study was to evaluate the efficiency, thrombus-device interaction and potential complications of the stent-like Solitaire FR Revascularization Device for immediate flow restoration and mechanical thrombectomy in-vivo.
Material and methods: The device was evaluated in an established animal model in the swine. Flow restoration effect (immediately after deployment = T0, after 5 minutes = T5 and 10 minutes = T10), recanalization rate after retrieval, thromboembolic events and complications were assessed. Radio-opaque thrombi (10mm length) were used for the visualization of thrombus-device interaction during application and retrieval of the device. The Solitaire FR (4x20 mm) was assessed in 15 vessel occlusions.
Results: Immediate flow restoration after deployment was achieved in 80.0% of vessel occlusions. Mean recanalization rate at T0 was 30.8%, at T5 30.7% and at T10 25.4% of initial vessel diameter. Re-occlusion occurred in 20.0% between T0 and T5 and in 13.3% between T5 and T10. Complete recanalization (TICI 3) after retrieval was achieved in 86.7%. In two cases (13.3%) partial recanalization was achieved with remaining thrombus in a side branch (TICI 2b). No thromboembolic event was observed during deployment or retrieval. Thrombus-device interaction illustrated the compression of the thrombus against the vessel wall during deployment leading to partial flow restoration. During retrieval the thrombus was retained by the stent meshes without significant thrombus compression. No vessel perforation, dissection nor fracture of the device was observed.
Conclusion: The Solitaire FR is a safe and effective combined flow restoration and thrombectomy device in-vivo. Maximal flow and thrombus compression is achieved immediately after deployment with decreasing effect with time indicating the need for retrieval to achieve recanalization.

150

Preoperative MR-Angiography with blood-pool agent at 3 Tesla. Analysis of arterial spinal cord blood supply in patients with thoracoabdominal aortic aneurysm

M. El-Koussy[1], P. Mordasini[2], M. Ith[2], J. Gralla[1], J. Schmidli[3], G. Schroth[1], H. Hoppe[2]
[1]Dept. Neuroradiolgy, Univ. Bern, Bern, Switzerland, [2]Dept. Radiology, Univ. Bern, Bern, Switzerland, [3]Dept. Vascular Surgery, Univ. Bern, Bern, Switzerland

Introduction: The operative repair of thoraco-abdominal aortic aneurysms carries an up to 5% risk of postoperative spinal cord ischemia causing complications including paraplegia. Preoperative mapping of the arteries supplying the spinal cord including the Adamkiewicz artery can help avoid postoperative ischemic complications. Steady-state MR angiography (MRA) provides a high spatial resolution, while gadolinium-based blood-pool-agent gadofosveset allows extended blood-plasma retention time.
Methods: Twenty-four consecutive patients underwent a preoperative spinal MRA in a 3-Tesla-scanner (MAGNETOM Verio, Siemens). The sequence applied was a steady-state coronal 3D-FLASH MRA with 0.7-mm isotropic voxels after injecting gadofosveset trisodium at 3 ml/sec. Postprocessing included multiplanar reconstructions and maximum-intensity-projection for the Adamkiewicz artery and its segmental artery mapped from aortic origin to the spinal canal entry. Assessment of the images was performed by three independent observers.
Results: Identification and localization of the Adamkiewicz artery and its segmental artery as major arterial supply of the spinal cord was successful including the level of aortic origin and spinal canal entry. The interobserver variance for the overall image quality and anatomy depiction was high.
Conclusion: Preoperative 3-Tesla-MRA with blood-pool agent provides a non-invasive and efficient tool for identification of the Adamkiewicz artery and its segmental artery with regard to the level of aortic origin and spinal canal entry. Further optimization is needed to combine steady-state and time-resolved MRA to overcome the venous overlap and enhance temporal information.

151

Quantification of Fat Infiltration in Oculopharyngeal Muscular Dystrophy: Comparison of Three Magnetic Resonance Imaging Methods

M. Gloor[1], A. Fischmann[2], S. Fasler[2], T. Haas[2], O. Bieri[1], K. Scheffler[1], D. Fischer[3]
[1]Radiological Physics, University of Basel Hospital, Basel, Switzerland, [2]Neuroradiology, University of Basel Hospital, Basel, Switzerland, [3]Neurology, University of Basel Hospital, Basel, Switzerland

Introduction: Oculopharyngeal muscular dystrophy (OPMD) is an autosomal-dominant muscle disorder, which appears in individuals with a mutation on the nuclear poly(A) binding protein gene [1] and is characterized by bilateral, progressive muscle fiber necrosis and muscle infiltration by fatty tissue. In this magnetic resonance (MR) imaging study, three quantitative measures of muscular fat infiltration are evaluated with regard

to applicability for longitudinal studies of the pattern and involvement of fat infiltration in OPMD patients.
Methods: Imaging on 8 OPMD patients 5 healthy volunteers was performed on a 1.5 T MR scanner. Two axial slice groups were chosen at predefined distances from the knee joint, one in the thigh and one in the calf. The protocol consisted of a T1-weighted turbo spin echo sequence for anatomical reference (fig. 1), two gradient echo sequences for 2-point Dixon imaging [2], a multi-contrast TSE sequence for quantification of transverse relaxation times T2, and a steady-state free precession (SSFP) sequence for histogram analyses (total acquisition time 20:44 min). Regions of interest (ROI) were drawn in 11 thigh and 10 calf muscles (fig. 1).
Results: Mean fat infiltration in the whole thigh and calf (fig. 2a) of all patients significantly differed from values of the healthy controls according to all methods except for the thigh muscles of patient 7. All techniques suggest that patients 2 and 4 are most affected by fat infiltration. Figure 2b exemplary illustrates the quantification of fat infiltration in the individual thigh muscles based on T2 values. The T2 values enabled a differentiation between patients and controls in 74%, the 2-point Dixon method in 58% and the SSFP method in 52% of the 168 examined patient muscles. Furthermore, a strong linear correlation is observed between the three quantitative methods ($0.78 < R^2 < 0.94$).
Conclusions: This work demonstrates that non-invasive quantification of fat infiltration in OPMD patients can be performed with different MR imaging methods. The mean fat fractions across all muscles can provide an impression of muscle degeneration. A detailed pattern of individual muscle involvement may help on the understanding of the disease and serve as a baseline for longitudinal studies. For an optimal assessment of therapy effectiveness, objective measures of muscle tissue integrity, such as multiecho Dixon techniques and quantitative T2 determination, are indispensable.
References: 1 Brais B, et al. Nat Genet. 1998;18:164–7. 2 Dixon WT. Radiology. 1984;153(1):189–94.

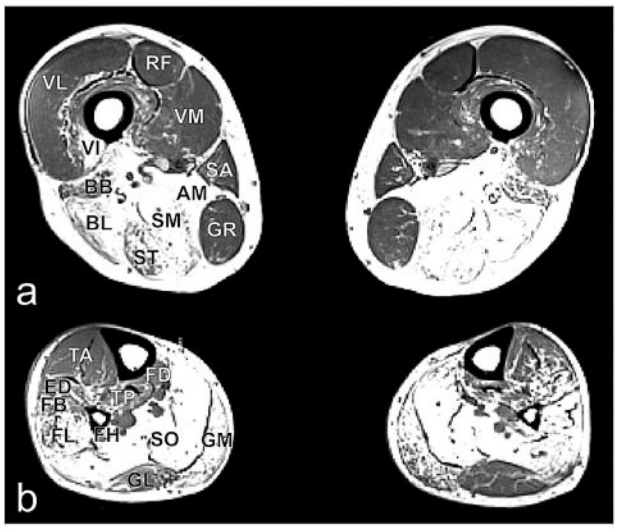

Figure 1
Exemplary T1-weighted images of thigh and calf muscles of an OPMD patient. (a) Abbreviations of thigh muscles: adductor longus (AL), adductor magnus (AM), biceps femoris caput breve (BB), biceps femoris caput longum (BL), gracilis (GR), rectus femoris (RF), sartorius (SA), semimembranosus (SM), semitendinosus (ST), vastus intermedius (VI), vastus lateralis (VL), vastus medialis (VM). (b) Abbreviations calf muscles: extensores longi digitorum et hallucis (ED), fibularis brevis (FB), flexor digitorum longus (FD), flexor hallucis longus (FH), fibularis longus (FL), gastrocnemius caput laterale (GL), gastrocnemius caput mediale (GM), soleus (SO), tibialis anterior (TA), tibialis posterior (TP).

Figure 2
(a) Mean fat fractions (primary y-axis) using the 2-point Dixon (2PD) method and SSFP histogram analysis, and mean T2 values (secondary y-axis) across left/right side and all muscles (first y-axis). Mean value and 2SD of 5 healthy controls and results of the individual OPMD patients are displayed.
(b) Quantification of fat infiltration in the individual thigh and calf muscles based on T2 values. Mean value (± 2 SD) across all healthy volunteers are shown for each muscle and opposed to values in individual muscles of OPMD patients (P1-P8). Muscles are sorted according to the mean values across all subjects in descending order.

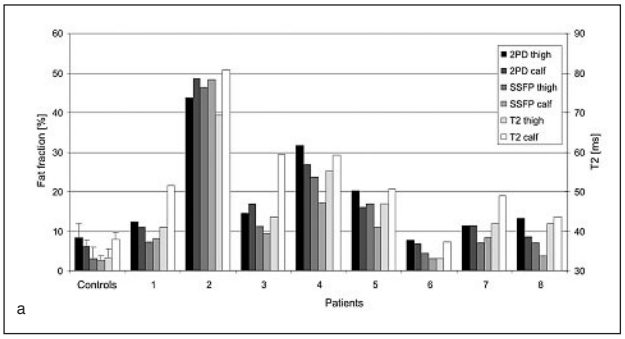

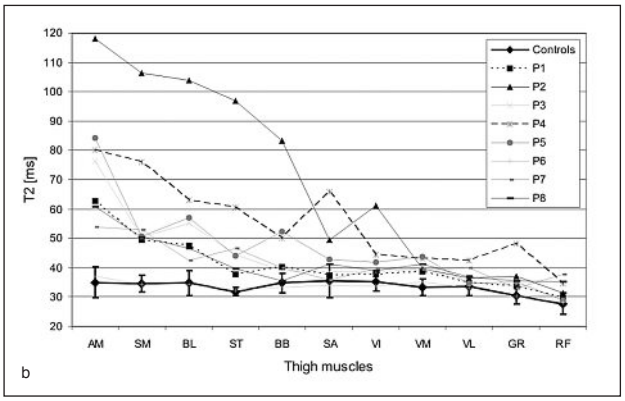

152

Quantitative Clinical Routine Magnetic Resonance Spectroscopy: Problems, Requirements and Solutions

J. Slotboom[1], D. Graveron[2], D. Stefan[3], C. Brekenfeld[1], D. van Ormondt[4]
[1]Institute for Diagnostic and Interventional Neuroradiology, Bern, Switzerland, [2]Laboratoire Creatis-LRMN, CNRS UMR 5220, Inserm U630, Université Claude Bernard LYON 1, CPE, Lyon, France, [3]ALTER Systems, Lyon, France, [4]Applied Physics, Delft University of Technology, Delft, Netherlands

Introduction: Localized in vivo magnetic resonance spectroscopy (MRS) is a technique that enables the non-invasive determination of metabolite concentrations of human tissues. Although many advances have been made in the available hardware, recording techniques and processing tools for MRS in recent years, its clinical applicability is still limited. Since the functionality of available MRS-quantification software on commercial scanners is still limited, the clinician still needs to export the spectrum manually, transfer it to a PC and process it with an external, state of the art, MRS quantification program, like e.g. jMRUI, LC-Model or TDFDFIT, which is tedious and time consuming and error prone. On the other hand, the quantitative results obtained by these external tools cannot be transferred back into to PACS systems. Additionally, the above mentioned quantification programs do not allow for the simultaneous examination of MR-images and 1D-MRS-data within the-same application.
Methods: Our new plug-in functionality of jMRUI enables the user to extend the functionality of this state of the art MRS quantification tool. In order to improve the applicability of MRS in the clinical routine, we developed the following plug-ins that solve the mentioned problems: I. DICOM network listener, allowing direct network transfer of DICOM files via the DICOM-

network protocol to jMRUI; II. automatic DICOM file-renaming into meaningful file names; III. display and advanced analysis of MR-images, with spectroscopic voxel projected into them; IV. automatic image pixel intensity determination at spectroscopy voxel location; V. reading of the proprietary Siemens spectroscopy DICOM-wrapper files; VI. signal reliability testing; VII. signal artefact reduction by order statistic filtering.
Results: Features I.-VII. have been implemented in JAVA and tests passed successfully.
Discussion: The currently added software was tested with raw DICOM image and spectroscopy files as generated by default on Siemens scanners. With the new plug-ins jMRUI is now the first advanced spectroscopy quantification software that enables the clinician to correlate image pixel information with MRS information in a simple way. Plug-ins for reporting quantitative MRS results to PACS-nodes is now under development.
Conclusion: The functionality of the state of the art jMRUI software package has been extended, massively simplifying the usage of quantitative in vivo MRS in clinical routine.

153

The diagnostic value of super-selective catheterization of the inferior petrosal sinus in Cushing's syndrome

L. Andereggen[1], G. Schroth[1], J. Gralla[1], RW. Seiler[2], L. Mariani[2], J. Beck[2], E. Christ[3], C. Ozdoba[1]
[1]Institute of Diagnostic and Interventional Neuroradiology, University of Bern, Bern, Switzerland, [2]Department of Neurosurgery, University Hospital, Inselspital Bern, Bern, Switzerland, [3]Division of Endocrinology, University Hospital, Inselspital Bern, Bern, Switzerland

Introduction: Identifying a micro adenoma in ACTH-dependent Cushing's syndrome remains a difficult issue. We describe the use of super-selective catheters in bilateral petrosal sinus sampling performed in 23 patients with Cushing's syndrome and ambiguous MR findings and discuss the accuracy of this method in comparison to MR imaging.
Methods: In 23 patients with Cushing's syndrome and normal or non-specific MR finding bilateral inferior petrosal sinus sampling (BIPSS) was performed. Briefly, inferior petrosal sinus was catheterized bilaterally with Hi-Flow Tracker 18 catheters. A third catheter was placed in a peripheral vein. ACTH blood concentration was measured from each of the three catheters before and 3, 5, and 10 minutes after i.v. stimulation with ovine corticotropine releasing hormone.
Results: In 21 of 23 patients, hyperplasia of ACTH producing cells or an adenoma could be histologically proven. In 18 of 20 cases where transsphenoidal partial hypophysectomy was performed based on BIPSS findings, adenoma was histological confirmed. Retrospective analysis of the MRI datas after BIPSS showed erroneous reports in 50%. MRI yielded a significant lower sensitivity with 53% compared to 95% in BIPSS and a specificity of 33% compared to 66% in BIPSS, respectively.
Conclusions: In cases of Cushing disease, bilateral inferior petrosal sinus sampling is far superior to MR imaging in the accurate detection of pituitary pathology.

154

The value of stereolithographic models for advanced treatment planning in complex giant aneurysms

L. Andereggen[2], J. Gralla[2], M. Peterhans[3], S. Weber[3], G. Schroth[2], M. Reinert[1], A. Raabe[1]
[1]Department of Neurosurgery, University of Bern, Inselspital, Bern, Bern, Switzerland, [2]Institute of Diagnostic and Interventional Neuroradiology, University of Bern, Bern, Switzerland, [3]ARTORG Center for Biomedical Engineering Research, University of Bern, Bern, Switzerland

Introduction: Treatment of complex giant aneurysms remains a difficult issue. Even though modern imaging technologies like 3D-rotational angiography and CT-angiography may help to better understand the often difficult anatomic configuration, there may be challenges in visualization. We wanted to evaluate if this novel technique of 3D models may improve visualization and decision making.
Methods: Stereolithographic biomodelling is a new technology that allows integration of imaging data sets such as CT, CTA and 3D-RA to accurately manufacture solid plastic replicas. Based on the information gained from these imaging studies, several different modalities could be analyzed simultaneously like the shape and extends of the aneurysm, thrombosis, vascular implants of a previous surgery or endovascular intervention as well as the courses of target and donor vessels were defined. The 3D-stereolithographic model integrated these structures within a 3D object.
Results: Four patients presented with a fusiform giant aneurysm of the MCA, one patient with a giant aneurysm of the PCA. In all of them, a 3D-stereolithographic model could be adequately achieved showing the relevant anatomical structures down to an object size of one millimeter.
Conclusions: Treatment of giant aneurysms either by endovascular or microsurgical or combined approach remain a complex task. Our series of 3D stereolithographic models demonstrates the feasibility and clinical utility of a new visualization medium for cerebrovascular neurosurgery in giant partially thrombosed aneurysm foreseen for an EC-IC bypass.

155

Virtopsy: Feasibility of Postmortem CT Angiography in Neuropathological Cases

P.M. Flach[1], P.M. Flach[2], S. Ross[2], S. Ross[3], G. Hatch[2], T. Ruder[2], T. Germerott[2], W. Zech[2], G. Ampanozi[2], G. Schroth[1], M. Thali[2]
[1]Department of Interventional and Diagnostic Neuroradiology, Inselspital Bern, Bern, Switzerland, [2]Centre for Forensic Imaging and Virtopsy, Institute of Forensic Medicine, University of Bern, Bern, Switzerland, [3]Department of Interventional, Pediatric and Diagnostic Radiology, Inselspital Bern, Bern, Switzerland

Introduction: Postmortem imaging provides a minimally invasive method to examine victims for causes of deaths. Still there is little information of the vasculature due to a lack of contrast. Pathologies of the cervicocranial junction are cumbersome to dissect during autopsy whilst only target-orientated preparation is feasible and simultaneously destruction of potential forensic findings will occur. Lately established postmortem CT Angiography (pmCTA) is performed in order to provide precise display of vascular and tissue lesions. The purpose of this case study was to show the potential of pmCTA as adjunct to autopsy in detection of vascular and parenchymal pathologies of the craniocervical region.
Methods: Five selected cases (3 m, 2f; 24–31 yrs) with neuropathological findings were studied and underwent autopsy. The ethics committee of the university approved this study. Unenhanced pmCT (Emotion6, Siemens Medical, Erlangen, Germany) was executed, followed by subsequent access to the femoral vessels (16 Fr artery; 20 Fr vein, Medtronic, Switzerland) in order to perform pmCTA with arterial and venous injection. A contrast media mixture of poly ethylene glycol (PEG200, Schaerer & Schlaepfer AG, Switzerland) and Imagopague 300 (Amersham Health, UK) was administered. Raw data acquisition was performed with the following settings: collimation 6x1 mm whole body; unenhanced pmCT with 130 kV;160 mAs and pmCTA with 110 kV;160 mAs. Spiral imaging of the head was standard with calculation of brain tissue/bone weighted algorithm (5 mm/1.25 mm). Due to potential forensic evidence the forensic pathologist had to be aware of the results detected in pmCTA prior to autopsy. Autopsy was considered as gold standard.
Results: All findings of pmCTA could be validated by autopsy. All cases showed severe neuropathological findings depicted by pmCTA and not detectable by unenhanced pmCT/pmMRI only. The leading cause of death was CRP in 4 cases. One case died due to cardiac arrest. Vascular lesions were present in 3 cases. Rupture of the brain stem occurred in 2 cases, and 1 showed hemorrhage to the brainstem and shearing injuries. Brain edema was present in 2 cases. All cases depicted intracranial hemorrhage.
Conclusions: PmCTA provided the basis of a focused and quality-improved preparation of the craniocervical junction by revealing pathologies that are frequently missed during classic autopsy. The newly implemented method of pmCTA proved to be a potential adjunct to classic autopsy detecting neuropathological causes of death.

156

White matter diffusion abnormalities after epilepsy surgery

D. Nguyen, M.I. Vargas, M. Seeck, K.O. Lovblad, S. Haller
Geneva University Hospital, Geneva, Switzerland

Introduction: Diffusion-tensor-imaging (DTI) techniques demonstrated diffuse bilateral temporal and extra-temporal abnormalities of white matter in patients presenting mesial temporal lobe epilepsy with hippocampal sclerosis (HS) [1-

3]. The aim of this study is to assess the reversibility of these diffusion changes following temporal lobe surgery, by applying a novel voxel-based tract-based spatial statistics (TBSS) [4] technique for whole-brain analysis of fractional anisotropy (FA).
Material and methods: The study included 23 patients with unilateral HS. Twelve patients underwent temporal lobe surgery. Follow-up MRI was done in a mean interval of 4 months. Pre-processing and statistics analysis of FA maps with TBSS was done using FSL tools [5]. Pre-operative FA asymmetry in all 23 patients was assessed within subjects between lesional and contralateral hemispheres with TBSS with threshold-free cluster enhancement (TFCE)[6] correction. The post-operative dataset of 12 patients was compared with the corresponding pre-operative dataset using voxel-wise and volume of interest (VOI) statistical analysis with a paired t-test.
Results: Within a mean interval time of 6.3 months after surgery, the majority of the included patients was seizure free (n = 10, 83.3%). The pre-operative comparison between lesional and contralateral hemispheres showed a significant FA reduction in the ipsilateral hippocampus, fornix and corpus callosum. Voxel-wise comparison between post and pre-operative dataset did not show supra-threshold voxels. VOI statistical analysis showed significant FA decrease in ipsilateral fornix and significant increase in contralateral fornix and bilateral white matter after surgery.
Conclusion: The ipsi-lesional fornix showed decreased FA after surgery, consistent with Wallerian degeneration. In contrast, contra-lesional fornix and bilateral large white matter fiber tracts demonstrated increasing FA indicating recovery of axonal integrity. This might be due to the removal of spreading epileptogenic activity after temporal lobe surgery. References:
1. Assaf B, Mohamed F, Abou-Khaled K, et al. Diffusion Tensor Imaging of the Hippocampal Formation in Temporal Lobe Epilepsy. AJNR. 2003;24:1857–62. 2. Concha L, Beaulieu C, Gross D. Bilateral limbic diffusion abnormalities in unilateral temporal lobe epilepsy. Ann Neurology. 2004;57:188–96. 3. Thivard L, Lehéricy S, Krainik A, et al. Diffusion tensor imaging in medial temporal lobe epilepsy with hippocampal sclerosis. NeuroImage. 2005;28:682–90. 4. Smith S, Jenkinson M, Johansen-Berg H, et al. Tract-based spatial statistics: Voxelwise analysis of multi-subject diffusion data. NeuroImage. 2006;31:1487–505. 5. Smith S, Jenkinson M, Woolrich M, et al. Advances in functional and structural MR image analysis and implementation as FSL. NeuroImage. 2004;23:208–19. 6. Smith S, Nichols T. Threshold-free cluster enhancement: Addressing problems of smoothing, threshold dependance and localisation in cluster inference. NeuroImage. 2009;1:83–98.

157

Extent of atherosclerotic lesions and plaque echogenecity on standard carotid ultrasound is correlated with plaque neovascularization detected by contrast-enhanced carotid ultrasound imaging

Sasan Partovia, Daniel Staub[b,c], Markus Aschwanden[b], Heiko Uthoff[b], Thomas Baldi[b], Sven Stein[b], Christoph Stippich[a], Steven B. Feinstein[c], Kurt A. Jaeger[b]
[a]Department Neuroradiology, University Hospital, Basel, Switzerland, [b]Department Angiology, University Hospital, Basel, Switzerland, [c]Department of Internal Medicine, Section of Cardiology, Rush University Medical Center, Chicago

Introduction: Current risk stratification of carotid atherosclerotic lesions is based on the evaluation of degree of stenosis and plaque morphology using standard ultrasound. High degree stenosis and echolucent plaques corresponding to histological features of plaque instability are at high risk for cerebrovascular events. Vasa vasorum derived neovascularization are known to be important features in plaque development and vulnerability triggered by inflammation and hemorrhage. As recently shown, contrast-enhanced carotid ultrasound (CEUS) provides direct visualization of plaque neovascularization. The purpose of this study was to correlate the extent of carotid atherosclerosis and plaque echogenicity with neovascularization on CEUS.
Methods: 175 subjects (mean age 67 ± 10 years, 65% male) with 293 atherosclerotic lesions underwent standard carotid ultrasound and CEUS. Echogenecity (class I: uniformly echolucent, class II: predominantly echolucent, class III: predominantly echogenic, class IV: uniformly echogenic, class V: extensive calcification) and degree of stenosis at standard ultrasound were evaluated for each lesion. Degree of neovascularization on CEUS was categorized as absent (grade 1), moderate (grade 2), or extensive (grade 3).
Results: Different characteristics of the atherosclerotic lesions are presented in table 1. Echogenicity was significantly correlated with the grade of neovascularization (p = 0.002). More echolucent plaques had higher degree of neovascularization compared with more echogenic ones (figure 1A). Lesion severity assessed by degree of stenosis and maximal thickness was significantly associated with grade of neovascularization (p <0.001). Lesions with higher degree of luminal narrowing had higher grade of neovascularization (figure 1B), and maximal thickness increases with the grade of neovascularization (grade 1: 2.6 ± 0.9 mm, grade 2: 2.8 ± 0.9 mm, and grade 3: 3.6 ± 0.9 mm; p <0.001 for trend).

Table 1

Characteristics	Atherosclerotic carotid lesions (n=293)
Severity, n (%)	
Stenosis < 50%	226 (77)
Stenosis 50-69%	49 (17)
Stenosis = 70%	18 (6)
Maximal plaque thickness, mean±SD (mm)	2.68±0.90
Echogenicity, n (%)	
Class I	30 (10)
Class II	99 (34)
Class III	111 (38)
Class IV	7 (2)
Class V	46 (16)
Neovascularization, n (%)	
Grade 1	178 (61)
Grade 2	96 (33)
Grade 3	19 (6)

Figure 1

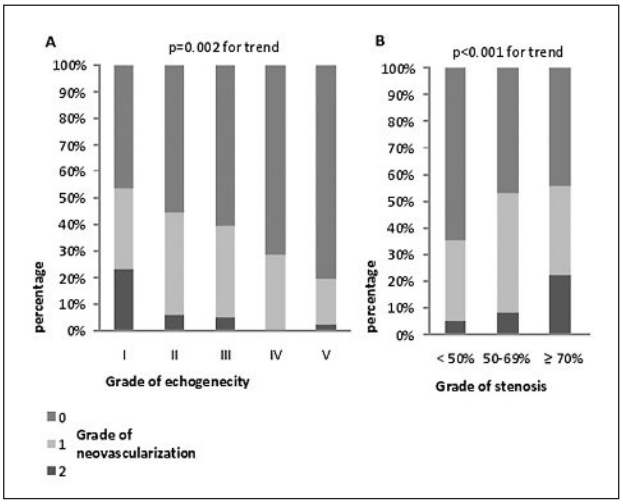

Conclusions: These findings support our hypothesis that neovascularization on CEUS is correlated with the extent of atherosclerotic lesions and with morphological features of plaque instability. The positive relationship between plaque density and contrast-agent enhancement is in agreement with the pathophysiological concept that more vulnerable plaques with higher risk for cerebrovascular events are more likely to have a greater degree of neovascularization. We conclude that CEUS is a valuable tool for risk stratification of atherosclerotic lesions.

158

Diffusion tensor imaging in spinal cord injury

J.A. Petersen[1], B. Wilm[3], J. von Meyenburg[2], M. Schubert[1], V. Dietz[1], S.S. Kollias[2]
[1]Spinal cord Injury Center, University Hospital Balgrist, Zürich, [2]Institute of Neuroradiology, University Hospital Zürich, Zürich, [3]Institute for Biomedical Engineering, University & ETH Zürich, Zürich

Introduction: Due to poor image quality and limited resolution, Diffusion Tensor Imaging (DTI) has rarely been applied to investigate disorders of the spinal cord. Recent improvements in MR pulse sequence design have overcome these problems, thereby providing a new instrument for the assessment of Spinal cord injury (SCI).
Methods: DTI data of 19 traumatic SCI subjects (level of lesion C3 to C8, mean age 59.7 years, time since injury 2 months to 8 years) and of 28 healthy volunteers (mean age 58 years) were acquired on a Philips Achieva 3 T MR scanner using an outer volume suppressed reduced field of view (FOV) acquisition with oblique slice excitation and a single-shot EPI readout. Fractional anisotropy (FA) and apparent diffusion coefficient (ADC) maps were calculated at cervical (C2 and C5), thoracic (T5) and lumbar (L1) levels of the spinal cord. Diffusivity values were evaluated in 10 regions of interest (ROIs) comprising the cross sectional area and certain parts of gray and white matter where motor and sensory tracts are located. Surface areas of spinal cord cross sections were compared.
Results and conclusion: In SCI subjects, FA values as compared to volunteers were decreased at all four spinal levels. At level C2, the decrease was statistically significant for the cross sectional area and for motor and sensory tracts ($p < 0.05$). Surface area of the injured spinal cord was decreased at all levels. The low FA values in the SCI subjects group are likely to reflect demyelination and axonal degeneration. Significant reduction of FA in the upper cervical segments suggests that regions remote from the injury site might be affected by progressive degeneration distant to the traumatic lesion. The reductions in surface area suggest atrophy. In conclusion, DTI provides useful, quantitative parameters for the objective evaluation of disease progression and potentially for monitoring treatment response.

159

Functional Organization of the primary motor cortex in congenital and chronic Acquired paraplegia

Magdalini Tozakidou[1], Michael Akbar[2], Maria Blatow[3], Ernst Nennig[3], Julia Reinhardt[1], Christoph Stippich[1]
[1]Department of diagnostic and Interventional Neuroradiology, University Hospital Basle, Switzerland, [2]Department of Orthopedic surgery, University of Heidelberg, Medical Center, Germany, [3]Department of Neuroradiology, University of Heidelberg, Medical Center, Germany

Introduction: The functional organization of the primary motor cortex in paraplegic patients is largely unexplored as research in the field is concentrated on the spinal lesion itself. However, the complete motor and somatosensory system is affected and may undergo functional changes on cortical, subcortical and spinal levels. In this research we focus on functional changes in the primary motor cortex associated with complete thoracic spinal lesions to better understand the underlying pathomechanisms. This is the first study to assess the somatotopic organization of M1 in patients with congenital and chronic acquired paraplegia using fMRI.
Material and methods: Ten right-handed patients with congenital paraplegia and thirteen patients with chronic acquired complete paraplegia (ASIA-Score grade A) due to thoracic spinal lesions underwent standardized BOLD-fMRI (executed tongue and finger movements, imagined foot movements) at 1.5 T or 3.0 T to study M1-somatotopy. Patient data were processed and evaluated on an individual basis using BrainVoyager® and compared to normative data obtained from healthy volunteers.
Results: Detailed anatomico-functional correlations revealed normal somatotopic organization of M1 in the patients with chronic acquired paraplegia as compared to healthy controls. The cortical representations were not significantly different. In contrast patients with congenital lesions had abnormal representations of the lower limb with a marked cranio-ventro-lateral shift of 3.1 mm (z-axis), 17.6 mm (y-axis), and 9.2 mm (x-axis) in the right hemisphere and 2.8 mm (z-axis), 11.8 mm (y-axis), and 9.0 mm (x-axis) in the left hemisphere (statistical means).
Conclusions: Patients with chronic acquired paraplegia due to complete thoracic spinal lesions show a normal functional organization of the primary motor cortex, where as patients with congenital paraplegia exhibit abnormal representations of the lower limbs. This indicates an important role of intact somatosensory affenrences and efferent functional loops for correct functional establishment of cortical body representations during CNS-development.

160

Perioperative strokes following resection of high grade gliomas

J.M. Lieb[1], G. Hartwigsen[2], J.W. Henson[3], F.G. Barker[3], F.J. Ahlhelm[1], C. Stippich[1], S. Ulmer[1,3]*
[1]Diagnostic and Interventional Neuroradiology, University Hospital Basel, Switzerland, [2]Departement of Neurology, University Hospital Schleswig-Holstein, Germany, [3]Pappas Center for Neuro-oncology, Massachusetts General Hospital, Boston, USA

Introduction: Postoperative MR imaging plays an important role in patient's management. Early resection control is mandatory to prove the extend of tumor resection and to rule out perioperative complications.
Material and methods: Fifty consecutive patients underwent postoperative MR imaging including a T1-weighted sequence with and without intravenous contrast administration, a diffusion weighted sequence (b value = 1000) and a T2 weighted TSE or FLAIR sequence. The images were analyzed by two neuroradiologists in consensus for restricted diffusivity and residual tumor burden. Follow-up exams were also reviewed (3 months postoperatively).
Results: Restricted diffusivity was detected in 70% of our patients. Areas of restricted diffusion were located in the depth or along the rim of the resection cavity. T1-weighted images were compared to rule out any artificial restriction caused by blood products in the resection cavity postoperatively. In follow-up MR scans, areas of restricted diffusivity as depicted by immediately performed MR imaging showed the typical appearance of encephalomalacia in 91% of these patients and adjacent contrast enhancement in 43% that regressed in further follow-up MR imaging.
Discussion: The amount of tumor resection has been found to be well correlated with long term survival. Detection of an early recurrence is the pivotal question in follow-up MR imaging. Nodular enhancement at the border of a resection cavity in follow-up MRI is often regarded as tumor progress. We have demonstrated that enhancement can also be caused by perioperative ischemia resembling progressive disease, however; this enhancement is a well known disruption of the blood brain barrier of a very special type of territorial stroke. Diffusion weighted imaging in immediately performed MRI is mandatory to be able to differentiate recurrent disease for perioperative strokes. These strokes can additionally cause new neurologic symptoms postoperatively.

161

Segmentale Beweglichkeit nach anteriorer zervikaler Dekompression – eine Vergleichsstudie

F. Ahlhelm, J. Lieb, S. Ulmer, A. Nabhan, D. Pape, C. Stippich

Purpose: Artifical disc replacement by disc prosthesis seems to be a promising treatment of symptomatic degenerative disc disease. To relieve overstraining of adjacent discs segmental motion should be preserved which is very difficult to evaluate and has not yet been proven. The aim of the current study was first to analyze segmental motion following artificial disc replacement using disc prosthesis. A second aim was, to compare both segmental motion as well as clinical result to the current surgical gold standard (ACDF).
Methods and materials: This is a prospective controlled study. 49 patients with cervical disc herniation were enrolled and assigned to either study groups (receiving a disc prosthesis) or control group (receiving ACDF, using a cage with bone graft and an anterior plate.). 8 patients were excluded from the study. Radio Stereometric Analysis (RSA) was used to quantify intervertebral motion immediately as well as 6, 12 weeks, 6 months as well as 1 and 2 years postoperatively. Also, clinical

results were judged using visual analog scale and neuro-exam at each RSA follow-up.
Results: Cervical spine segmental motion decreased over time in the presence of both disc prosthesis or fusion device. However, the loss segmental motion is significantly higher in the fusion group. We observed significant pain reduction in neck and arm postoperatively, without significant difference between both groups.

Conclusion: Cervical spine disc prosthesis remains segmental motion within 2 years after surgery. The clinical results are the same when compared to the early results following ACDF.

Abela E 25 S
Abu-Isa J 43 S
Achtnichts L 31 S, 38 S
Ackermann KA 5 S
Ahlhelm F 50 S
Allali G 31 S, 41 S
Amaxopoulou C 43 S
Amor F 28 S
Amort M 40 S
Andereggen L 48 S
Annoni JM 28 S
Arnold M 31 S, 37 S
Azakir BA 23 S, 29 S

Bellut D 9 S, 13 S, 16 S
Beltagy ME 18 S
Bijlenga P 19 S
Bloch A 32 S
Boëx C 24 S
Bogni S 18 S
Bohlhalter S 32 S
Bonati LH 35 S, 37 S
Bregy A 15 S, 17 S, 18 S

Capper-Loup C 23 S
Cereda CW 38 S

De Marchis GM 8 S
Di Fulvio S 26 S
Diserens K 29 S

El-Koussy M 42 S, 46 S
Engelter ST 24 S, 36 S
Erhardt S 12 S, 14 S
Everts R 21 S

Faber PL 3 S
Fischer U 39 S
Flach PM 48 S
Fluri F 31 S, 34 S

Gautschi OP 11 S, 17 S
Geiser E 41 S
Gloor M 46 S
Goeggel Simonetti B 22 S
Graumann U 13 S
Grujic GJ 37 S
Grunt S 20 S
Gschwind M 40 S
Guggisberg AG 6 S

Haefeli J 4 S
Haller S 43 S, 45 S
Hardmeier M 5 S
Hatz F 26 S, 27 S
Hauf M 44 S
Hosp JA 24 S

Jequier Gygax M 21 S
Jetzer AK 10 S
Jost GF 16 S

Kaech DL 19 S
Kassouha A 30 S
Khateb A 36 S
Kinter J 29 S
Klamroth-Marganska V 25 S
Klein A 20 S
Kockro RA 14 S
Kothbauer KF 10 S
Kotowski M 8 S
Krestel HE 7 S

Lascano AM 34 S
Lieb JM 50 S
Lisitchkina H 30 S
Lönnfors-Weitzel T 42 S
Lysandropoulos AP 30 S

Marbacher S 8 S, 9 S, 12 S
Mehling M 32 S
Meier N 36 S
Mihaylova V 35 S
Mono M-L 32 S, 36 S
Mordasini P 6 S, 46 S
Müller M 39 S

Nguyen D 48 S
Nirkko AC 3 S

Ochsenbein A 15 S
Oertel MF 17 S

Partovia S 49 S
Payer AK 34 S
Perren F 6 S
Petersen JA 50 S
Peyer AK 35 S
Pignat JM 38 S
Pizza F 6 S
Poretti A 20 S, 22 S
Poryazova RP 25 S
Ptak R 41 S

Ramelli GP 21 S
Ritz M-F 26 S
Rossetti AO 29 S
Rouge E 28 S
Rummel C 3 S

Sailer M 11 S
Salzmann A 22 S
Sarikaya H 27 S, 28 S, 33 S
Scheidegger O 7 S, 45 S
Schlachter E 12 S
Schober H 19 S
Schubert M 42 S
Schubring-Giese M 34 S
Schwyzer L 15 S
Seidel K 11 S
Seule MA 9 S
Sherif C 10 S
Simioni S 27 S, 40 S
Slotboom J 44 S, 46 S, 47 S
Sokolov AA 39 S
Stienen MN 16 S, 23 S

Tomasi O 13 S
Tozakidou M 50 S
Tyrand R 30 S

Valcarenghi C 26 S
Vanbellingen TV 23 S
Vassella E 14 S
von Meyenburg J 4 S
Vulliémoz S 41 S

Westermann B 13 S
Wider 33 S
Wiest R 3 S, 43 S
Wingeier K 21 S
Winkler DT 37 S

Zecca C 7 S
Zosso SZ 18 S
Zubler C 45 S
Zumofen W 8 S, 15 S
Zutter D 33 S